AIR QUALITY RESEARCH PROGRAM

Texas Commission on Environmental Quality
Contract Number 582-10-94300
Awarded to The University of Texas at Austin

Quarterly Report

March 1, 2015 through May 31, 2015

Submitted to

David Brymer
Texas Commission on Environmental Quality
12100 Park 35 Circle
Austin, TX 78753

Prepared by

David T. Allen, Principal Investigator
The University of Texas at Austin
10100 Burnet Rd. MC R7100
Austin, TX 78758

June 10, 2015

Texas Air Quality Research Program

Quarterly Report

March 1, 2015 – May 31, 2015

Overview

The goals of the State of Texas Air Quality Research Program (AQRP) are:

(i) to support scientific research related to Texas air quality, in the areas of emissions inventory development, atmospheric chemistry, meteorology and air quality modeling,

(ii) to integrate AQRP research with the work of other organizations, and

(iii) to communicate the results of AQRP research to air quality decision-makers and stakeholders.

On April 30, 2010, the Texas Commission on Environmental Quality (TCEQ) contracted with the University of Texas at Austin to administer the AQRP. For the 2010-2011 biennium, the AQRP had approximately $4.9 million in funding available. Following discussions with the TCEQ and an Independent Technical Advisory Committee (ITAC) concerning research priorities, the AQRP released its first request for proposals in May, 2010. Forty-five proposals, requesting $12.9 million in research funding were received. After review by the ITAC for technical merit, and by the TCEQ for relevancy to the State's air quality research needs, the results of the reviews were forwarded to the AQRP's Advisory Council, which made final funding decisions in late August, 2010. A total of 15 proposals were selected for funding. All projects were completed as of November 30, 2011, and final reports have been posted to the AQRP website.

In June 2011, the TCEQ renewed the AQRP for the 2012-2013 biennium. Funding of $1,000,000 for the FY 2012 period was awarded in February 2012. An additional $1,000,000 for the FY 2013 period was awarded in June 2012. At the same time an additional $160,000 was awarded for FY 2012, to support funding for two specific air quality projects recommended by the TCEQ. A call for proposals was released in May 2012. Thirty-two proposals, requesting $5 million in research funding were received. The proposals were reviewed by the ITAC and the TCEQ. The Advisory Council selected 14 projects for funding.

In June 2013, the TCEQ issued Amendment 9 to the AQRP grant.   This amendment had two purposes, 1) it renewed the AQRP for the 2014-2015 biennium (but did not award any funding for that biennium), and 2) it awarded an additional $2,500,000 in FY 2013 funds. Ten percent (10%) of these funds were allocated for Project Administration, and the remaining funds were allocated to the Research program per the terms of the AQRP grant. A portion of the research funds were awarded to the 2012-2013 Discover-AQ Ground Sites Infrastructure Support project, in order to expand logistical support for the Discover-AQ study, at the request of TCEQ and with the Advisory Council's approval.

All 2012 – 2013 research projects were completed by November 30, 2013. The final reports for the projects have been posted to the AQRP website. All FY 2012 funds were fully expended and the remaining FY 2013 funds were held for use on future projects.

After the TCEQ issued Amendment 9 to renew the grant, the AQRP developed the FY 2014/2015 research priorities and submitted them to the ITAC for input and to the TCEQ for review. Funding of $1,000,000 for FY 2014 and $1,000,000 for FY 2015 was awarded via Amendment 10 in October 2013. A call for proposals was released and by the November 22, 2013 due date, 31 proposals requesting $5.8 million in research funding were received. In December and January the ITAC and the TCEQ reviewed the proposals. On February 21, the Advisory Council selected 15 projects for funding, with one project on hold while TCEQ completed their review. These projects were funded with a combination of FY 2013, 2014, and 2015 funds.

In early March 2014, project Principal Investigators (PIs) were notified of the decision of the Advisory Council. AQRP Project Managers and TCEQ Project Liaisons were assigned to each funded project. A kick-off call was held with each project team to discuss the development of the Work Plans which consist of the project scope of work, budget and justification, and quality assurance project plan (QAPP). The TCEQ completed their review of the final projects to be recommended for funding and the Council approved the final project on April 2, 2014.

All projects began work as their Work Plans were approved. In August, the AQRP was notified by the PI of Project 14-023 that the site where the project work was to take place was no longer able to participate in the project and an alternate site could not be located. A decision was made to end Project 14-023 and return the unspent funds to the Research Program account. The TCEQ then performed a relevancy review of the projects that were not funded in the first round, and forwarded a ranking to the AQRP Review Panel, with a recommendation to fund 5 additional projects. The Review Panel concurred with that recommendation. The Advisory Council then reviewed the proposals and approved funding for the 5 additional projects recommended by the Review Panel.

During the period covered by this report, the final agreements were executed with the University of Alabama at Huntsville and George Mason University. All projects (with the exception of 14-023 described above) are in progress. An AQRP Workshop, that will provide updates on on-going research projects, has been scheduled for June 17 and 18, 2015.

BACKGROUND

Section 387.010 of HB 1796 (81st Legislative Session), directs the Texas Commission on Environmental Quality (TCEQ, Commission) to establish the Texas Air Quality Research Program (AQRP).

> Sec. 387.010. AIR QUALITY RESEARCH. (a) The commission shall contract with a nonprofit organization or institution of higher education to establish and administer a program to support research related to air quality.
>
> (b) The board of directors of a nonprofit organization establishing and administering the research program related to air quality under this section may not have more than 11 members, must include two persons with relevant scientific expertise to be nominated by the commission, and may not include more than four county judges selected from counties in the Houston-Galveston-Brazoria and Dallas-Fort Worth nonattainment areas. The two persons with relevant scientific expertise to be nominated by the commission may be employees or officers of the commission, provided that they do not participate in funding decisions affecting the granting of funds by the commission to a nonprofit organization on whose board they serve.
>
> (c) The commission shall provide oversight as appropriate for grants provided under the program established under this section.
>
> (d) A nonprofit organization or institution of higher education shall submit to the commission for approval a budget for the disposition of funds granted under the program established under this section.
>
> (e) A nonprofit organization or institution of higher education shall be reimbursed for costs incurred in establishing and administering the research program related to air quality under this section. Reimbursable administrative costs of a nonprofit organization or institution of higher education may not exceed 10 percent of the program budget.
>
> (f) A nonprofit organization that receives grants from the commission under this section is subject to Chapters 551 and 552, Government Code.

The University of Texas at Austin was selected by the TCEQ to administer the program. A contract for the administration of the AQRP was established between the TCEQ and the University of Texas at Austin on April 30, 2010 for the 2010-2011 biennium, and was renewed in June 2011 for the 2012-2013 biennium and in June 2013 for the 2014-2015 biennium. Consistent with the provisions in HB 1796, up to 10% of the available funding is to be used for program administration; the remainder (90%) of the available funding is to be used for research projects, individual project management activities, and meeting expenses associated with an Independent Technical Advisory Committee (ITAC).

RESEARCH PROJECT CYCLE

The Research Program is implemented through a 9 step cycle. The steps in the cycle are described from project concept generation to final project evaluation for a single project cycle.

1.) The project cycle is initiated by developing (in year 1) or updating (in subsequent years) the strategic research priorities. The AQRP Director, in consultation with the ITAC, and the TCEQ, develop research priorities; the research priorities are released along with a Request for Proposals.

2.) Project proposals relevant to the research priorities are solicited. The Request for Proposals can be found at http://aqrp.ceer.utexas.edu/ .

3.) The Independent Technical Advisory Committee (ITAC) performs a scientific and technical evaluation of the proposals.

4.) The project proposals and ITAC recommendations are forwarded to the TCEQ. The TCEQ evaluates the project recommendations from the ITAC and comments on the relevancy of the projects to the State's air quality research needs.

5.) The recommendations from the ITAC and the TCEQ are presented to the Council and the Council selects the proposals to be funded. The Council also provides comments on the strategic research priorities.

6.) All Investigators are notified of the status of their proposals, either funded, not funded, or not funded at this time, but being held for possible reconsideration if funding becomes available.

7.) Funded projects are assigned a Project Manager at UT-Austin and a Project Liaison at TCEQ. The project manager at UT-Austin is responsible for ensuring that project objectives are achieved in a timely manner and that effective communication is maintained among investigators involved in multi-institution projects. The Project Manager has responsibility for documenting progress toward project measures of success for each project. The Project Manager works with the researchers, and the TCEQ, to create an approved work plan for the project.

   The Project Manager also works with the researchers, TCEQ and the Program's Quality Assurance officer to develop an approved Quality Assurance Project Plan (QAPP) for each project. The Project Manager reviews monthly, annual and final reports from the researchers and works with the researchers to address deficiencies.

8.) The AQRP Director and the Project Manager for each project describe progress on the project in the ITAC and Council meetings dedicated to on-going project review.

9.) The project findings are communicated through multiple mechanisms. Final reports are posted to the Program web site; research briefings are developed for the public and air quality decision makers; and a bi-annual research conference/data workshop is held.

Steps 1 – 9 have all been completed for both the 2010-2011 and 2012 - 2013 biennia. For the 2014-2015 biennium Steps 1 through 6 have been completed. Steps 7-9 are in progress.

PROJECT TIMELINE

During the project period covered by this report (March 1, 2015-May 31, 2015), the following activities took place:

- A Master Agreement with to George Mason University was fully executed.
- Task Orders were executed with the University of Alabama at Huntsville and George Mason University for the 5th additional project (14-022).
- The AQRP Workshop was scheduled for June 17 and 18, 2015, in Austin, Texas.
- Project funding was rebudgeted across fiscal years. Several projects that were previously assigned to FY 14 or FY 15 funds were split between FY 14 or FY 15 and FY 13 in order to ensure the most efficient use of the research funds.
- Several projects requested and were granted extensions to their end dates from June 30, 2015 to no later than September 30, 2015.

RESEARCH PROJECTS

FY 2014- 2015 research project activities are described below for all active projects. Some projects are analyzing the results of the Discover AQ program. A brief description of that program is provided for reference:

Discover AQ

In September of 2013, the DISCOVER-AQ (Deriving Information on Surface Conditions from Column and Vertically Resolved Observations Relevant to Air Quality) program deployed NASA aircraft to make a series of flights with scientific instruments on board to measure gaseous and particulate pollution in the Houston, Texas area. The purpose, for NASA, of this campaign was to better understand how satellites could be used to monitor air quality for public health and environmental benefit.

To complement the NASA flight-based measurements, and to leverage the extensive measurements being funded by NASA to better understand factors that control air quality in Texas, ground-based air quality measurements were made simultaneously by researchers from collaborating organizations, including research scientists and engineers funded wholly or in part by the AQRP and the TCEQ. Because of the opportunity to leverage NASA measurements, projects related to DISCOVER-AQ were a high priority for the 2012-2013 biennium, and analysis of data collected during DISCOVER-AQ was a high priority for the 2014-2015 biennium.

FY 2014 – 2015 Projects

Project 14-002	**STATUS: Active – June 6, 2014**

Analysis of Airborne Formaldehyde Data Over Houston Texas Acquired During the 2013 DISCOVER-AQ and SEAC4RS Campaigns

University of Colorado - Boulder – Alan Fried
University of Maryland – Christopher Loughner
AQRP Project Manager – Gary McGaughey
TCEQ Project Liaison – Jim Smith

Funding Amount: $199,895
($150,508 UC-Boulder, $49,387 U of Maryland)

Executive Summary

During summer months the greater Houston-Galveston-Brazoria Metropolitan Area (HGBMA) often experiences elevated levels of ozone exceeding federal standards, particularly during hot and stagnant wind conditions. Although significant progress has been achieved understanding the major causes of these events over the past 10 years, there are still major unanswered questions related to sources of ozone from highly reactive volatile organic compounds (HRVOC's) emitted by large petrochemical facilities throughout the HGBMA. The toxic trace gas formaldehyde (CH_2O) is produced as an intermediate when these HRVOCs break down in the atmosphere, and ozone and radicals are formed when CH_2O further breaks down. Therefore a comprehensive understanding of CH_2O emissions, photochemical production rates, and transport processes is needed. Unfortunately, despite extensive efforts and advances from past studies, there are still major gaps in understanding related to the importance of directly emitted CH_2O from sources such as petrochemical flaring operations and automotive emissions relative to secondarily produced CH_2O from HRVOCs produced downwind, affecting large geographic areas far removed from the petrochemical facilities. Updating the emission inventories and temporal trends for CH_2O and its HRVOC precursors are two additional areas requiring attention.

To address these issues, a collaborative team, comprised of scientists from the University of Colorado, the University of Maryland, and the NASA Goddard Space Flight Facility, will analyze ambient measurements of CH_2O they acquired on the NASA P3 and DC-8 aircraft during the 2013 DISCOVER-AQ (Deriving Information on Surface Conditions from Column and Vertically Resolved Observations Relevant to Air Quality) and 2013 SEAC^{4}RS (Studies of Emissions and Atmospheric Composition, Clouds and Climate Coupling by Regional Surveys) studies, respectively.

The analysis will rely on the Community Multiscale Air Quality (CMAQ) model with Process Analysis, in very high-resolution mode (1 km resolution), driven by the WRF (Weather Research and Forecasting) meteorological model. The analysis will begin by identifying favorable time periods, such as Sept. 25, 2013, when sampling large petrochemical and refinery plumes under favorable meteorological conditions as well as other clearly identifiable sources (e.g., ship plumes, etc.) close to their source and downwind. The high resolution WRF-CMAQ model results will be compared with observations downwind at various times to arrive at updated emission rates for CH_2O and to help in validating the model meteorology and chemistry. The CMAQ model will be run in the Process Analysis Mode to quantify the relative importance of

the major CH_2O sources. The analysis will conclude with an effort to compare select airborne CH_2O measurements with 24-hour averaged cartridge measurements acquired by The Texas Commission on Environmental Quality (TCEQ) every 6th day at the Clinton, Deer Park and Channelview sites as a means to further validate and/or provide error bounds, for such long-term CH_2O data in the greater HGBMA.

Project Update

The Community Multi-scale Air Quality (CMAQ) modeling effort at 4 and 1-km resolutions have been completed, and we have embarked on efforts this quarter to: 1) employ this modeling capability in conjunction with the NASA P3 aircraft measurements to determine the relative contributions to the formaldehyde (HCHO) levels observed in the greater Houston Metropolitan from direct emissions, particularly from petrochemical flaring operations, relative to secondary photochemical production; and 2) improve facility emission estimates of HCHO and its highly reactive precursors ethene and propene, when isolated industrial plumes can be identified. Both efforts are in their formative stages, and will be presented in subsequent reports. This report instead focuses on a more detailed examination of the accuracy and limitations of the CMAQ HCHO modeling results. The panels of Figures 1 show daily composite HCHO biases (CMAQ-Measurements) for the planetary boundary layer (PBL) and the free troposphere (FT).

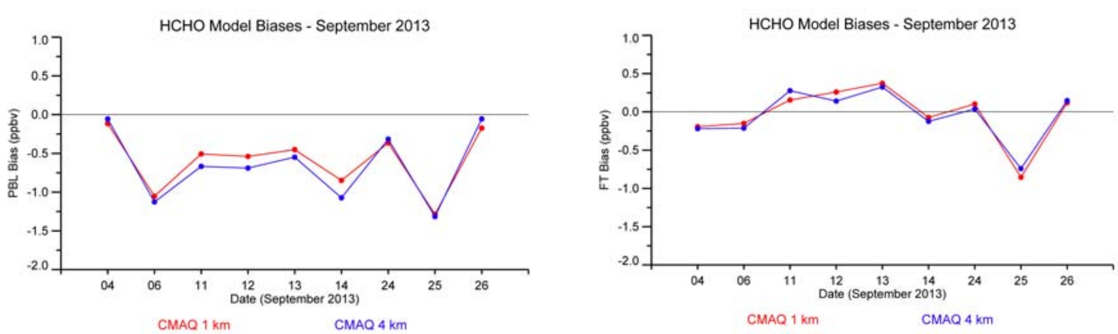

Figure 1: Average HCHO model bias from the new 1 and 4 km CMAQ simulations as compared to P-3B observations on each flight day within the PBL (left) and FT (right).

Although useful for providing an overview, such plots do not reveal the temporal and spatial behavior for the model-measurement comparisons. In this report, we examine in greater detail comparisons for select time periods on September 13 and September 25. As can be seen, the former exemplifies typical results for many of the days studied, while the latter illustrates results from extreme petrochemical emission events from the Baytown Exxon/Mobil and Deer Park facilities later in the month.

Figure 2 shows this comparison for the 2nd P3 circuit on September 13. It is important to note that in contrast to model results, which calculate relatively constant 5-minute average HCHO concentrations in ± 1km grid boxes, the 1-second P3 HCHO measurements often reflect large changes in airmasses as the P3 traverses ~ 0.1km each second. This results in large measurement variance compared to model results. To facilitate comparisons, the longer temporally and spatially-averaged model results are determined at each 1-second P3 sampling time. Although the true variance is smoothed out in the model, one can still compare results for select time periods for a given spatial region with common sources at relatively constant altitudes. In Figures 2& 3, these time periods are denoted by dark horizontal traces, where the blue and red lines respectively represent the average HCHO measurement and CMAQ model results. These traces are only meant to graphically show the overall biases for the select time periods. The actual (CMAQ-Measurement) biases are determined by point-to-point differences over the select time periods and these values along with their standard deviations are given in the plots. As can be seen, although there are differences, the measurements and model values follow the same overall trends. Fig. 2 shows 4 FT and 3 PBL time periods for comparison. Combining the 3 PBL legs yields an average overall (CMAQ-Measurement) difference of -705 ± 158 pptv (-17% ± 4%), which we attribute to low biases in HCHO and its precursor emission sources employed as input in the CMAQ model. Our follow up studies will attempt to address this. These values are slightly different than Fig. 1 since these are a subset of the Fig. 1 dataset. Not surprising, the largest bias occurs during the PBL leg from Smith Point to Moody Tower over Galveston Bay and the Houston Ship channel, where many of the petrochemical facilities are located. The corresponding PBL comparisons for CO yield a much smaller (CMAQ-Measurement) bias of -2.8 ± 1.5 ppbv (-2.2% ± 1.2%), which supports the veracity of the CMAQ model results both in terms of CO emissions and transport. By contrast, three of the four FT comparisons for both HCHO (CMAQ-Measurement = 660 ± 250 pptv) and CO (CMAQ-Measurement = 39.8 ± 2.0 ppbv, 50.5% ± 1.4%) suggest a problem in the FT CMAQ calculations, perhaps in the transport from the PBL to the FT during this day.

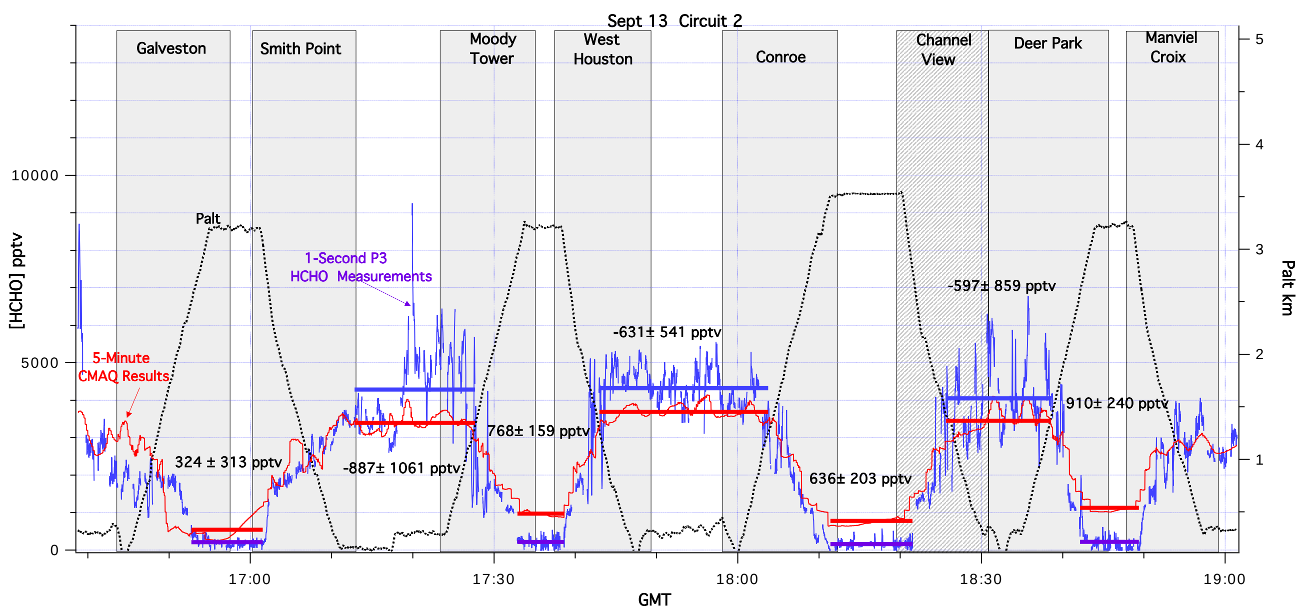

Figure 2: P3 HCHO measurements (1second data, blue trace) and 5-minute CMAQ model results (red trace) for the 8 spiral sites during the 2nd circuit of the September 13, 2013 DISCOVER-AQ flight. The dark horizontal blue and red traces are averaged values over the select PBL and FT time periods, with the resultant point-by-point average (CMAQ-Measurement) differences and standard deviation given for each period.

Figure 3 shows the corresponding plot for the 1st circuit of Sept. 25, which is a day with significant petrochemical emissions of HCHO (due to flaring) and its highly reactive precursors ethene and propene, as well as significant photochemical production of HCHO downwind. The results for the select periods shown in Fig. 3 for this day (4 FT legs, and 4 PBL legs) are significantly different than Sept. 13. The composite PBL results yield an average point-by-point HCHO (CMAQ-Measurement) difference of -5025 ± 4492 pptv (-45% ± 32%) and a corresponding CO difference of -124 ± 53 ppbv (-42% ± 9%), values that reflect significant petrochemical emissions that are not accounted for in the CMAQ emissions input for both HCHO and CO. With the exception of the Smith Point PBL leg (during this 1st circuit), the remaining 3 PBL legs over the Baytown Exxon/Mobil complex, over central Houston, and over the Deer Park Shell facility, all show significant model negative biases, with the largest bias over the Exxon/Mobil facility, where we have evidence of a flaring event. The 4 FT legs of Fig. 3 also show different behavior than Sept. 13. In contrast to the potential CMAQ transport issue discussed, the FT comparisons of Sept. 25 yield excellent agreement for both HCHO (average (CMAQ-Measurement) = -14 ± 57 pptv, -2% ± 18%) and CO (average (CMAQ-Measurement) = 11 ± 2 ppb, 13% ±2%).

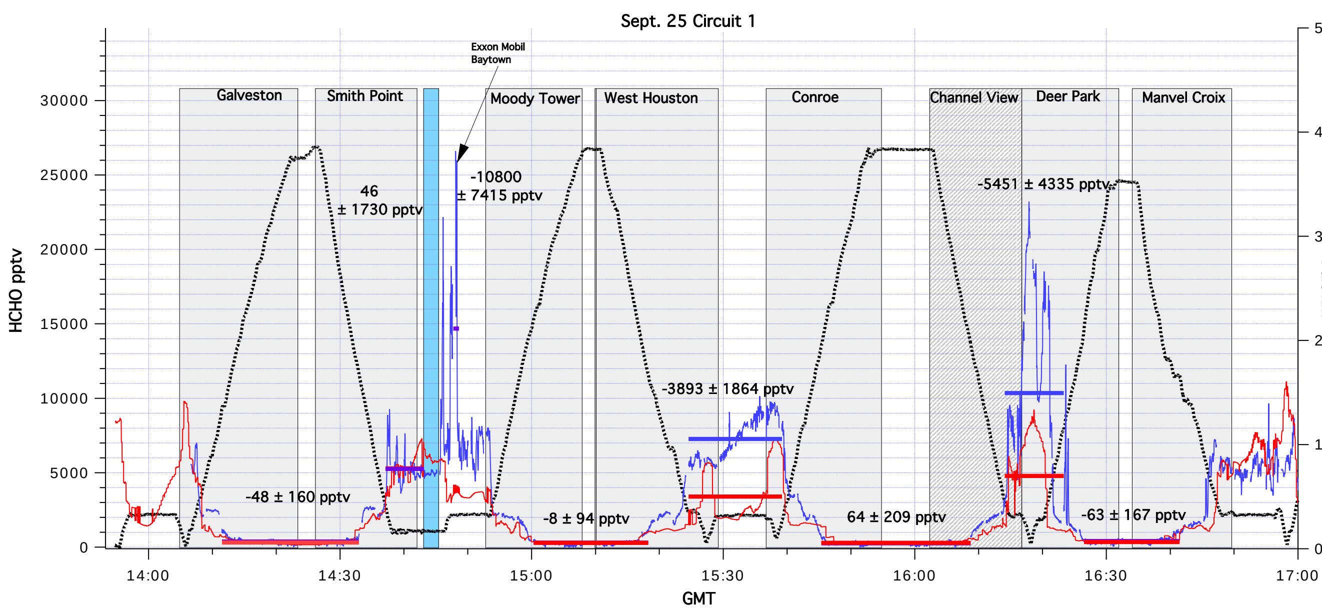

Figure 3: P3 measurements and CMAQ model results for Sept. 25, 2013 in the same format as Fig 2. This time period accentuates emission inventory biases.

In addition to the two aforementioned efforts discussed at the beginning of this report, our efforts in the near term will also: 1) present an analysis of P3 and 24-hour CMAQ modeling data over the Deer Park DNPH cartridge sampling facility on Sept. 13 as one means to assess the accuracy of the DNPH cartridge measurements; and 2) further examine HCHO (CMAQ-Measurement) biases in an attempt to understand the differences noted above for the FT.

Project 14-003	STATUS: Active – May 28, 2014

Update and evaluation of model algorithms needed to predict Particulate Matter from Isoprene

University of North Carolina – Chapel Hill – William Vizuete

AQRP Project Manager – Elena McDonald-Buller
TCEQ Project Liaison – Jim Price

Funding Amount: $200,000

Executive Summary

Terrestrial vegetation emits into the atmosphere large quantities (~500 teragrams C) of the reactive di-olefin isoprene (C_5H_8). Isoprene emissions in eastern Texas and northern Louisiana are some of the largest in the United States. Photochemical oxidation of isoprene leads to significant yields of gas-phase intermediates that contribute to fine particulate matter (PM2.5). The production of isoprene-derived PM2.5 is enhanced when mixed with anthropogenic emissions from urban areas like those found in Houston. To predict PM production from isoprene requires fundamental parameters needed to describe the efficiency with which gas phase intermediates react on the surface of atmospheric particles. Recently, EPA updated a regulatory chemical mechanism to include the formation of these new gas-phase isoprene-derived intermediates. Furthermore, the project investigators recently collaborated with the EPA to update the CMAQ model to predict isoprene-derived PM explicitly across the eastern US. This updated gas- and aerosol-phase framework found in CMAQ remains to be validated against systematically conducted chamber experiments. Thus, we first will conduct a series of new experiments at UNC to quantitatively measure the reactive uptake of the two predominant isoprene-derived gas phase intermediates to PM of different inorganic compositions. By providing these new fundamental measurements, we will be able to more directly evaluate the aerosol-phase processes added to the model. This work will produce a model evaluation of isoprene SOA formation against existing UNC outdoor smog chamber experiments. This project will also deliver performance data needed to bound uncertainties in key parameters used by CAMx to predict isoprene derived PM. This work directly addresses the stated priority area of investigating the transformation of gas-phase pollutants to particulate matter that impact Texas air quality.

Project Update

Project activities are described by task number below.

1. Integration of Gas-Phase Epoxide Formation and Subsequent SOA Formation into UNC MORPHO Box Model

This task is complete. The study team members are confident in the QA/QC testing of the algorithms for the predicted uptake of gaseous IEPOX onto an aerosol of variable acidity, temperature, and relative humidity. They have generated simulations necessary for QA of data from the model including the predicted bulk SOA formation in our indoor chamber using reactive uptake coefficients we recently derived in flow tube studies (Gaston et al., 2014, ES&T).

2. Synthesis of Isoprene-derived Epoxides and Known SOA Tracers
All syntheses needed for the project including the generation of the QA/QC data are complete.

3. Indoor Chamber Experiments Generating SOA Formation Directly from Isoprene-Derived Epoxides
Table 1 shows the experiments that are now completed. Processing and quality assuring the data collected from the completed experiments is nearly finalized.

Table 1. Indoor experiments to be conducted at UNC.

Expt. #	Epoxide	[Epoxide] (ppb)	Seed Aerosol Type	Initial Seed Aerosol ($\mu g/m^3$)	RH (%)	T (^oC)
1	IEPOX	300	$(NH_4)_2SO_4$	~20-30	~50-60	~20-25
2		300	$(NH_4)_2SO_4$ + H_2SO_4	~20-30	~50-60	~20-25
3	MAE	300	$(NH_4)_2SO_4$	~20-30	~50-60	~20-25
4		300	$(NH_4)_2SO_4$ + H_2SO_4	~20-30	~50-60	~20-25
5	none		$(NH_4)_2SO_4$	~20-30	~50-60	~20-25
6	none		$(NH_4)_2SO_4$ + H_2SO_4	~20-30	~50-60	~20-25
7	IEPOX	300	none	none	~50-60	~20-25
8	MAE	300	none	none	~50-60	~20-25

0.6 M (NH4)2SO4 + 0.6 M H2SO4

4. Modeling of Isoprene-derived SOA Formation From Environmental Simulation Chambers
The first modeling analysis has resulted in a published manuscript in Environmental Science & Technology Letters entitled "Heterogeneous Reactions of Isoprene-Derived Epoxides: Reaction Probabilities and Molar Secondary Organic Aerosol Yield Estimates." For this task the team has completed modeling to constrain two uncertain parameters central to SOA formation from isoprene-derived gas phase precursors:

(1) Rate of epoxide heterogeneous uptake to the particle phase

(2) Molar fraction of gas phase precursors that are reactively taken up and contribute to SOA (ϕ_{SOA}).

Flow reactor measurements of the *trans*-β-isoprene epoxydiol (*trans*-β-IEPOX) and methacrylic acid epoxide (MAE) aerosol reaction probability (ɣ) were completed on atomized aerosols with compositions similar to those used in chamber studies. Observed ɣ ranges for *trans*-β-IEPOX and MAE were 6.5×10^{-4}–0.021 and 4.9×10^{-4}–5.2×10^{-4}. Through the use of a time-dependent chemical box model initialized with chamber conditions and the ɣ measurements, ϕ_{SOA} for *trans*-β-IEPOX and MAE on different aerosol compositions was estimated between 0.03–0.21 and 0.07–0.25, with MAE ϕ_{SOA} showing more uncertainty.

It is unclear how ɣ and ϕ_{SOA} are affected when a significant fraction of S_a is represented by epoxide-derived SOA. This warrants further investigation as it could be relevant in regions like eastern Texas during summer where isoprene SOA can account for a substantial portion of $PM_{2.5}$ mass and therefore S_a. The results presented here, and in a previous study,[Gaston] which constrain all reactions contributing to IEPOX- and MAE-derived SOA, could be beneficial in regional and/or global models to help constrain predictions of IEPOX- and MAE-derived SOA, especially since only a few known aqueous-phase reaction rates constrain current models.

The study team is currently finalizing the most recent results for a manuscript for publication and will also provide those findings in the final report to AQRP.

All funds allocated to the project are intended to be utilized by June 30, 2015.

Reference

Gaston, Cassandra J., Riedel, Theran P., Zhang, Zhenfa, Gold, Avram, Surratt, Jason Douglas, and Thornton, Joel A.; "Reactive Uptake of an Isoprene-derived Epoxydiol to Submicron Aerosol Particles" Environ. Sci. Technol. 2014, 48, 11178−11186. http://pubs.acs.org/doi/abs/10.1021/es5034266

Project 14-004	STATUS: Active – June 20, 2014

Emission Source region contributions to a high surface ozone episode during DISCOVER-AQ

University of Maryland – Christopher Loughner
Morgan State University – Melanie Follette-Cook
AQRP Project Manager – Gary McGaughey
TCEQ Project Liaison – Doug Boyer

Funding Amount: \$109,111
(\$55,056 Univ. of Maryland, \$54,055 Morgan State Univ.)

Executive Summary

The highest ozone air pollution episode in the Houston, TX region in 2013 occurred September 24-26, which coincided with the DISCOVER-AQ (Deriving Information on Surface Conditions and Vertically Resolved Observations Relevant to Air Quality) field campaign. The maximum 8-hour average ozone peaked on September 25 at LaPorte Sylvan Beach reaching 124 ppbv. We will analyze this air pollution episode to quantify how emissions from various source regions (i.e., Houston, Dallas, Beaumont/Port Arthur, Lake Charles, LA, Oklahoma, etc.) contributed to Houston's poor air quality. This work will examine the importance of regional emissions and transport on local air quality.

The investigators will use a combination of model simulations and space-, aircraft-, and ground-based observations to investigate the roles of both regional transport and local emissions on air quality in Houston, TX for this event. This work will improve understanding of ozone formation and accumulation by examining the spatial patterns of emissions within and outside of Texas and the transport processes that contributed to high ozone in Houston.

The investigators will use Weather Research and Forecasting (WRF) and Community Multi-scale Air quality (CMAQ) model output along with ground- and aircraft-based observations obtained during the DISCOVER-AQ field campaign to identify plumes that entered the Houston metropolitan area and contributed to high surface ozone concentrations. The investigators will identify the origins of plumes by calculating back trajectories from the WRF simulation. CMAQ simulations performed with source apportionment will be analyzed to determine the contributions of various source regions on surface ozone concentrations in the Houston metropolitan area. In addition, satellite observations (Ozone Monitoring Instrument (OMI) tropospheric nitrogen dioxide, OMI ozone profiles, Measurement Of Pollution In The Troposphere (MOPITT) carbon monoxide, and Moderate Resolution Imaging Spectrometer (MODIS) and Visible Infrared Imaging Radiometer Suite (VIIRS) aerosol optical depth) will be analyzed to determine if they were able to detect the regional transport of air pollution and subsequent buildup in the Houston metropolitan area.

Project Update

As discussed in the previous quarterly report, we used improved model inputs and a new modeling technique to improve WRF and CMAQ simulations of the Houston surface ozone episode in late September 2013. Back-trajectories calculated from the improved 4 km WRF model output initialized over LaPorte Sylvan Beach on September 25 and 26 at 2 PM CST are shown in Figures 1 and 2. The September 25 back-trajectory shows transport from the Dallas metropolitan area and the September 26 back-trajectory shows transport from the Beaumont, TX/Lake Charles, LA area. Based on this analysis, we identified the following regions to select for an ozone source apportionment simulation: 1) Houston; 2) Dallas; 3) Beaumont; 4) Lake Charles; 5) marine areas; and 6) remaining areas. A CMAQ simulation with ozone source apportionment has been completed and results are being analyzed to quantify how anthropogenic emissions from these source regions impacted surface ozone in the Houston metropolitan area on September 25 and September 26.

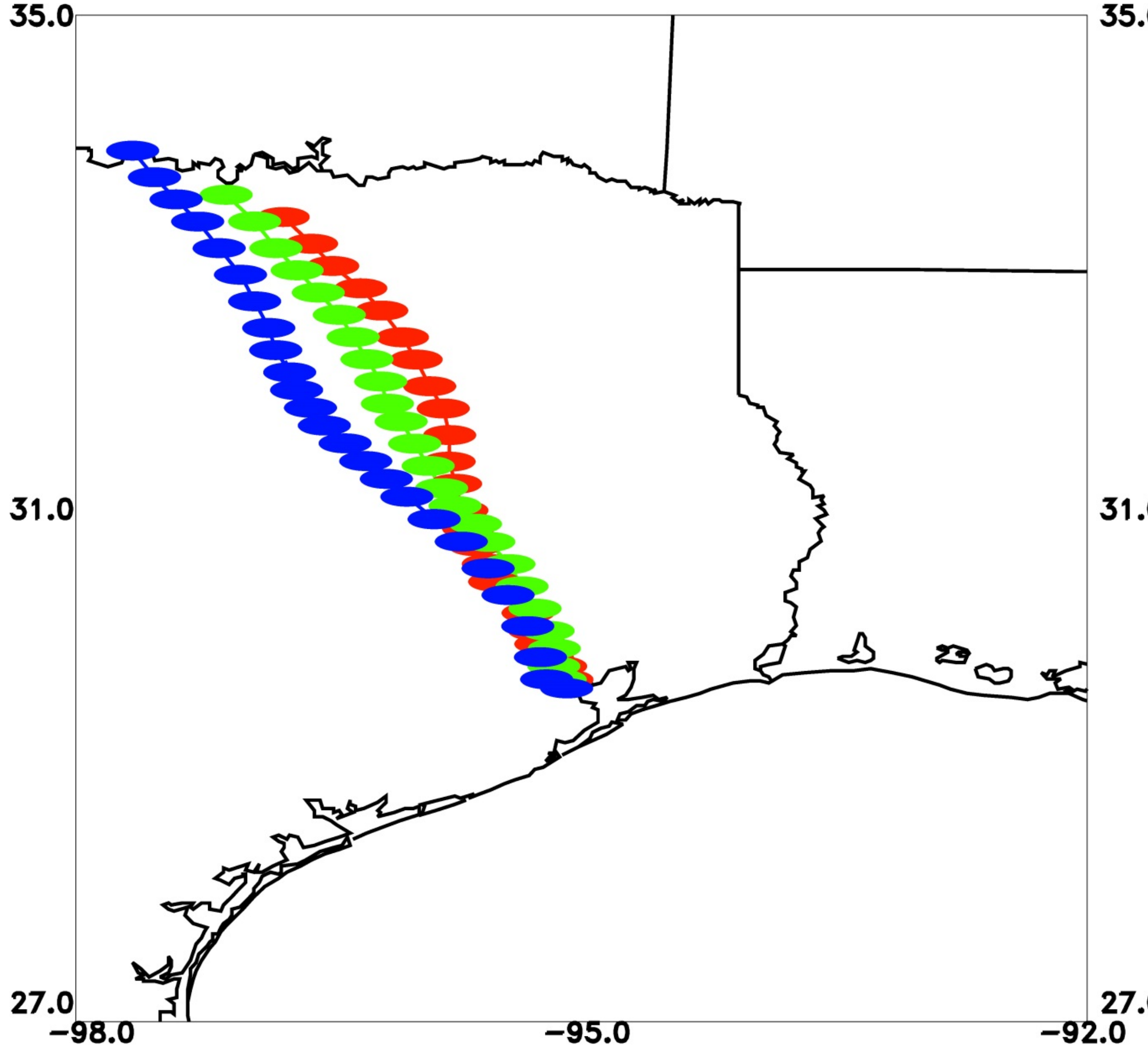

Figure 1: 24 hour back trajectories from 4 km WRF output initialized at 2 pm CST September 25 over La Porte Sylvan Beach at 0.5 km (red), 1.0 km (green), and 2.0 km (blue) AGL. Trajectories pass over Dallas.

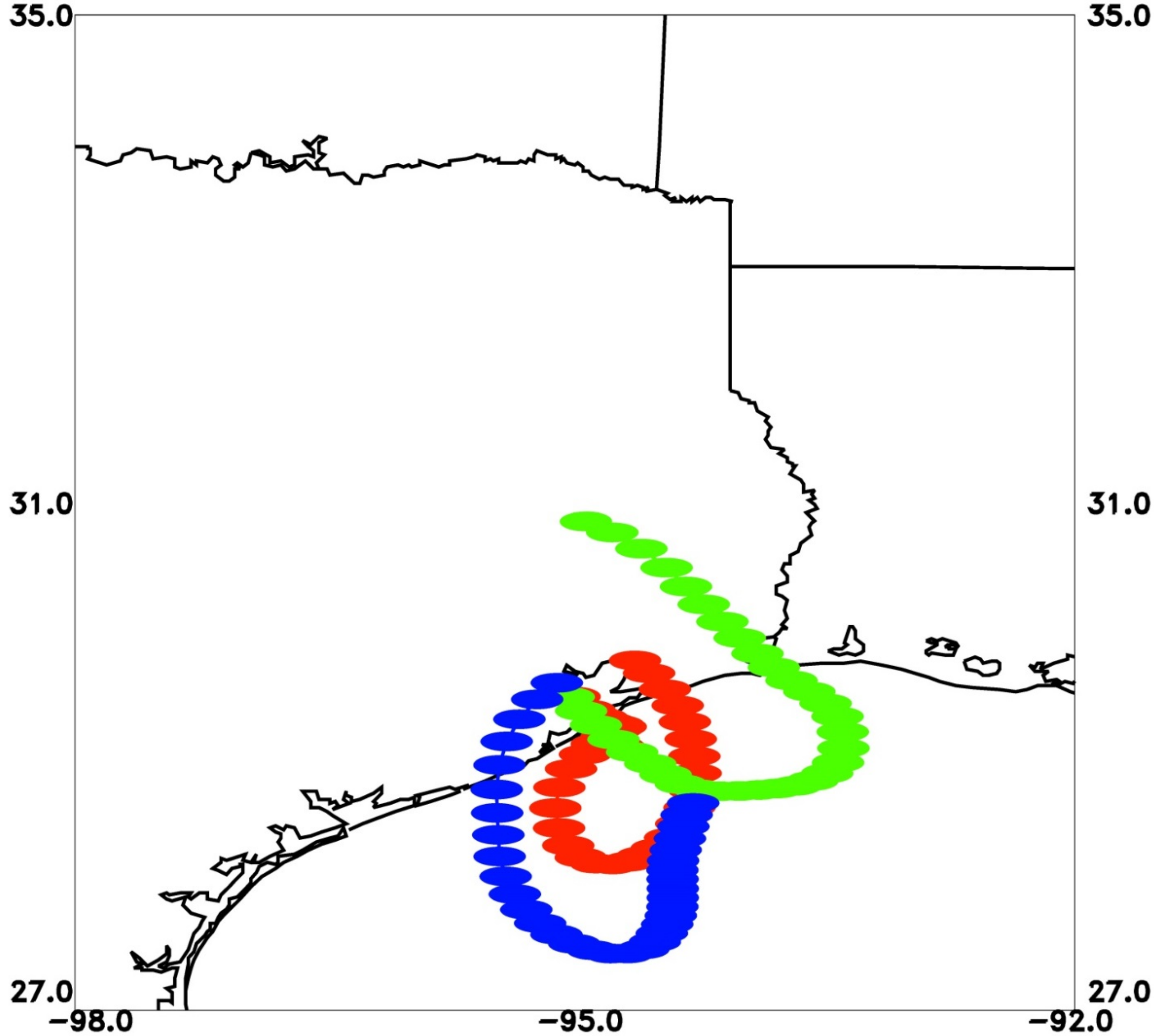

Figure 2: 33 hour back trajectories from 4 km WRF output initialized at 2 pm CST September 26 over La Porte Sylvan Beach at 0.5 km (red), 1.0 km (green), and 2.0 km (blue) AGL. Trajectories show recirculation of local air and transport from Beaumont, TX / Lake Charles, LA area.

Project 14-005	STATUS: Active – February 5, 2015

Sources and Properties of Atmospheric Aerosol in Texas: DISCOVER-AQ Measurements and Validation

Texas A&M – Sarah Brooks

AQRP Project Manager – Vincent Torres
TCEQ Project Liaison – Jim Price

Funding Amount: $103,890

Executive Summary
Tropospheric air quality is degraded by local aerosol sources and gas phase precursors as well as aerosol transported over long distances. While the availability of recent satellites such as the Moderate-resolution Imaging Spectroradiometer (MODIS) and the Cloud-Aerosol Lidar with Orthogonal Polarization (CALIOP) offer improved accuracy and global coverage of aerosol, such measurements still rely on broad assumptions in determination of aerosol source and composition. During the fall of 2013, the Houston area was the site of the 2nd field intensive of the NASA Deriving Information on Surface conditions from COlumn and VERtically Resolved Observations Relevant to Air Quality (DISCOVER-AQ) campaign. During DISCOVER-AQ, this project's research team operated a new scattering instrument, the Cloud and Aerosol Spectrometer with Polarization (CASPOL), which measures the depolarization ratio of individual particles in the aerosol population. The polarization capabilities of CASPOL facilitate an effective approach to validate space-borne aerosol retrieval, particularly CALIOP aerosol type classification. The CASPOL was operated on top of the 60 m tall Moody Tower (MT) on the University of Houston campus, a central urban location and site of many complementary measurements during DISCOVER-AQ. In this study, the CASPOL data set will be analyzed to determine the concentration, size distribution, and optical properties of aerosol from the wide variety of sources, including urban pollution sources from downtown Houston, the industrial Ship Channel, and transported aerosol. Combined with additional measurements of organic carbon, black carbon and ozone, the CASPOL data set provides an opportunity to determine the primary aerosol sources and impacts of aging due to ozone modified aerosol optical properties. These in-situ data will be compared to MODIS and CALIOP aerosol measurements to determine the sensitivity of remote sensing to changes in surface aerosol properties and air quality. Results from the project will improve the linkage between column observations provided by satellite instruments and near-surface atmospheric composition, which is relevant to air quality and human health in the short term and the relationship between future air quality and climate.

Project Update
Project activities are described by task number below.

1. CASPOL Data Collection and Quality Control.
From August 28 through October 4, 2013, the CASPOL was located on top of the Moody Tower, at 29.7176° N, -95.3414° W, approximately four kilometers south of downtown Houston, Texas. The inlet was located on top of the building which is ~70 meters tall. This height is low enough that the aerosols being sampled are representative of the aerosols at the surface, but tall enough to allow for substantial mixing. This tower has been the location of many previous and current

field campaigns (Brooks et al., 2010; Lefer et al., 2010; Rappenglück et al, 2010; Wong et al., 2011). During the first quarter of this project, all CASPOL data collected during DISCOVER-AQ was quality controlled. Data collected during and after precipitation events have been eliminated from the data set. Periods during which the CASPOL was operating offline for maintenance, drying, or flow testing have also been removed.

2. Separation of All Data-Controlled CASPOL Data According to Source Location.
There are 4 major sources of aerosols characterizing the air masses arriving at the Moody Tower. Sources include the Houston Ship Channel, a heavily industrialized area on the east side of Houston, the densely populated urban center of Houston, a marine source, which consists of transported aerosols from the Gulf of Mexico and potentially further (Goudie and Middleton, 2001), and aerosol from the less densely populated or semi-urban zones of Southwest Houston. Conveniently, these sources come from four different wind directions relative to the Moody Tower. The NOAA, Atmospheric Resources Laboratories Hybrid Single Particle Lagrangian Integrated Trajectory (HYSPLIT) model (Draxler and Hess, 1997, 1998; Draxler et al., 1999) was used to create five day back trajectories with one hour intervals using Global Data Assimilation (GDAS) model data with 0.5 degree resolution for all CASPOL data. All CASPOL data was then classified as Ship Channel cases, Urban cases, and Ocean aerosol type, according to the back trajectories. No Semi-Urban/Rural air masses were identified during the time period of the campaign.

A technique for identifying particle type by the patterns in plotted optical properties for ensembles of sampled particle was developed by Glen and Brooks (2013). To create the patterns, referred to here as scattering signatures, the backscatter intensity and depolarization ratio data for all particles observed in a time segment are first discretized. The depolarization ratio is plotted on the x axis, and the backscatter intensity on the y axis. Next, the frequency of particles that have intersecting values of depolarization ratio and backscatter intensity are placed at each intersection. In Figure 1, the composite scattering signatures of all of the data from each of the three sources are shown. The color of each intersecting value indicates the percentage of particles at that intersecting value. The Ocean/Transported case has the strongest backscatter intensity, approaching 400, and is the most depolarizing. The data collected under the Ship Channel conditions (Figure 1B) is slightly depolarizing but the backscatter intensity is around half of the Ocean data at around 210. The Urban data has an even lower backscattering intensity of 200 and is the least depolarizing at approximately 0.1 (Figure 1C).

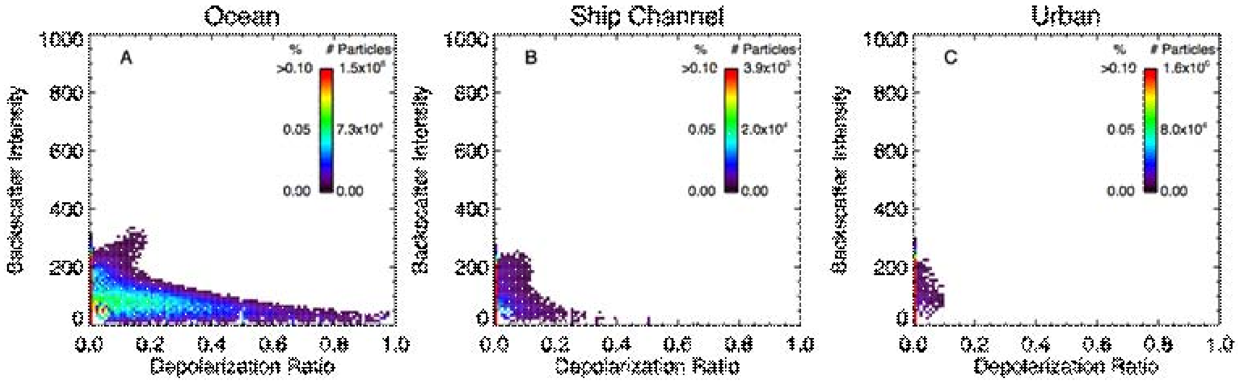

Figure 1. The scattering signatures for all of the data in the Ocean, Ship Channel, and Urban sources.

Each of these scattering signatures is unique in shape from the others. By using this scattering signature technique, the CASPOL can distinguish aerosol source regions in the Houston area. The CASPOL's ability to distinguish aerosol source shows that a potential exists for the CASPOL to be a useful tool in air quality monitoring. Provided that a significant number of particles have been detected ($\sim 10^6$), an optical signature can be generated and the dominant aerosol type may be assigned. For each satellite comparison, the CASPOL data was sorted combing all data collected 4 hours before and after each satellite overpass time, and generating an optical plot from each data set. This ensures that a sufficient number of particles are available to generate high quality optical signature plots.

<u>3. Data summary table for time periods in which satellite and in-situ data are collocated.</u>

MODIS - CASPOL Comparison
Simultaneous comparisons of MODIS aerosol optical depth (AOD) retrievals (Collection 6) and CASPOL aerosol settings are reported in Table 1. MODIS data is available from the instrument available on the Terra satellite and a second on the Aqua satellite. The Terra satellite passes the Houston areas near 12:00 pm Central Daylight Time (CDT). The Aqua satellite passes the Houston areas in the afternoon, ~around 15:00 CDT. The ground-based AErosol RObotic NETwork (AERONET) has been used to validate satellite aerosol retrievals in previous studies. There is an AERONET site located at the Moody Tower (Univ_of_Houston, 29.7178°N, 95.0428°W). Hence, for additional comparison, we include AERONET AOD from this location in Table 1.

In the existing MODIS algorithm (Collection 6), MODIS aerosol types are chosen based on location and season. Naturally, the actual aerosol population may vary during this season, and therefore such aerosol type settings may not be accurate for all the retrievals. We found that for all the cases in Table 1 and 2, the MODIS aerosol retrieval algorithm, the fine mode aerosol type assignment was "weakly absorbing". This study an example where there is likely a need for a more detailed typing decision tree incorporated into the MODIS analysis. The CASPOL data types may better represent the actual aerosols and may improve MODIS aerosol retrievals.

The results in Table 1 show that MODIS aerosol optical depth (AOD) retrievals over the Houston urban area are overestimated compared to the AERONET in nine of the ten cases (with a 1% significance level). So, while the MODIS treats all cases as weakly absorbing, fine-tuning this would lead to MODIS AODs which are further from, rather than more similar to, AERONET. Our intent was to test whether the agreement between MODIS AOD and AERONET AOD varied between air mass types as determined by the CASPOL. However, in the collocated MODIS-CASPOL data sets in Table 1 and 2, there are only 2 Ship Channel cases, and 1 Urban case. Hence we will need a revised approach for comparing CASPOL to MODIS.

Table 1. Collocated MODIS (Terra) and CASPOL Data

Date	Time (CDT)	Terra AOD (Aerosol Optical Depth)	AERONET AOD	CASPOL Aerosol Type
6 September	12:30	0.262	0.233	Ship Channel
8 September	12:20	0.278	0.105	Transported
13 September	12:34	0.312	0.203	Urban
22 September	12:29	0.098	0.050	Transported
25 September	11:24	0.152	0.090	Transported
26 September	12:04	0.133	0.060	Transported

Table 2. Collocated MODIS (Aqua) and CASPOL Data

Date	Time (CDT)	Aqua AOD	AERONET AOD	Aerosol Type
12 September	15:05	0.100	0.103	Ship Channel
18 September	14:30	0.146	0.103	Transported
25 September	14:35	0.132	0.119	Transported
26 September	15:20	0.137	0.086	Transported

CALIOP - CASPOL Comparison

To compare CASPOL to the available CALIOP data sets, we resort the CASPOL data combining all data collected 4 hours before and after each satellite overpass time as we did above for MODIS collocation. Rather than compare CALIOP identified aerosol type directly with the CASPOL aerosol type, we compared the depolarization measured by CASPOL to the CALIOP depolarization ration product. In each case, the CALIOP DRP is the mean of all in the lower troposphere along the 50 km segment. In Table 3, the latitudes and longitudes are the locations of the nearest profiles to the Moody Tower. The distance is the horizontal distance between each of the nearest profiles to Moody Tower in km. The CALIOP DPR on 16 September is not available, because no aerosol layer is identified by CALIOP within the corresponding 50 km segment. The differences between CASPOL and CALIOP depolarization ratios for the other three cases are 0.0018, -0.0087, and -0.0065, one order of magnitude less than the theoretical results. The largest absolute difference among the three cases is present on 23 September, in which the track of the CALIOP is farthest to Moody Tower.

Table 3. Cases of Collocated CASPOL and CALIOP

Date	Latitude	Longitude	Distance (km)	CALIOP DPR	CASPOL DPR	CASPOL Backscatter Intensity
11 Sep	29.85	-96.08	73.07	0.014	0.016	64.8
16 Sep	29.81	-94.95	39.33	NA	0.026	40.2
23 Sep	29.51	-96.38	102.89	0.013	0.005	60.1
27 Sep	29.85	-96.04	68.98	0.014	0.007	60.9

*NA is short for not available.

As seen in Table 3, 4 cases of collocated CASPOL and CALIOP are available during DISCOVER-AQ, and in one of these, the CALIOP reports that the value of depolarization ratio is too small to be reported. Based on the low number of data collocated sets available, it is difficult to make a reliable comparison. At this time, we are investigating alternative approaches.

In conclusion, an adequate number of cases (10) of collocated MODIS and CASPOL data have been found. Additional analysis will include further analysis of data collected during these time periods, including CASPOL mean backscattering, mean depolarization ratio, particle size distribution, and derived fine mode fraction and MODIS derived fine mode fraction. In contrast, there are not enough cases in which CASPOL data is available for 8 continuous hours centered on the CALIOP overpass. Therefore, no strong conclusions can be drawn from these data. The 8 hour time requirement was chosen to be consistent with the initial MODIS-CASPOL comparisons and is specifically required for the generation of CASPOL optical signatures. However, CASPOL depolarization ratios require less data points than optical scattering signatures. Thus, in the future we will attempt to compare CALIOP to shorter segments of CASPOL data. We hope that modifying this requirement will provide a larger number of CASPOL-CALIOP cases for comparison.

Deliverables:

Task 1 Deliverables: (Task 1 was completed during the first quarter.)

A file has been produced for each day which contains for all quality controlled data collected that day CASPOL time, total particle number, size distribution. Next, the data was classified according to source location. For each period in which the CASPOL continuously sampled under constant source conditions, a file was created containing single particle backscattering, and depolarization data, which was used to generate optical signature plots in Task 2 below.

Task 2 Deliverable: Task 1 was initially completed during the first quarter. However, Task 2 was revisited and modified during the second quarter, once it was realized that the CASPOL data time periods must be chosen based on satellite overpass times.

HYSPLIT back trajectories have been run for all quality controlled CASPOL DATA. Based on the back trajectories, all CASPOL data has been sorted into categories, i.e. urban pollution, industrial pollution from the Ship Channel, or transported aerosol. From these files, CASPOL data from has been used to generate optical signature plots (backscattering vs. depolarization) for each time period of data of 6 or more continuous hours of CASPOL data collected in a single category.

Task 3. Summary table of time periods in which satellite and in-situ data are collocated.

3A. Summary table of time periods in which MODIS, and CASPOL are collocated. AERONET data is also included for each time (Table 1 above).

3B. Summary table of time periods in which CALIOP and in-situ data are collocated.

References Cited:

Brooks, S., Luke, W., Cohen, M., Kelly, P., Lefer, B., and Rappengluck, B.: Mercury species measured atop the Moody Tower (TRAMP) site, Houston, Texas, Atmospheric Environment, 44, 4045 – 4055, doi: http://dx.doi.org/10.1016/j.atmosenv.2009.02.009

Draxler, R. R. and G.D. Rolph. (2003), HYSPLIT (Hybrid Single-Particle Lagrangian Integrated Trajectory) model, Air Resource Laboratory, NOAA, Silver Spring, Md. (Available at http://www.arl.noaa.gov/ready/hysplit4.html).

Eck, T., B. Holben, J. Reid, O. Dubovik, A. Smirnov, N. O'Neill, I. Slutsker, and S. Kinne (1999), Wavelength dependence of the optical depth of biomass burning, urban, and desert dust aerosols, *Journal of Geophysical Research: Atmospheres (1984–2012)*, *104*(D24), 31333-31349.

Glen, A. and Brooks, S. D.: A new method for measuring optical scattering properties of atmospherically relevant dusts using the Cloud and Aerosol Spectrometer with Polarization (CASPOL), Atmospheric Chemistry and Physics, 13, 1345–1356, 2013.

Goudie, A. and Middleton, N.: Saharan dust storms: nature and consequences, Earth-Science Reviews, 56, 179–204, 2001

Lefer, B., Rappenglück, B., Flynn, J., and Haman, C.: Photochemical and meteorological relationships during the Texas-II Radical and Aerosol Measurement Project (TRAMP), Atmospheric Environment, 44, 4005 – 4013, doi:http://dx.doi.org/10.1016/j.atmosenv.2010.03.011, 2010.

Quinn, P., Coffman, D., Kapustin, V., Bates, T., and Covert, D.: Aerosol optical properties in the marine boundary layer during the First Aerosol Characterization Experiment (ACE 1) and the underlying chemical and physical aerosol properties, Journal of Geophysical Research: Atmospheres (1984–2012), 103, 16 547–563, 1998.

Rappenglück, B., Dasgupta, P. K., Leuchner, M., Li, Q., and Luke, W.: Formaldehyde and its relation to CO, PAN, and SO_2 in the Houston-Galveston airshed, Atmospheric Chemistry and Physics, 10, 2413–2424, doi:10.5194/acp-10-2413-2010, 2010.

Wong, K. W., Oh, H.-J., Lefer, B. L., Rappenglück, B., and Stutz, J.: Vertical profiles of nitrous acid in the nocturnal urban atmosphere of Houston, TX, Atmospheric Chemistry and Physics, 11, 3595–3609, doi:10.5194/acp-11-3595-2011, 2011.

Project 14-006	STATUS: Active – June 12, 2014

Characterization of Boundary-Layer Meteorology during DISCOVER-AQ Using Radar Wind Profiler and Balloon Sounding Measurements

Sonoma Technology, Inc. – Clinton MacDonald
Valparaiso University – Gary Morris

AQRP Project Manager – Gary McGaughey
TCEQ Project Liaison – Dave Westenbarger

Funding Amount: $65,588
($49,979 Sonoma Technology, $15,609 Valparaiso)

Executive Summary

As part of the DISCOVER-AQ (Deriving Information on Surface Conditions from Column and Vertically Resolved Observations Relevant to Air Quality) program in August and September 2013, Sonoma Technology, Inc. and the National Oceanic and Atmospheric Administration, with support from the AQRP, operated radar wind profilers (RWPs) at four sites in the greater Houston area to collect boundary layer wind data. In addition, a permanent network of three RWPs also provided data during this study. Also, Pennsylvania State University and the Valparaiso University/University of Houston team conducted daily meteorological and ozone soundings on most days during DISCOVER-AQ. The combination of these data offers a rich source of boundary layer meteorological data and can be used to provide insight into the processes that influence the air quality in Houston.

To address questions about meteorological conditions during the DISCOVER-AQ study and to provide useful information to other researchers, this project will (1) characterize boundary layer meteorological processes on all aircraft flight days and high ozone days during the DISCOVER-AQ study period; (2) provide context to the DISCOVER-AQ boundary layer characteristics by comparing them to characteristics observed on high ozone days during the TexAQS-II project in 2005 and 2006 and over the past 10 years for the month of September; and (3) provide continuous daytime boundary layer height data at the seven RWP sites for the entire study period. The results from this project will be documented in a final report, distributed to other researchers, and presented at an end-of-project meeting in Austin in 2015.

Project Update

Over this period, the project team

- Completed the comparison of meteorological conditions observed during the 2013 NASA DISCOVER-AQ program in Houston to those observed during the 2005-2006 TexAQS program;
- Completed the comparison of meteorological conditions observed during the 2013 NASA DISCOVER-AQ program to September average conditions for Houston;
- Completed and delivered a draft final report of the analyses and findings;
- Began preparing a presentation for the Texas AQRP Workshop scheduled for June 2015.

The final report for this Texas AQRP project will provide a basis for understanding key meteorological processes that were observed during the 2013 DISCOVER-AQ campaign in the

Houston area. Meteorological and air quality data from standard surface monitors, radar wind profilers, ozonesondes (“ozone balloons”), weather satellites and radar, and air parcel trajectory models were analyzed by meteorologists at Sonoma Technology, Inc. (STI) and Prof. Gary Morris, Ph.D. (St. Edwards Univ.) to characterize atmospheric boundary layer conditions and relate those findings to observed air quality during the DISCOVER-AQ campaign, as well as on some days with high ozone levels that occurred following the campaign.

A summary of key findings from this analysis is provided below.

- Two general meteorological regimes were identified during the DISCOVER-AQ period: 1) Deep onshore flow (southeasterly winds, blowing from water to land) with lower ozone concentrations, and 2) Weak offshore flow (northerly or northeasterly winds, blowing from land to water) and complex local flows with higher ozone concentrations.

- In agreement with previous analyses, the highest ozone concentrations occurred during periods of weak offshore flow, typically following the passage of a surface cold front. In these cases, the location of highest ozone concentrations in the Houston area is related to the strength, inland progression, and interaction of the Bay breeze (easterly winds from Galveston Bay) and Gulf breeze (southeasterly winds from the Gulf of Mexico). Two such events were identified during the time period analyzed in this report: September 25 and October 8, 2013.

- On high ozone days, mixing heights were typically low (at or below 500 m) at coastal and inland locations during the early- to mid-morning hours, before increasing rapidly to near 2000 m inland during the late-morning and early-afternoon hours while remaining steady at the coast. In contrast, mixing heights on low ozone days showed less diurnal and spatial variation. The mixing height is the height in the atmosphere from the ground to which turbulence/mixing causes atmospheric features (such as winds, moisture, and air pollutants) to be relatively uniform.

- Surface ozone concentrations were more spatially and diurnally variable on high ozone days compared to low ozone days, due to the presence of complex, local wind patterns.

Over the next month, work will focus on revisions to the Draft Final Report, submitting the Final Report, and preparing and delivering a presentation for the end of project meeting in Austin in June.

Project 14-007	**STATUS: Active – June 23, 2014**

Improved Analysis of VOC, NO2, SO2 and HCHO data from SOF, mobile DOAS and MW-DOAS during DISCOVER-AQ

Chalmers University – Johan Mellqvist
University of Houston – Barry Lefer
AQRP Project Manager – David Sullivan
TCEQ Project Liaison – John Jolly

Funding Amount: $97,260
($74,179 Chalmers, $23,081 UH)

Executive Summary

Mobile optical remote sensing measurements by the SOF and mobile DOAS techniques were carried out in the Houston area during September 2013 as part of the NASA Discover Air Quality experiment. Atmospheric gas column measurements of SO_2, NO_2, HCHO and VOCs were carried out in a box around the Houston Ship channel, in parallel with flights by two aircraft from NASA. In this project the collected optical remote sensing data will be reanalyzed, improved and compared to other data. In particular, the investigators will work with radiative transfer modeling to minimize cloud effects.

In addition, during the 2013 field campaign a new VOC sensor was used to map ratios of the ground concentrations of alkanes and aromatic VOCs downwind of various industries. In this project the investigators will refine the spectral analysis for measurements of the aromatic VOCs from this sensor and compare the data to parallel measurements with other techniques and write a scientific paper.

This project will support the AQRP priority research area: "Improving the understanding of ozone and particulate matter (PM) formation, and quantifying the characteristics of emissions in Texas through analysis of data collected during the DISCOVER-AQ and SEAC4RS campaigns."

Project Update

During the period March to May the primary focus has been on compiling the final data from our own measurements and the ones recently made available by NASA for the final report.

We have also worked on reanalyzing data from a new VOC sensor that was used in the 2013 campaign to map ratios of the ground concentrations of alkanes and aromatic VOCs downwind of various industries. The sensor is an open path Differential Optical Absorption Spectroscopy (DOAS) system coupled to a custom made multiple-pass cell working in the UV region between 250-280 nm. We e have refined the spectral analysis for measurements of aromatic VOCs from this sensor and compared it's data to parallel data from a proton transfer mass spectrometer (PTRMS) and canister sampling and subsequent GC-FID. The results are included in the draft final report, including also a manuscript for a scientific paper.

We have improved the evaluation of formaldehyde (HCHO) from the mobile DOAS spectra by rerunning the spectral retrieval with HCHO cross sections from [Meller and Moortgat 2000] instead of the ones previously used from [Cantrell 1990]. These data are used to estimate emissions of the latter species.

Project 14-008	STATUS: Active – April 17, 2014

Investigation of Input Parameters for Biogenic Emissions Modeling in Texas during Drought Years

The University of Texas at Austin – Elena McDonald-Buller

AQRP Project Manager – David Sullivan
TCEQ Project Liaison – Barry Exum

Funding Amount: $175,000

Executive Summary
The role of isoprene and other biogenic volatile organic compounds (BVOCs) in the formation of tropospheric ozone has been recognized as critical for air quality planning in Texas. In the southwestern United States, drought is a recurring phenomenon and, in addition to other extreme weather events, can impose profound and complex effects on human populations and the environment. Understanding these effects on vegetation and biogenic emissions is important as Texas concurrently faces requirements to achieve and maintain attainment with the National Ambient Air Quality Standard (NAAQS) for ozone in several large metropolitan areas. Previous research has indicated that biogenic emissions estimates are influenced by potentially competing effects in model input parameters during drought and that uncertainties surrounding several key input parameters remain high. The primary objective of the project is to evaluate and inform improvements in the representation of one of these key input parameters, soil moisture, through the use of simulated and observational datasets. The Model of Emissions of Gases and Aerosols from Nature (MEGAN) will be used to explore the sensitivity of biogenic emission estimates to alternative soil moisture representations.

Project Update
Project activities are described by task number below.

Task 1. Investigation and Evaluation of Soil Moisture Datasets
The primary datasets used in this study were observations of soil moisture at 5/10/20/50/100cm (where available) collected by the Soil Climate Analysis Network (SCAN) and U.S. Climate Research Network (USCRN) during 2006-2013 at multiple monitoring locations throughout the South Central US and eastern Texas. These in-situ results were compared to predictions from the North American Land Data Assimilation System-Phase II (NLDAS-2) Mosaic, Noah, Noah with multi-parameterization (Noah-MP), and Variable Infiltration Capacity (VIC) land surface models (LSMs). The seasonal and inter-annual variability of these soil moisture datasets were investigated individually as summarized in previous quarterly reports.

Task 2. Comparison of Simulated and Observed Soil Moisture
The in-situ measurements and NLDAS-2 predictions were evaluated within the 12-km grid domain that covers Texas and surrounding states for years 2006-2013. Comparison with available in-situ observations shows that all NLDAS-2 LSMs capture relative changes in the overall spatial and temporal variations of soil moisture such as the extent and evolution of

drought potentially important for BVOC emission modeling. Depending on the specific location and season, Noah-MP, Mosaic, or Noah may have the best agreement with observations in the near-surface layers while the models predict substantially drier soil moisture at deeper soil layers compared to observations. However, absolute model biases may be large, with the magnitude partially dependent on LSM, soil depth, and location. In particular, absolute soil moisture values are consistently predicted as too wet by VIC for the near-surface layers and hence cannot capture extreme wet/dry events. In contrast, Noah-MP exhibits overly weak temporal variation at deeper layers in eastern Texas and so fails to reproduce conditions during the wet year of 2007 and drought events in 2011.

Task 3. Preparation of MEGAN Simulations
As discussed in previous quarterly reports, MEGANv2.1 simulations were generated to predict isoprene emissions for years 2006 2007, and 2011 during March through October on the 4-km grid domain at 1-km horizontal spatial resolution. Datasets processed for input to MEGAN included National Centers for Environmental Predictions North American Regional Reanalysis (NCEP-NARR) meteorological data (temporal/spatial resolution: 3 h/32 km), MODIS 4-day LAI product (MCD15A3; spatial resolution: 1 km), Photosynthetically Active Radiation (PAR) produced using solar insolation data from the Geostationary Operational Environmental Satellites (GOES; temporal/spatial resolution: 1 h/4 km) that were obtained from the University of Alabama in Huntsville, and the TCEQ land cover products. Emission factors were those specified by the default MEGAN gridded maps. Simulations were performed using results from each of the examined NLDAS-2 LSMs, i.e., Mosaic, Noah, Noah-MP, and VIC.

Task 4. Sensitivity of Biogenic Emission Estimates to Soil Moisture
The primary geographic focus of MEGAN simulations was on five eastern Texas climate regions: North Central, South Central, East, Upper Coast, and eastern portions of Edwards Plateau. Utilization of the Noah, Noah-MP, and VIC soil moisture databases within MEGAN to predict isoprene emissions during drought showed regionally-averaged isoprene reductions within 15% of the base case (i.e., impact of soil moisture not considered). In contrast, the simulations that employed the Mosaic database often predicted large emissions reductions during drought. Analysis of the Mosaic results show that emissions reductions were sometimes predicted even during non-drought periods especially in regions dominated by clay soils. The substantial differences in Mosaic isoprene predictions from the other models are due, in part, to the relatively high wilting point database employed by Mosaic.

A complete discussion of all analysis and results, including suggestions for future work, have been provided in the draft final report delivered to AQRP on May 18, 2015. All funds allocated to the project are intended to be utilized by June 30, 2015.

Project 14-009	STATUS: Active – July 1, 2014

Analysis of Surface Particulate Matter and Trace Gas Data Generated during the Houston Operations of DISCOVER-AQ

Rice University – Robert Griffin
University of Houston – Barry Lefer

AQRP Project Manager – Elena McDonald-Buller
TCEQ Project Liaison – Shantha Daniel

Funding Amount: $219,232
($109,867 Rice, $109,365 UH)

Executive Summary

In recent years, the National Aeronautics and Space Administration (NASA) has placed considerable emphasis on the use of satellite remote sensing in the measurement of species such as O_3 and PM that constitute air pollution. However, additional data are needed to aid in the development of methods to distinguish between low- and high-level pollution in these measurements. To that end, NASA established a program titled Deriving Information on Surface Conditions from Column and Vertically Resolved Observations Relevant to Air Quality (DISCOVER-AQ). DISCOVER-AQ began in summer 2011 with work in the Mid-Atlantic Coast that featured satellite, airborne, and ground-based sampling. The DISCOVER-AQ program conducted operations in and near Houston in September 2013.

During the Houston operations of DISCOVER-AQ, there was a need for ground-based measurement support. The predecessor to this project filled that need by providing quantitative measurements of sub-micron particle size and composition and mixing ratios of volatile organic compounds (VOCs) and other photochemically relevant gases such as O_3 and oxides of nitrogen (NO_x = nitric oxide (NO) plus nitrogen dioxide (NO_2)). The instrumentation for these measurements was deployed using the University of Houston (UH) mobile laboratory. The current project focuses on the analysis of data generated during the mobile laboratory operations during DISCOVER-AQ.

Project Update

The importance of secondary processes in determining the concentrations of particulate matter (PM) in Houston was first evaluated by investigating the composition of the particles measured by a high-resolution time-of-flight aerosol mass spectrometer (HR-ToF-AMS) aboard the UH/Rice mobile air quality laboratory MAQL. Organic material (a mix of primary and secondary material) was the dominant species across the city, followed by sulfate, ammonium, and nitrate, the three of which predominantly form via secondary processes. Based on the HR-ToF-AMS data, a statistical modeling technique called positive matrix factorization was used to split the organic material into factors that represent primary organic aerosol (POA) and two forms of secondary organic aerosol (SOA) - one that is more aged and one that is relatively fresh. Averaged across the city, the fresh SOA accounts for almost two thirds of the organic aerosol, with an equal split of the remainder between POA and the aged SOA. With regard to the relative aging, the southeastern portion of the city (named here Zone 3) shows a degree of oxidation typically associated with the most aged SOA; wind typically moves the PM through the central part of the city (named here Zone 2) where the relative aging decreases due to the injection of

POA. Downwind (to the northwest) of the city (named here Zone 1), the fresh SOA appears to increase in importance, probably because of reactions between volatile organic compounds (VOCs) and oxidants in the urban plume. However, additional statistical work using a technique called principal component analysis indicates that local oxidation of anthropogenic VOCs is likely more important than that of biogenic volatile organic compounds (BVOCs) (specifically in the form of BVOCs known as monoterpenes) and that formation of sulfate aerosol is likely to occur on a regional rather than a local scale. The PM data collected using HR-ToF-AMS also have been used in a computer model to estimate the liquid water content (LWC) associated with the PM. Comparisons between LWC and other aerosol constituents have been made within each of the Zones defined above. In each Zone, LWC was well correlated with the inorganic aerosol constituents. Relative to Zones 1 and 3, Zone 2 exhibited the strongest relationship between LWC and organic aerosol mass and between LWC and HR-ToF-AMS markers of aging.

Previous work showed that the O_3 monitoring instrument (OMI) satellite has a hard time capturing the spatial variability of NO_2 in an urban region. As a result, a new technique was applied to downscale OMI data to a finer spatial resolution. This downscaling takes the OMI NO_2 mass for each satellite pixel and uses Community Multi-Scale Air Quality (CMAQ) model output to derive a spatial weighting kernel to distribute the NO_2 measured by OMI at the CMAQ scale. This technique has been applied in Houston and compared to DISCOVER-AQ Pandora (ground-based total column) and P-3B (airplane *in situ*) measurements. Improvements were observed for the Houston Ship Channel area for the P-3B comparison, but the Pandora instruments did not observe this improvement. The different spatial footprints of the two measurements make a large difference in the result and highlight the importance of understanding spatial resolution when comparing different measurement techniques.

The MAQL data (filtered by nitrogen oxide (NO_x) mixing ratios below 100 parts per billion to ensure sampling was not occurring within a motor vehicle exhaust plume) were used to constrain the Langley Research Center photochemical model to estimate O_3 formation, destruction, and net production (formation minus destruction) rates in two greater Houston locations: Conroe (to the northwest of central Houston) and Manvel Croix (directly south of central Houston). Because of instrumental malfunction, VOC data were derived from other measurements throughout Houston using regression techniques, wind directions to show airmass history, and CMAQ model output (as opposed to MAQL data). It was found that simulation of net O_3 production in both locations was extremely sensitive to the BVOC mixing ratios used. Current work is focused on determining the most appropriate BVOC mixing ratios to use for this effort as a result of the sensitivity of the results to BVOC. Once that is complete, final model output describing O_3 dynamics (as well as the sensitivity of those dynamics to NO_x) and radical formation will be generated.

Project 14-010	STATUS: Active – January 26, 2015

Impact of large-scale circulation patterns on surface ozone concentrations in HGB

Texas A&M Galveston – Yuxuan Wang

AQRP Project Manager – Vincent Torres
TCEQ Project Liaison – Mark Estes

Funding Amount: $79,325

Executive Summary
The Bermuda High (BH) is a key driver of large-scale circulation patterns in Southeastern Texas in summer. The variations in the location and strength of the Bermuda High are expected to influence surface ozone concentrations and cause high- or low-ozone years in HGB through modulating the southerly flows that bring marine air with lower ozone background from the Gulf of Mexico. This project aims at establishing a statistical relationship from historical observations to quantify the impact of the BH variations on the variability of surface O_3 in HGB during the ozone seasons. Such a relationship will then be used to improve the GEOS-Chem simulation of background ozone inflow from the Gulf of Mexico through development of a bias correction scheme. The more than decade-long observational record of ozone and meteorology (1998 – 2012) during the ozone season (April 1 – October 31) will be analyzed to characterize the complex effects of the BH on surface ozone variations in HGB. The ozone variability will be defined for maximum daily 8-h average (MDA8) at the monthly and interannual time scales (i.e., the timescale of determining air quality attainment or nonattainment). A variety of indices to define the location and strength of the Bermuda High (BH Index; BHI) will be adopted from the literature and new BHI of better relevance to Texas air quality will be proposed. Statistical relationships between the variability of surface ozone concentrations and BHI will be constructed based on observations. The observed relationship will then be used as a mechanistic basis to design a bias correction scheme in the GEOS-Chem global CTM to improve its simulation of background O_3 associated with maritime inflow to HGB. The results will benefit the regulatory models of TCEQ through improved boundary conditions at the Gulf of Mexico model domain.

Project Update
Progress on Project 14-010 is summarized below by Task:

Task 1: In addition to the datasets collected in the last period, the project team has also collected Palmer Drought Severity Index (PDSI) for HGB on NOAA website. It is a meteorological drought index developed in 1965 by Wayne Palmer to measure the departure of the moisture supply. The PDSI is calculated based on precipitation and temperature data, as well as the local Available Water Content (AWC) of the soil. From the inputs, all the basic terms of the water balance equation can be determined, including evapotranspiration, soil recharge, runoff, and moisture loss from the surface layer.

In this reporting period, we analyzed the influence of the Bermuda High on surface ozone concentrations over HGB on the seasonal and monthly time scale. Figure 1 shows the seasonal variations of BH-Lon, BHI and HGB-mean MDA8 ozone. Zhu and Liang (2013) used the SLP difference over Gulf of Mexico (25.3°–29.3°N, 95°–90°W) and the southern Great Plains (35°–

39°N, 105.5°–100°W) to define BHI. Similar to their definition, our BHI is defined as the SLP difference over (25.3°–29.3°N, 92.5°–87.5°W) and (35°–39°N, 105.5°–100°W). Results show that BH-Lon explains the seasonal variations of HGB ozone from May to September (Figure 1). The trough of ozone in July is accompanied by the most westward extension of the BH of the year (i.e., July sees the lowest numerical value of BH-Lon of the year as west longitude being negative by definition). BHI shows an increase from winter to summer, and a decrease from summer to winter, which is consistent to the seasonal variations of HGB ozone, but it does not explain the ozone trough in July. Given the non-linear variations of BH-Lon and ozone from late spring to early fall, we focus on the interannual variations of monthly ozone. During May of some years (e.g. 2005), the 1560-gpm isoline does not exist over the Bermuda region. Considering the instability of the BH in May, we only calculate BH-Lon from June to September in the monthly timescale analysis.

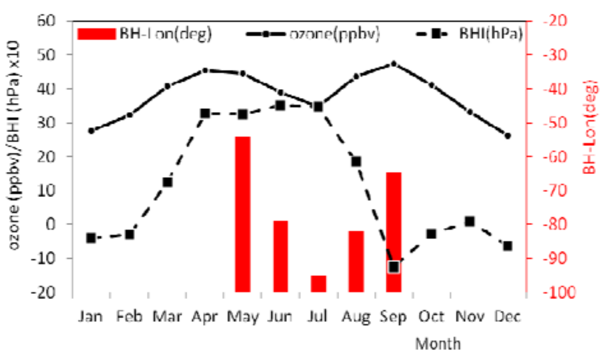

Figure 1.Seasonal variations (1998-2013 mean) of BH-Lon, BHI and mean MDA8 ozone concentrations over HGB.

In the prior analysis, we used the 1560-gpm isoline to define the BH-Lon for the whole study period. Since the Bermuda High is weaker in August and September than that in June and July, we tried other isolines to adjust for this seasonal variability of BH in our definition of BH-Lon for August and September. We got the best results (in terms of correlation with HGB ozone) when the 1556-gpm isoline was used to define BH-Lon for August and the 1536-gpm isoline for September. Figure 2 shows the detrended HGB ozone and BH-Lon for June, July, August and September respectively. Note that the BH-Lon for Jun and July is defined using the 1560-gpm, while that for August and September is defined using the 1556- and 1536-gpm respectively. The time series of ozone concentration is detrended by subtracting the 3-year moving average from the raw data; BH-Lon is detrended by subtracting the best straight-line fit from the raw data. In the strong-BH months (June and July), the interannual variations of ozone is well captured by BH-Lon. However, in the weaker-BH months (August and September), the correlation is not as good. There may be other indicators influencing HGB ozone in those weaker-BH months. For example, the regression residual of ozone in 2011 is quite large for all the months examined here, and 2011 happened to be a drought year. Thus, we speculate that drought may be an indicator to explain some high ozone events in August and September. Indeed, high ozone in August 2011 and September 2011, which cannot be well explained by BH-Lon, corresponds with negative PDSI (severe drought). Thus, we include the drought index as a predicting variable when constructing the multiple linear regression (MLR) model in Task 2.

In addition to mean MDA8 ozone over HGB, other metrics of ozone were tested for their associations with the BH variability, including median MDA8 ozone, mean and median background ozone, and ozone enhancement above background. The background ozone data were provided by TCEQ. Monthly median MDA8 ozone is calculated as the mean of monthly median ozone of all the sites. Mean/median ozone enhancement is the difference between mean/median MDA8 ozone and mean/median background ozone. Median ozone is typically lower than the mean, suggesting the median value may be less sensitive to high ozone events. The interannual variability of monthly mean background ozone is very similar to that of the mean MDA8 total ozone, especially in June (r=0.97).

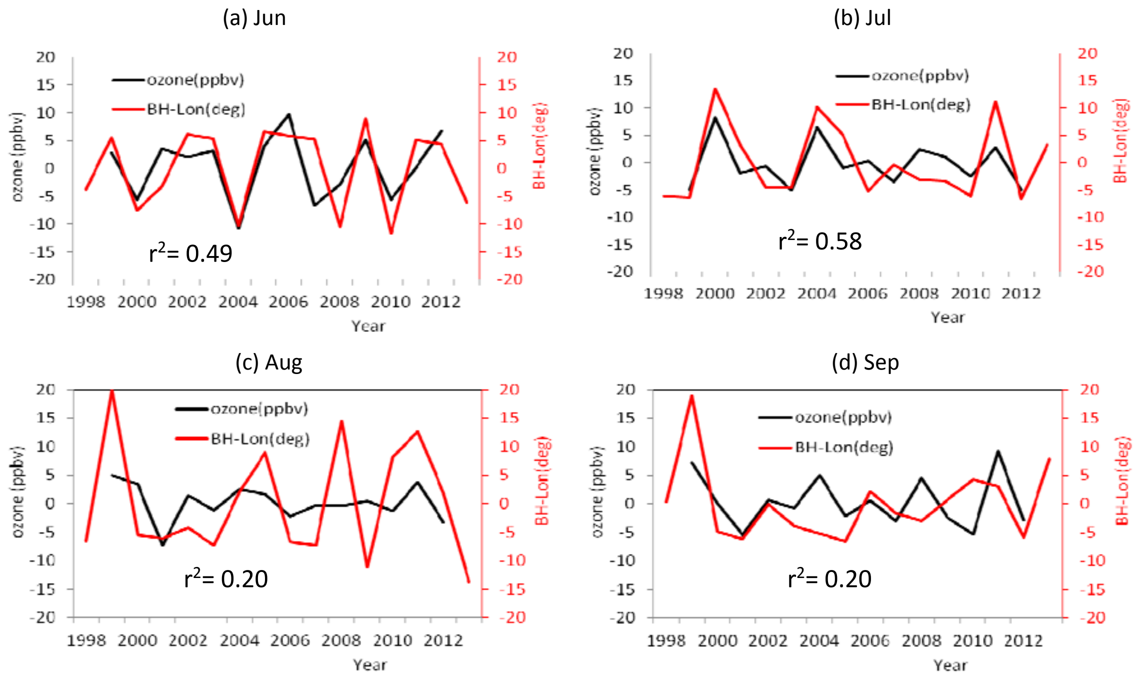

Figure 2. The interannual variations of the detrended monthly mean surface ozone and BH-Lon for June, July, August and September.

We calculated the correlation coefficients between different monthly ozone metrics and BH-Lon by month. In June and July when the correlations between total ozone and BH-Lon are stronger, there are also significant correlations between background ozone and BH-Lon. However, in August and September, there are no significant positive correlations between background ozone and BH-Lon, probably due to the reduced influence of maritime inflow on background ozone.

We also examined the correlations between BHI and different metrics of ozone. BHI is the conventional index of the Bermuda High and is found to correlate well with LLJ (Zhu et al., 2012), which is an indicator of the strength of the meridional winds. Therefore, we speculate that BHI can explain to some extent high ozone events over HGB that are typically brought in by northerly winds. Indeed, the correlation coefficients between BHI and HGB ozone were found to be typically negative, with the strongest correlation being in September (figure not shown). Therefore, the BHI is chosen as another independent variable in the MLR model to be constructed in Task 2.

To elucidate any connection of the BH-Lon variability with known climate modes, we examined the relations between ENSO and BH-Lon on a longer time scale (1991-2010). The Bivariate ENSO time series were obtained from NOAA (http://www.esrl.noaa.gov/psd/data/climateindices/list/). We tested the correlations of BH-Lon with the ENSO index for the same months as well as up to a 2-month lag. The only significant correlation is between the BH-Lon of June and the Bivariate ENSO index in April (Figure 3) and that correlation is only moderate. This analysis suggests that ENSO may not play a significant role in affecting the variability of HGB ozone and therefore it is not included in the MLR.

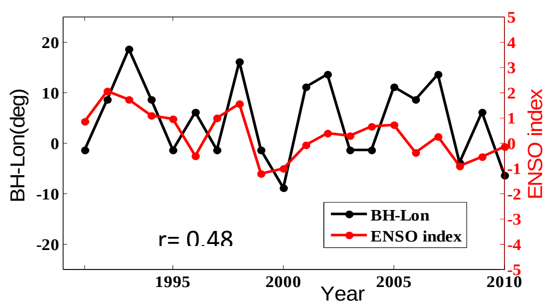

Figure 3. Time series of BH-Lon in June and the ENSO index in April from 1991 to 2010.

Task 2: We applied a multiple linear regression (MLR) model to construct the statistical relationship between different metrics of HGB ozone and the indices selected in Task 1, including BH-Lon, BHI, and PDSI.

The MLR equations for each month are as follows:

$$y_{Jun}=0.54\times x_1-0.22\times x_2-0.26\times x_3,\quad y_{Jul}=0.70\times x_1-0.13\times x_2-0.19\times x_3$$

$$y_{Aug}=0.37\times x_1+0.05\times x_2-0.32\times x_3,\quad y_{Sep}=0.37\times x_1-0.48\times x_2-0.32\times x_3$$

where y represents detrended mean total ozone, and x_1, x_2, x_3 represent BH-Lon (detrended), BHI and PDSI, respectively. Figure 4 displays the MLR-predicted mean total ozone when BH-Lon, BHI and PDSI are used as predicting variables. The MLR-fitted ozone captures 55%, 61%, 31% and 53% of the variance in HGB ozone in June, July, August and September, respectively.

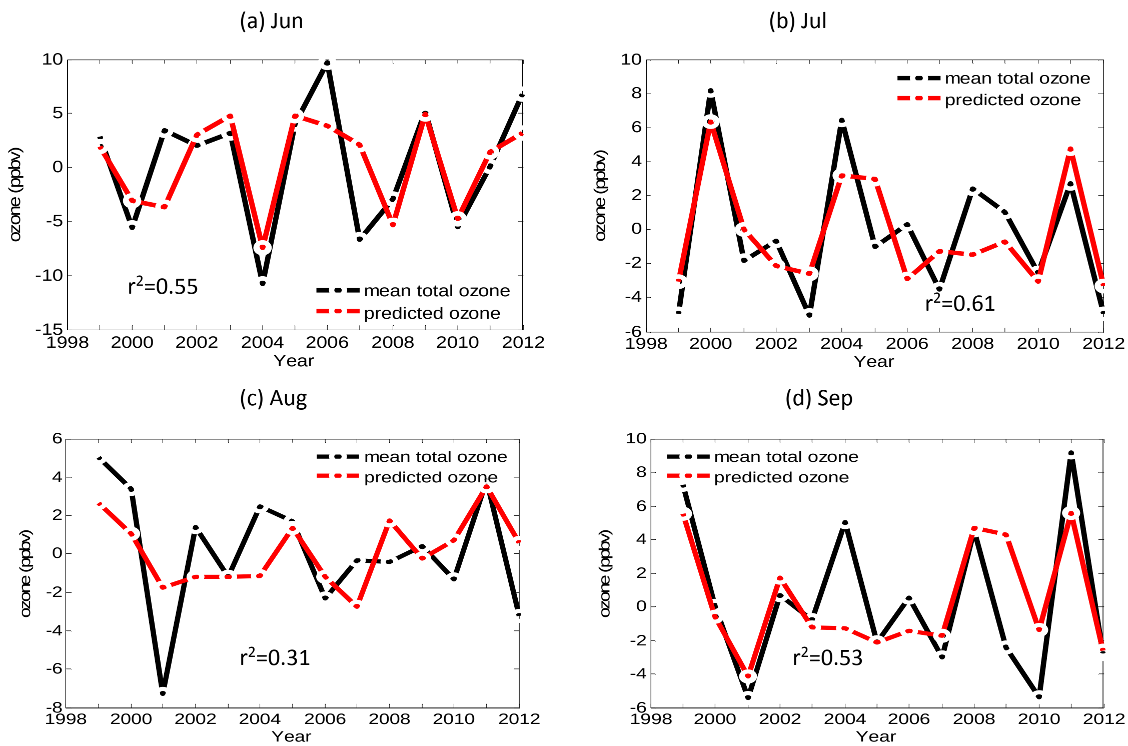

Figure 4. Observed (black) and MLR-predicted (red) mean MDA8 ozone over HGB by month.

Task 3: GEOS-Chem simulations have been conducted for June from 2004 to 2012 using the GEOS-5 assimilated meteorology and EPA NEI inventory with year-to-year changes of emissions. The model resolution is 0.5° x 0.667°. Further analyses of GEOS-Chem simulation results will be carried out during the next reporting period.

Targeted Improvements in the Fire Inventory from NCAR (FINN) Model for Texas Air Quality Planning

The University of Texas at Austin – Elena McDonald-Buller
Environ – Christopher Emery

AQRP Project Manager – David Sullivan
TCEQ Project Liaison – Jim MacKay

Funding Amount: $179,586
($151,167 UT-Austin, $28,419 Environ)

Executive Summary
Wildland fires and open burning can be substantial sources of ozone precursors and particulate matter. The influence of fire events on air quality in Texas has been well documented by observational studies. During the 2012-2013 fiscal year of the Air Quality Research Program (AQRP), Dr. Elena McDonald-Buller, Dr. Christine Wiedinmyer, and Mr. Chris Emery led a project (#12-018) that evaluated the sensitivity of emissions estimates from the Fire INventory from NCAR (FINNv1; Wiedinmyer et al. 2011) to the variability in input parameters and the effects on modeled air quality using the Comprehensive Air Quality Model with Extensions (CAMx; ENVIRON, 2011). The project included an analysis of the climatology of fires in Texas and neighboring regions, comparisons of fire emission estimates between the FINN and BlueSky/SmartFire (Larkin 2009; Chinkin et al., 2009) modeling frameworks, evaluation of the sensitivity of FINN emissions estimates to key input parameters and data sources, and assessment of the effects of FINN sensitivities on Texas air quality. Among the many findings of the study were the needs for targeted improvements in land cover characterization, burned area estimation, fuel loadings, and emissions factors. These needs were particularly pronounced in areas with agricultural burning. This project addresses specific improvements in FINN that will support fire emissions estimates for Texas and the next public release of the FINN model. Fire emissions and air quality modeling will focus on 2012 to support TCEQ's air quality planning efforts.

Project Update
Project activities are described by task number below.

Task 1. Regional Land Cover Characterization
Processing of ArcGIS raster files for the land cover datasets in the WGS84 coordinate system has been completed. In addition to the MODIS Land Cover Type Product, these datasets include the Global Land Cover (GLC) - SHARE product from the United Nations Food and Agriculture Organization (FAO), the European Space Agency's (ESA's) Climate Change Initiative Land Cover (CCI-LC) product, the Fuel Characteristic Classification System (FCCS) database and U.S. Department of Agricultural (USDA) National Agricultural Statistical Service (NASS) Cropland Data Layer (CDL) both of which are available for the continental United States, and a high resolution regional land use/land cover database for Texas and surrounding states developed

by Popescu et al. (2011). These land cover products are being used alone or in combination as FINN input. The study team also processed the recently released MODIS Vegetation Continuous Fields (VCF) product for 2012 (version 5.1), which contains proportional estimates for vegetative cover types: woody vegetation, herbaceous vegetation, and bare ground. MODIS VCF data is used in FINN to identify the density of the vegetation at active fire locations. Sensitivity studies will be conducted to estimate emissions of carbon monoxide (CO), nitrogen oxides (NO_x), and fine particulate matter ($PM_{2.5}$) associated with fire events during 2012.

Task 2. Mapping of Croplands Data

Cropland data has been obtained from the USDA CDL. Crop-specific emission factors, developed by Jessica McCarty at the University of Louisville have been added to the FINN default configuration. Fuel loading and CO emissions for the generic croplands classification used as the FINN default configuration are compared to those for specific crop types in Table 1 below.

Table 1. Fuel loading (kg m^{-2}) and carbon monoxide emission factors (g/kg) by crop type.

	Fuel Loading (kg/m^2)	CO Emission Factor (g/kg)
Crop (Generic)	0.66	53
Rice	0.67	64
Wheat	0.66	55
Cotton	0.38	73
Soy Bean	0.56	69
Corn	1.62	53
Sorghum	0.66	64
Sugar Cane	1.50	59

Task 3. Estimation of Burned Area

Development of the algorithms and ArcGIS tools used for processing of the MODIS Rapid Response fire detection records, quantifying burned area, and characterizing the underlying land cover has been largely completed. On-going work is examining burned area estimates for distinct agricultural fire events in the southeastern United States and wildfires throughout the southeastern and western United States.

Task 4. Sub-grid scale Partitioning of NO_x Emissions to NO_z in Fire Plumes

The study team conducted a literature review of various field studies and modeling approaches upon which to base NO_x partitioning into aged NO_z forms (HNO_3 and PAN) during EPS3 processing of the FINN emission estimates. Based on Alvarado et al. (2010) and Fischer et al. (2014), the GEOS-Chem model apportions 40% NO_x to PAN and 20% NO_x to HNO_3, leaving 40% as NO. These factors were derived from ARCTAS-B aircraft measurements within North American boreal fire plumes and were considered adequate for the 3-hour emission time scales applied in GEOS-Chem. In regulatory ozone modeling for the State of Louisiana using a 2010 FINN v1 inventory, ENVIRON and ERG (2013) apportioned 20% NO_x to PAN and 10% NO_x to HNO_3 and reduced remaining NOx to 20% of the original FINN value (a net reduction in total fire nitrogen of 50%). The NO_x reduction was applied to align NO_x:CO values closer to Alvarado et al (2010). Hecobian et al. (2011) evaluated ARCTAS measurements within numerous fire plumes throughout North American and Asia. Their results will be evaluated and compared to the NO_z:NO_x values from Alvarado et al. (2010) to assess consistency. More recently, Alvarado et al. (2013) developed look-up tables of NO_z:NO_x emission ratios as functions of vegetation type, temperature, and solar angle. Such tables would be ideal for incorporation into air quality models, as long as vegetation types could be adequately mapped to the land cover classification schemes used in the models. However, the availability of these data is unclear and such an approach is beyond the simpler methodology intended for this project. Look-up tables may be a good direction for future work.

The study team reviewed the EPS3 fire emissions processing chain and developed a straw-man approach to incorporate re-speciation of FINN NO_x to NO_z compounds as a function of fire size relative to grid resolution and fire plume rise. The general approach is to maximize NO_z:NO_x ratios for small fires relative to grid size and for fires with higher plume rise to account for longer aging times occurring during rise and dilution to grid scale. Conversely, NO_z:NO_x ratios would be minimized (or zero) for large fires relative to grid size and for fires with lower plume rise, in which case grid model chemistry would be a more appropriate mechanism to age the NO_x. The approach will also consider diurnal PAN:NO_x profiles to account for the fact that PAN is a photochemically-derived product.

Task 5. Comprehensive Air Quality Model with Extensions (CAMx) Sensitivity Studies

The TCEQ has provided the team with its 2012 CAMx episode. The base case simulation has been run at the Texas Advanced Computing Center (TACC). The output has been benchmarked for the base case against that of the TCEQ. Emissions estimates from fire events developed by the TCEQ for its 2012 CAMx base case have been summarized; these will be compared with estimates from the newly modified FINN processor using the default land cover database (MODIS LCT) as well as those obtained using other land cover products.

Project 14-014	STATUS: Active – January 27, 2015

Constraining NO_X Emissions Using Satellite NO_2 and HCHO Column Measurements over the Southeast Texas

University of Houston – Yunsoo Choi

AQRP Project Manager – Vincent Torres
TCEQ Project Liaison – Dave Westenbarger

Funding Amount: $84,927

Executive Summary
Ozone production depends not only on availability of Volatile Organic Compounds (VOCs) and Nitrogen Oxides (NO_x) but also on their relative concentrations, which can be expressed as a VOC/NO_x ratio. Over or under prediction of either component in an air quality model changes the VOC/NO_x ratio and limits the capability of an air quality model to predict ozone properly. Additionally, accurate predictions of meteorological variables are crucial to simulate atmospheric chemistry and consequently properly simulate ozone concentrations. In addition to ground and aircraft measurements obtained in Houston during the Deriving Information on Surface Conditions from Column and Vertically Resolved Observations Relevant to Air Quality (DISCOVER-AQ) campaign in September 2013, remote sensing data of NO_2 are available from Aura Ozone Monitoring Instrument (OMI). NO_2 column data products and can be used as a proxy for NO_x and their values in air quality models can be quantified and thus constrained. In this project, an analysis of the archived in-situ aircraft and ground measurements will be performed and satellite measurements of NO_2 will be utilized to improve the bottom-up NO_x emission inventories and study the impact of these improved emissions on ozone predictions. Objective analysis (OA) of meteorological simulations will be applied to improve predictions of meteorological parameters as well as ozone predictions.

The primary objectives of this project are to: (1) utilize satellite measurements of tropospheric NO_2 columns to quantify surface NO_x anthropogenic and soil emissions using inverse modeling; (2) evaluate model-simulated formaldehyde and isoprene concentrations (key drivers for ozone) using in-situ ground and/or aircraft measurements; (3) examine how the ratio of model-simulated NO_2/HCHO in Air Quality Forecasting system at UH (AQF-UH) varies and corresponds to remote sensing NO_2/HCHO column measurements, and (4) perform objective analysis (OA) of meteorological predictions to improve their predictions, and consequently, ozone predictions. The Air Quality Forecasting System will use the Community Multiscale Air Quality (CMAQ) Model with a 4 km resolution for Southeast Texas. The meteorological inputs will be provided by the Weather Research and Forecasting (WRF) model.

Project Update
The project team has finished the preparation of NEI2011, as well as a CMAQ simulation for the 2013 DISCOVER-AQ Texas period with the new inventory. The CMAQ simulation is based on a WRF run with 1-Hr OA. CMAQ model evaluation has also been finished.

The major work is to compare satellite OMI NO_2 daily data to model NO_2 output and update emission inventory using inverse modeling. For this, we have downloaded and processed OMI data and compared to CMAQ output. We are finalizing (analyzing and validating) the inverse modeling part and will report in next quarter.

<u>NEI2011 for CMAQ modeling</u>

We extracted the NEI2011 raw data files and created the input files for SMOKE 3.5.

The NEI 2011 platform v6.1 was developed in November 2014. It includes all the criteria air pollutants and precursors (CAPs) and the following hazardous air pollutants (HAPs): chlorine (Cl), hydrogen chloride (HCl), Benzene, Acetaldehyde, Formaldehyde and Methanol (BAFM). Another revision v6.2 includes a few newer inventories and especially the latest mobile emissions using the Motor Vehicle Emissions Simulator (MOVES) 2014. While some of the emissions data were developed specifically for this project and include improvements over the NEI 2011 platform v6.2 for this time period, the majority of the inventory data were from the NEI 2011 platform v6.1.

We have checked the inventory files prepared for CMAQ and found them to be reasonable. Plots of monthly mean SMOKE emissions (four sectors) are shown in Figure 1: NO emissions for biogenic and mobile emissions, NO_x emissions for area and point sources. Point sources are integrated from surface to the 27th vertical layers.

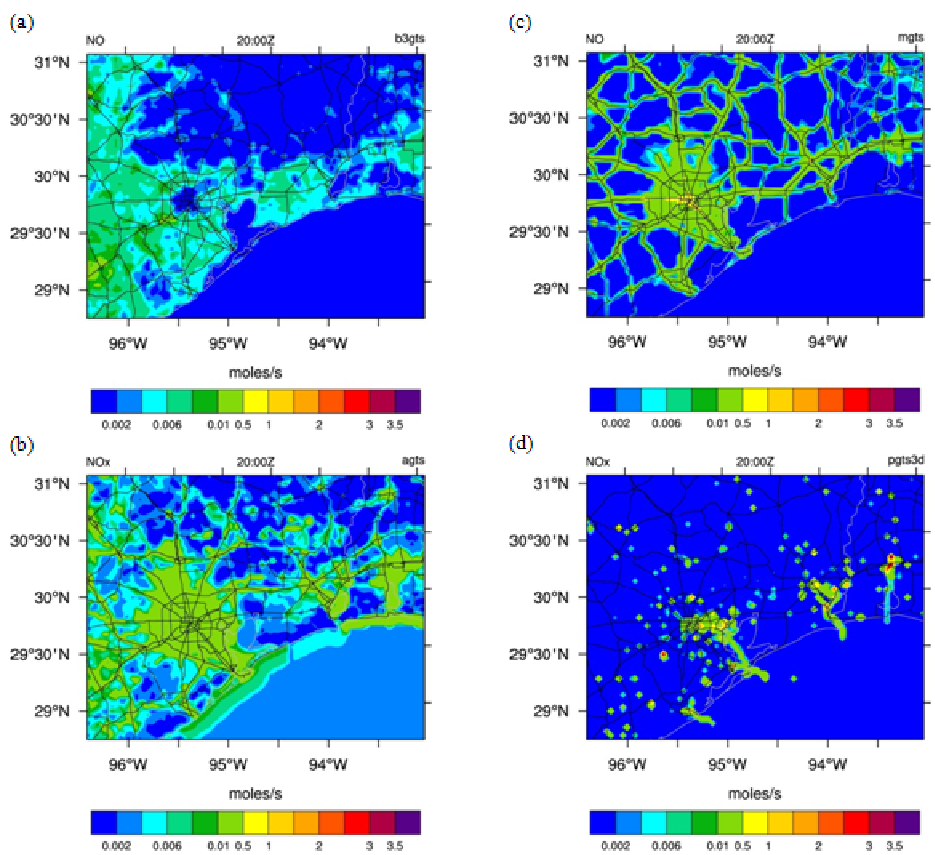

Figure 1: Monthly mean SMOKE four sector emissions based on National Emission Inventory (NEI) 2011: (a) biogenic (b) area (c) mobile (d) point source.

OMI NO2 data processing

We obtained OMI tropospheric NO_2 daily observations (level2) and managed to filter out noisy values. In order to visualize and compare the OMI data with the model output (and perform inverse modeling), we should firstly remove the influence of a priori gas profile from OMI, and secondly project the level2 product on a longitude-latitude grid using a reliable gridding approach. The following figure is the result of mapped OMI tropospheric NO_2 in 4km spatial resolution with and without applying AMF (Figure 2).

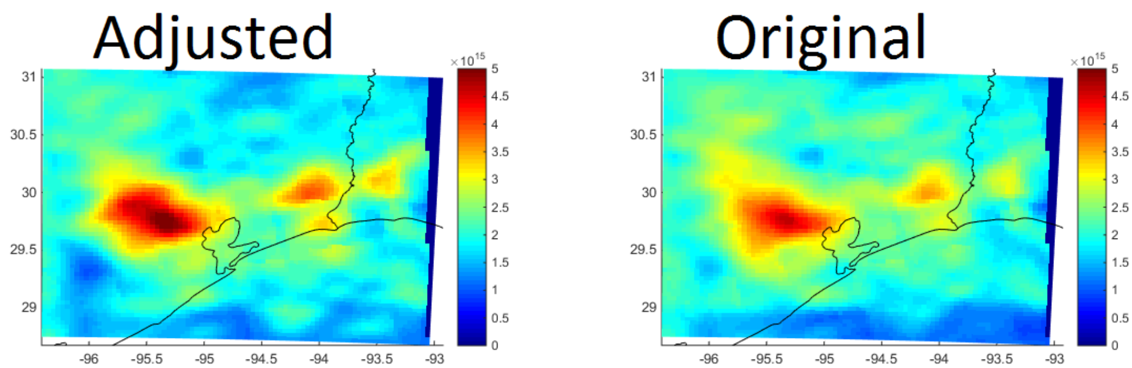

Figure 2. Left: mapped and adjusted OMI tropospheric NO_2 using the grid method and removing priori guess in 4km spatial resolution; right: mapped OMI tropospheric NO_2 using the grid method without performing the first step in the same resolution.

CMAQ Surface Ozone Evaluation with CAMS Data

The ozone statistics were displayed in Table 2. The correlation and IOA is 0.75 and 0.82, respectively. The mean bias is a positive 7.7 ppb, which can be attributed to overestimated model background ozone. Overall, the model ozone performance is quite decent. A comparison of model results from a coastal site (Galveston, C1034) and inland site (Conroe, C78) showed that model performed much better at C78 with a low bias and a high correlation. An examination of model performance at different sites shows that models tend to have much smaller biases at sites located farther inland than at those closer to the coast. This finding, as well as the low observed ozone at Galveston, suggests that model's background ozone (~40 ppb) is too high.

Table 1 Statistics of hourly surface ozone

Case	N	Corr	IOA	RMSE	MAE	MB	O_M	M_M	O_SD	M_SD
1Hr-OA	33308	0.75	0.82	13.8	11.1	7.7	24.4	32.2	16.5	15.9

N – data points; Corr – Correlation; IOA – Index of Agreement; RMSE – Root Mean Square Error; MAE – Mean Absolute Error; MB – Mean Bias; O – Observation; M - Model; O_M – Observed Mean; M_M – Model Mean; SD – Standard Deviation

- Units for RMSE/MAE/MB/O_M/M_M/O_SD/M_SD: ppb

CMAQ Aloft Ozone Evaluation with Aircraft Data

The ozone measurements from aircraft P3-B provided a more complete picture for 09/25's ozone evolution. During the day, P-3B flew around the industrial area, Galveston bay, and Galveston Island for about 9 hours. Of particular, the comparison of observation and model showed the largest difference on September 25th of 2013.

Figure 3 showed hourly ozone vertical profiles from 08 CST to 16 CST of September 25th, with ozone being displayed on x-axis and height on y-axis. One observation dot was averaged over all the grid cells in the same model layer. The 08 and 09 CST profiles showed there was a high ozone layer with average ozone of ~65 ppb, stretching from 450 m to 1200 m height. In comparison, model run had lower ozone, ~50 ppb, in this layer. Such difference certainly contributed to the model underprediction of surface ozone. The discrepancies between low surface ozone and ozone aloft may be explained by a reversal of aloft winds: winds at surface layer still showed light northwesterly in the early morning while winds aloft already changed to southerly.

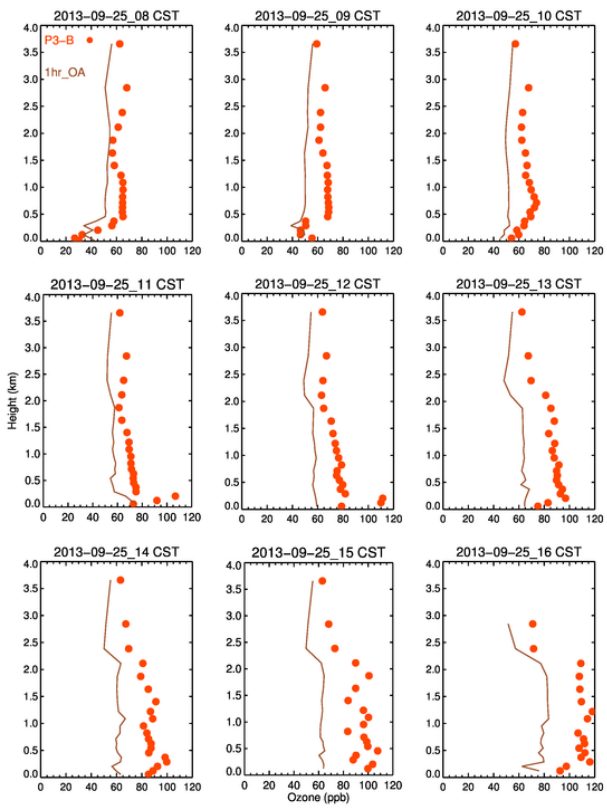

Figure 3. Vertical ozone profiles from 09/25_08 CST to 09/25_16 CST of 2013

CMAQ and OMI NO_2 Comparison

After simulating CMAQ model by using NEI2011 emissions, we once again removed the influences of a priori gas profile from OMI with new outputs and projected the resultant tropospheric OMI NO_2 on the same longitude-latitude grid defined in the model.

The results of tropospheric CMAQ NO_2 and OMI were shown in Figure 4. It demonstrated that simulated CMAQ NO_2 columns overpredicted in urban regions, while underpredicted in suburban/rural regions. The CMAQ modeling with new emissions appears to have a better performance in simulating NO_2 columns. There are discrepancies which should be adjusted by inverse modeling.

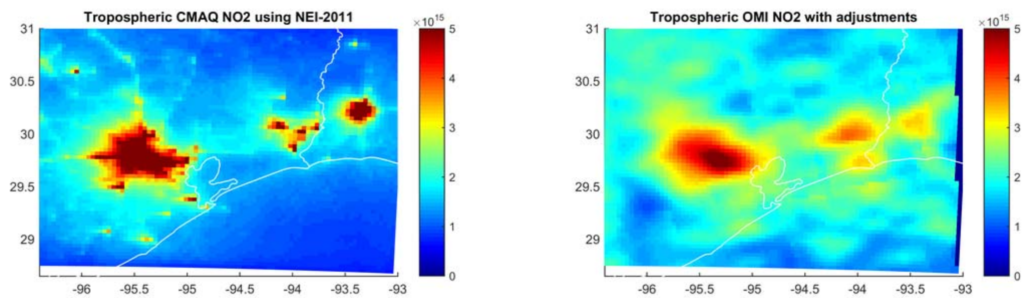

Figure 4: Comparison between CMAQ modeled NO_2 columns (average over September of 2013), left; and OMI NO_2 columns, right

Project 14-016	STATUS: Active – June 4, 2014

Improved Land Cover and Emission Factor Inputs for Estimating Biogenic Isoprene and Monoterpene Emissions for Texas Air Quality Simulations

Environ – Greg Yarwood

AQRP Project Manager – Elena McDonald-Buller
TCEQ Project Liaison – Mark Estes

Funding Amount: $271,911

Executive Summary

The exchange of gases and aerosols between the Earth's surface and the atmosphere is an important factor in determining atmospheric composition and regional air quality. Accurate quantification of emission fluxes is a necessary step in developing air pollution control strategies. In some cases emissions can be directly measured (e.g., point sources with continuous emission monitors) or can be estimated with reasonable confidence (e.g., point sources that have well-defined operating parameters). In contrast, large uncertainties are associated with area sources including emissions from vegetation, and in particular, emissions of biogenic volatile organic compounds (BVOCs). Vegetation is the largest source of VOC emissions to the global atmosphere. The oxidation of BVOCs in the atmosphere affects ozone, aerosol and acid deposition. Current BVOC emission estimates are based on measurements for individual plants that must be scaled up to represent landscapes and adjusted for environmental conditions. There is a critical need for independent BVOC emission inputs for air quality models.

AQRP Project 14-016 will use aircraft observations from the 2013 Southeast Atmosphere Study (SAS) and the 2006 Texas Air Quality Study (TexAQS) to assess and reduce uncertainties associated with a widely-used BVOC emissions model, namely the Model of Emissions of Gases and Aerosol from Nature version (MEGAN). The eddy covariance technique will be used to directly quantify BVOC emission fluxes for all suitable aircraft observations from the SAS study. Using the relationship between BVOC fluxes and concentrations derived from this subset of SAS aircraft data, BVOC emission fluxes will be estimated for 2013 SAS and 2006 TexAQS flights in the southeastern U.S. and Texas, respectively. In addition, the investigators will improve the land cover and emission factor input data sets that are considered the major uncertainties associated with BVOC emission estimates. The overall benefit of this project will be more accurate BVOC emission estimates that can be used in Texas air quality simulations that are critical for scientific understanding and the development of effective regulatory control strategies that will enhance efforts to improve and maintain clean air.

Project Update

Project activities are described by task number below.

<u>Task 1: Estimation of Terpenoid Emission Fluxes from Aircraft Data</u>

Work was done on the comparison between estimated isoprene emissions from the NOAA WP-3D and NCAR C-130 flights and the MEGAN v2.1 model (Figure 1). This extends the previous analyses that included the MEGAN v2.0 and BEIS models. Compared to MEGAN v2.0, the MEGAN v2.1 model correlates somewhat better with the measurements (r=0.69 for MEGAN v2.1vs. r=0.64 for MEGAN v2.0). In addition, the MEGAN v2.1 emissions also agree somewhat better quantitatively with those derived from the measurements (average model-to-measurement ratio is 1.92 for MEGAN v2.1 and 2.25 for MEGAN v2.0). Nevertheless, the MEGAN emissions still appear to overestimate the measured emissions. Another area of concern is the lower degree of correlation between, on the hand, the wavelet flux measurements from the C-130 and the inventories, and, on the other hand, the mixed boundary layer method emissions from the C-130 and the inventories. Work is in progress to understand these differences in more detail.

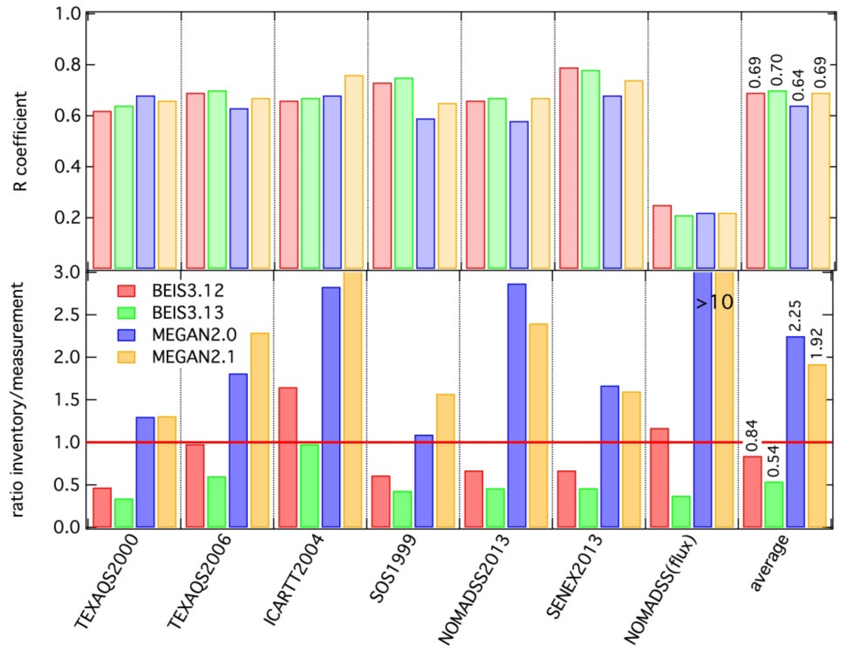

Figure 1: Comparison between the isoprene emissions estimated by the mixed boundary layer method (and the eddy covariance flux for NOMADSS (flux)) for different measurements campaign versus various emissions models. The top panel shows the degree of correlation between the emissions derived from the measurements and the models. The bottom panel shows the average ratios between the emissions from the models and from the measurements.

<u>Task 2: Development of High Resolution Land Cover Data for MEGAN Modeling in Texas and the Southeastern U.S.</u>
This task is completed.

<u>Task 3: Emission Factor Database Development</u>
PNNL continued working on improving the emission factor (EF) dataset by incorporating aircraft observations. The previous updated emission factor data (EFv2015) developed by PNNL included spatially averaged surface flux data derived from aircraft observations. We developed an experimental EF database (EFv2015x) by improving the footprint analysis and using the relationships between vegetation cover types, emission factors calculated based on observations

and land covers, to adjust emission factors for all vegetation types including those not covered by aircraft observations.

During footprint analysis, all existing vegetation types (EVTs) were categorized into 11 groups and average airborne EFs were calculated for 6 of the 11 groups. Scale factors were calculated based on EVT group averaged airborne EF and average land cover EFs (EFv2015) in the footprint areas for corresponding EVT groups. For EVT groups with no data available, an average scale factor was applied. The scale factors were then applied to all EVTs within corresponding groups to derive the EFv2015x dataset.

The limited information for the majority of EVTs prohibits a comprehensive modification of the updated MEGAN EF database (EFv2015). Despite the fact that a "full" modification is not possible, we still applied the valuable information presented in previous sections and developed an experimental EF database (EFv2015x). Due to data limitation, this dataset is considered rather preliminary and was developed for exploratory purposes only.

Task 4: Development of MEGAN Biogenic Emission Inventories and Inventory Evaluation using Regional Photochemical Modeling

ENVIRON prepared model-ready MEGAN emissions using MEGAN inputs provided by PNNL under Tasks 2 and 3 and ran the CAMx photochemical model with the MEGAN emissions. Three biogenic emission inventories were developed for use in the photochemical modeling. The initial inventory was a base-case biogenic emission inventory, which was developed using the MEGAN v2.1 default landcover database and default emission factors. Next, a second biogenic emission inventory was derived from the updated high-resolution landcover database and Texas and Southeastern U.S. emission factor database (EFv2015). Finally a third biogenic inventory was developed using the updated high-resolution landcover database and EFv2015x data. We compared the photochemical model concentrations for the simulations using default and updated biogenic emission inventories against observed concentrations from surface monitoring stations and the C-130 and P-3 aircraft.

Using both the default and updated MEGAN inventories, CAMx spatial patterns of high and low isoprene concentrations were similar to those of the aircraft observations. CAMx generally overestimated isoprene along the C-130 and P-3 aircraft flight tracks. Although the CAMx modeled high bias for isoprene relative to aircraft observations increased in the run using the updated (EFv2015) MEGAN emissions, the CAMx model's performance in simulating ground level ozone improved in the Houston area. The updated MEGAN inventory has significantly lower isoprene emissions in the Houston area, and this appears to reduce ground level ozone, bringing the model into closer agreement with observations.

In the CAMx run that used MEGAN emissions prepared with the EFV2015x data, the high bias against aircraft isoprene and isoprene products measurements from previous runs was significantly improved, while the value of r^2 was similar or slightly lower. The magnitude of the low bias for monoterpenes in increased relative to previous runs and the r^2 decreased slightly. Use of the MEGAN emissions with EFV2015x data had little effect on the modeled high bias for ozone when compared against aircraft ozone data. There were some small improvements in modeled ozone at surface monitoring sites in Texas and southeastern US, but a strong high bias persisted.

Three additional CAMx sensitivity tests were carried out using the updated MEGAN emissions with EFv2015 inputs.

1. We altered the CB6r2 chemical mechanism to increase the production of OH from the breakdown of isoprene following the mechanism of Peeters et al. (2013). The purpose of the test was to gauge the model's response to an isoprene mechanism that represents an upper limit on the production of OH from isoprene. Increasing OH production from isoprene reduces but does not eliminate the high bias in isoprene products.

2. Based on the high bias for isoprene noted in the CAMx run that used default MEGAN emissions, we reduced the MEGAN isoprene emissions by a factor of 2 for all grid cells and times and reran CAMx. For the P-3 data, the CAMx Base run high bias for isoprene products (114%) changed to a low bias of -7% in the sensitivity test as a result of the lower isoprene emissions and atmospheric concentrations. For the C-130 data, the CAMx bias for isoprene products changed from 48% to -33%. The reduction in the magnitude of bias for isoprene products in this sensitivity test suggests that the MEGAN isoprene emissions are overestimated in the default case.

3. In June 2013, Nguyen et al. (2015) measured dry deposition velocities (Vd) for biogenic trace gases in an Alabama forest during the Southern Oxidant and Aerosol Study (SOAS). Comparison of CAMx Vd against the measurements showed Vd was underestimated in the model. We increased CAMx dry deposition of these species to improve agreement with the SOAS measurements. The effects of this test on modeled ozone and isoprene and monoterpenes species were small.

CAMx model performance in the Base Run using default MEGAN emissions and the sensitivity tests in summarized in Figures 2 and 3, which indicate how the normalized mean bias (NMB) varied among the different CAMx runs as the model results were compared to measurements made aboard the C-130 and P-3 aircraft.

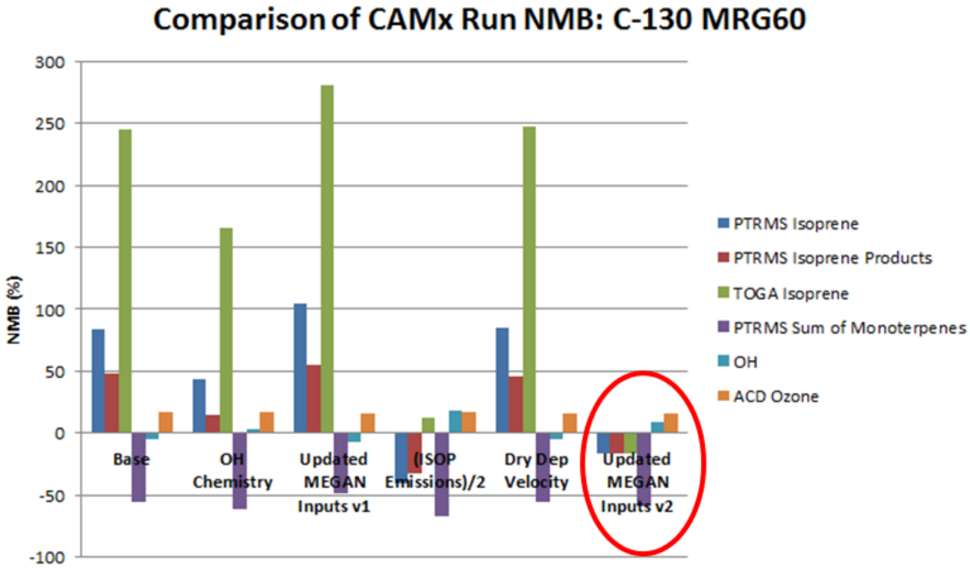

Figure 2. Summary of variation of NMB for the CAMx Base Run and sensitivity test results when model results were compared to C-130 measurements for a subset of key species.

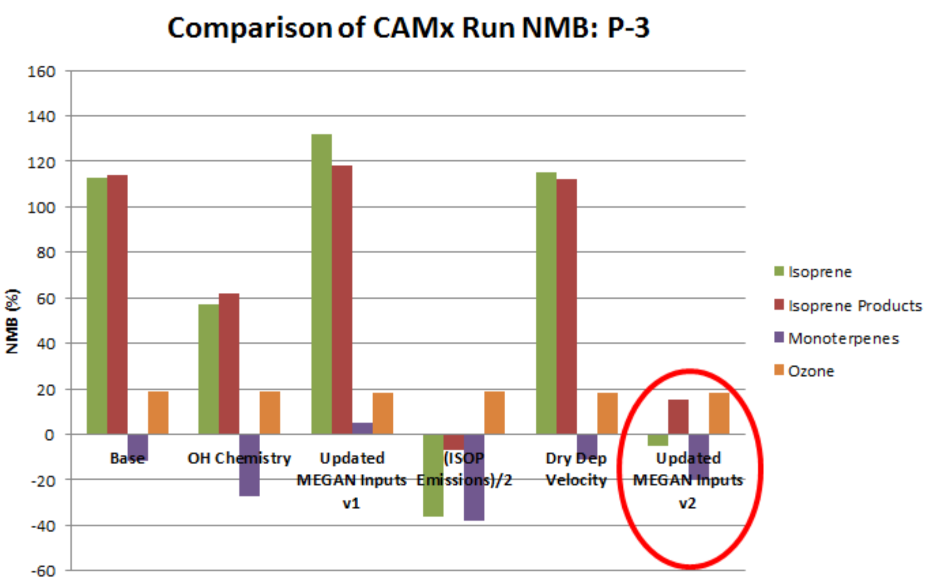

Figure 3. Summary of variation of NMB for the CAMx Base Run and sensitivity test results when model results were compared to P-3 measurements.

<u>Task 5: Project Management</u>
ENVIRON, NOAA and PNNL/Battelle prepared the draft final report and submitted it on May 18, 2015.

Delays or Technical Issues during the Reporting Period

The project remains on schedule for completion with delivery of the final AQRP-reviewed report by June 30, 2015. We intend to use all funds allocated to the project by 06/30/2015.

References

Nguyen, T., J. D. Crounse, A. P. Teng, J. M. St. Clair, F. Paulot, G. M. Wolfe, and P. O. Wennberg. 2015. Rapid deposition of oxidized biogenic compounds to a temperate forest. *PNAS*. www.pnas.org/cgi/doi/10.1073/pnas.1418702112.

Project 14-017	STATUS: Active – July 8, 2014

Incorporating Space-borne Observations to Improve Biogenic Emission Estimates in Texas

University of Alabama - Huntsville – Arastoo Pour Biazar
Rice University – Daniel Cohan

AQRP Project Manager – Elena McDonald-Buller
TCEQ Project Liaison – Mark Estes

Funding Amount: $199,982
($137,003 UAH, $62,979 Rice)

Executive Summary

One of the challenges in understanding the Texas air quality has been the uncertainties in estimating the biogenic hydrocarbon emissions. Biogenic volatile organic compounds, BVOCs, play a critical role in atmospheric chemistry, particularly in ozone and particulate matter (PM) formation. In southeast Texas, BVOCs (mostly as isoprene) are the dominant summertime source of reactive hydrocarbon. Despite significant efforts by the State of Texas in improving BVOC estimates, the uncertainties in emission inventories remain a concern. This is partly due to the diversity of the land use/land cover (LU/LC) over southeast Texas coupled with a complex weather pattern, and partly due to the fact that isoprene is highly reactive and relating atmospheric observations of isoprene to the emissions source (vegetation) relies on many meteorological factors that control the emission, chemistry, and atmospheric transport.

BVOC estimates depend on the amount of radiation reaching the canopy (Photosynthetically Active Radiation, PAR), and temperature. However, the treatment of temperature and PAR is not uniform across emissions models and still poses a problem when evaluating the inventories. Recent studies show that the largest uncertainty comes from the model solar radiation estimates and that using satellite-based PAR would be preferable. Emissions from soils also remain as one of the poorly quantified sources of NOx (nitrogen oxides) in most air quality models. Soils can be the largest source of NOx in rural regions where low-NOx conditions make ozone production efficiency especially high, contributing to background ozone levels.

The overall objective of the current activity is to advance our understanding of Texas Air Quality by utilizing satellite observations and the new advances in biogenic emissions modeling to improve biogenic emission estimates. This work specifically addresses a priority area in Texas AQ studies by improving biogenic emission estimates. In particular, the objectives are:

(1) To provide satellite-based PAR estimates for Texas during selected periods of 2006 and the Discover-AQ period (September, 2013).

(2) To produce an improved biogenic emission estimate for Texas and help in the evaluation of biogenic emission inventories over Texas by providing the best model representation of the atmospheric condition during the observations used for evaluation.

(3) To prepare and use a new soil NOx scheme that provides more mechanistic representation of how emissions respond to nitrogen deposition, fertilizer application, and changing meteorology.

The University of Alabama in Huntsville (UAH) currently generates a set of products from the Geostationary Operational Environmental Satellite (GOES) that includes surface incident short-wave radiation as well as cloud albedo and cloud top temperature. Under this activity, UAH will produce the Photosynthetically Active Radiation (PAR) needed in the estimation of biogenic hydrocarbon emissions. Satellite-derived PAR will be evaluated against previous satellite-based products as well as surface observations for the summer of 2006 and also during Texas Discover-AQ campaign. Furthermore, the new PAR retrievals will be used in MEGAN (the Model of Emissions of Gases and Aerosols from Nature) to generate BVOC emissions.

The new soil NOx scheme to be used is an implementation of the Berkeley-Dalhousie Soil NOx Parameterization (BDSNP) within MEGAN. A series of sensitivity simulations will be performed and evaluated against Discover-AQ observations to test the impact of satellite-derived PAR and the new soil NOx emission model on air quality simulations.

Project Update

The Rice team has adapted its implementation of the Berkeley Dalhousie Soil NO Parameterization (BDSNP) emission scheme from CMAQ into a stand-alone version that can be easily implemented for other air quality modeling platforms, such as CAMx, which is currently used as the host model for SIP modeling over Texas by TCEQ. The stand-alone BDSNP version does not require simulation of atmospheric processes by CAMx and therefore provides a computationally efficient approach to creating an offline soil NO emissions inventory. A new soil biome spatial map based on finer resolution land cover data and climate zone classification over the continental U.S. (CONUS) has been developed to link with published estimates for biome-specific base emission rates to produce more detailed NO emission estimates. The spatial pattern of this new soil biome map matches with the latest CONUS land cover GSI database from USGS and has much finer texture representations for the biome types with high base emission rates such as grassland, evergreen broadleaf forest and cropland. Furthermore, we are conducting a sensitivity test that replaces the existed world averaged soil biome base emission factors with the values derived from measurements over North America to better reflect local conditions.

For the biogenic VOC emission modeling, we have finished the evaluations of the University of Alabama-Huntsville (UAH) satellite insolation and photosynthetically active radiation (PAR) retrieval products by comparing with a different set of ground radiation network data over CONUS and Texas during August 2006. The UAH PAR/insolation product has much stronger correlations than a meteorological model (WRF) with observations in terms of temporal variations as well as spatial patterns. We also compared the UAH satellite PAR product with another PAR retrieval product from University of Maryland (UMD) at the same period and the results shown comparable statistic performance in terms of correlation and bias. However, the UAH PAR has much finer spatial texture than UMD PAR due to the high resolution (4km). We are conducting a series of WRF-MEGAN-CMAQ simulations by using different PAR inputs, namely the PAR from base case WRF, the PAR from a new WRF simulation with clouds assimilated by UAH, and the satellite-based PAR from UAH. The selected simulation time coincides with the DISCOVER-AQ Houston campaign in September 2013 so that we can take advantage of available measurement data for model evaluations. Comparisons of these simulations will enable us to evaluate the impact of these alternate inputs to ozone and particulate formation over Texas.

WRF simulations with cloud assimilation for 2013

The August and September 2013 WRF simulations were completed for three domains. Domain 1 is a 36 km grid covering the Continental United States (CONUS) region, domain 2 is a nested 12 km grid covering part of the Southern United States (SouthUS) and domain 3 is a nested 4 km grid covering Texas. This report will cover the model performance for all three domains with respect to clouds and surface measurements. The WRF configuration used for the simulations is given in Table 1.

The results of two different WRF simulations will be presented: the control (CNTRL) simulation and the GOES satellite assimilation (ASSIM) simulation. The CNTRL simulation only nudges in the NAM analysis temperature, wind, and mixing ratio data throughout the forecast time period, while the ASSIM simulation uses an analytical technique for assimilating in GOES satellite observations through the nudging field. Note that for domain 3, only winds were nudged into the model as indicated by Table 1. The main reason for this is that the nudging of analysis winds into WRF has been shown to reduce the positive wind bias that the WRF model produces. This also leads to smaller errors in the wind speed and direction.

Model Performance: To evaluate the model performance of the CNTRL and ASSIM simulations, the cloud agreement index (AI) and model statistics with respect to surface observations were calculated. The (AI) calculates how well the model does at producing clouds in the correct place and at the correct time when compared to GOES satellite observations. Thus, it will be used as the metric to rate the model cloud performance. The AI was calculated for each hour in the range 15:00-22:00 UTC in the August-September 2013 time frame. The time range was chosen to ensure maximum daylight coverage across the domain so that GOES imager observations are available. The hourly AIs were then averaged to produce the daily AI. To calculate model statistics with respect to surface observations, METSTAT was used to determine the model bias and root mean square error (RMSE) for wind speed, temperature, and mixing ratio.

Domain 1

The daily AI in Figure 1 shows that the ASSIM simulation has a greater AI than the CNTRL simulation for all days in the simulation time period. The average daily percentage increase in the AI from the CNTRL to the ASSIM simulation was found to be 12.71%. The individual hourly results similarly showed that the AI was greater for the ASSIM simulation than it was for the CNTRL simulation. The maximum hourly percentage increase was found to be 22.54%, while the minimum increase was 0.92%. These results show that this GOES assimilation technique, overall, does improve cloud placement in space and time relative to GOES satellite observations.

Table 1: WRF configuration

	Domain 1	Domain 2	Domain 3
Running Period	August – September 2013		
Horizontal Resolution	36 km	12 km	4 km
Time Step	90 s	30 s	10 s
Number of Vertical Levels	43		
Top Pressure of the Model	50 hPa		
Shortwave Radiation	RRTMG		
Longwave Radiation	RRTMG		
Surface Layer	Monin-Obukhov		
Land Surface Layer	Unified Noah (4-soil layer)		
PBL	YSU		
Microphysics	Thompson		
Cumulus Physics	Kain-Fritsch (with Ma and Tan 2009 trigger function)		None
Meteorological Input Data	NAM Analysis		
Analysis Nudging	Yes		Winds Only
U, V Nudging Coefficient	3×10^{-4}		3×10^{-4}
T Nudging Coefficient	3×10^{-4}		0
Q Nudging Coefficient	1×10^{-5}		0
Nudging within PBL	Yes for U and V, No for q and T		Yes for U and V

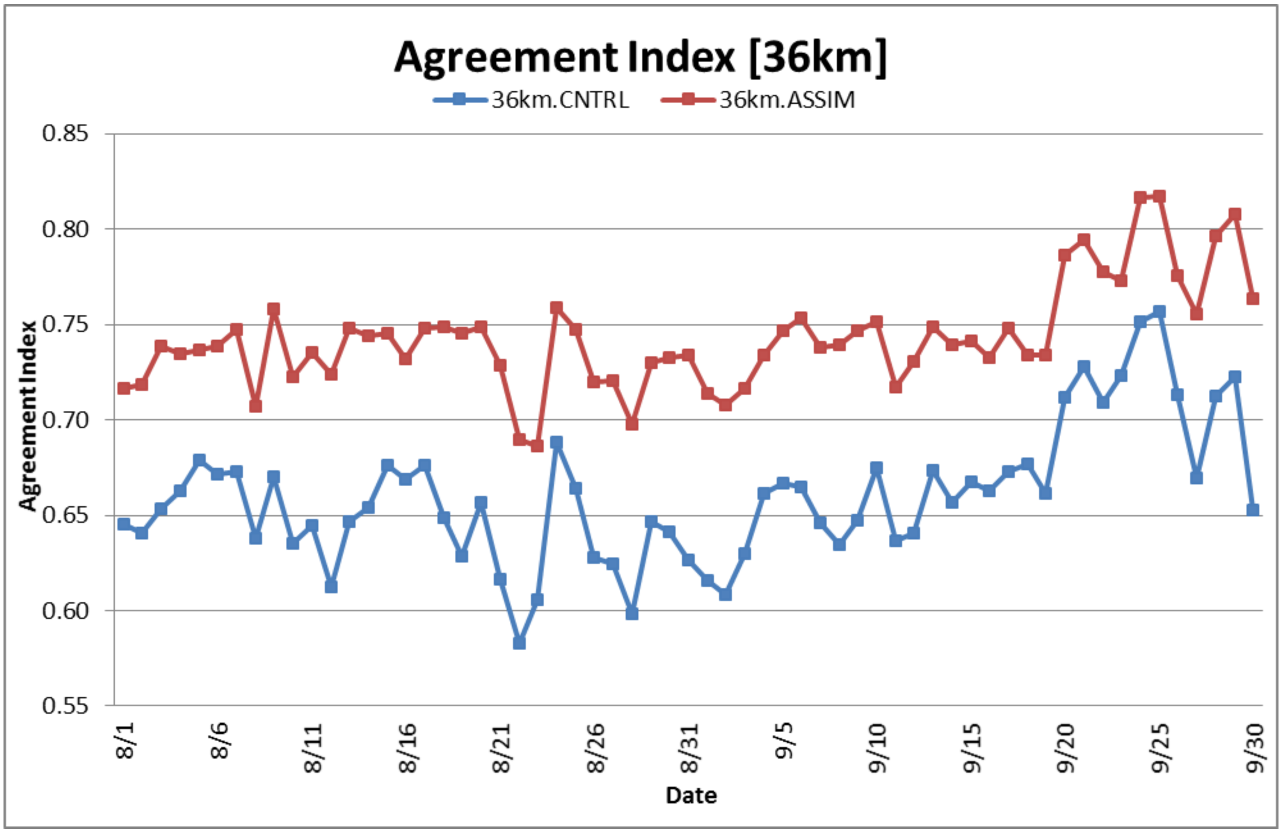

Figure 1: Daily agreement index for CNTRL and ASSIM 36 km WRF simulations over August-September 2013 using a 10% cloud albedo threshold.

Figure 2 shows a spatial plot of the agreement index for August 21, 2013 at 17 UTC. From Figure 2a, we see that the CNTRL simulation has trouble creating clouds in locations that GOES observes them as indicated by the large coverage of orange shading. Also, the CNTRL simulation tends to produce more clouds over the ocean than what is observed by GOES, as indicated by the red shading in Figure 2a. By assimilating GOES observations into WRF, the result is less overprediction and underprediction of clouds with respect to observations, as can be seen with the reduction of orange and red shading in Figure 2b when compared to Figure 2a.

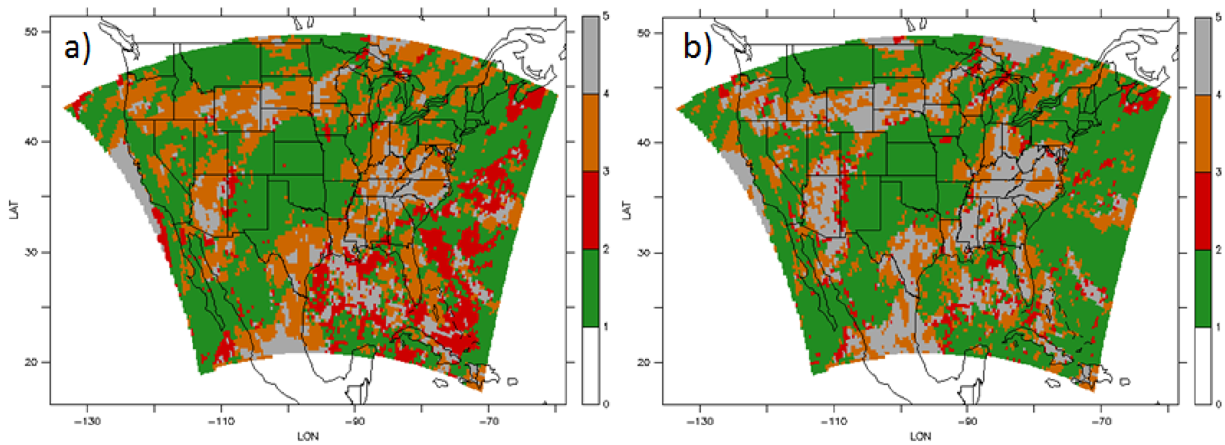

Figure 2: Agreement Index for August 21, 2013 at 17 UTC from a) CNTRL (AI=59.9%) b) ASSIM (AI=73.4%). Green indicates the model and GOES was clear, Red indicates locations where the model overpredicts clouds, Orange indicates locations where the model underpredicts clouds, and Grey indicates locations where the model and GOES are cloudy.

Wind speed and direction, temperature, and mixing ratio was also evaluated against surface observations. Overall, the results of the 36 km grid indicate that the assimilation technique led to better cloud agreement. In doing so, the ASSIM simulation increased the surface wind speeds across the domain and increased the surface moisture as well. The surface temperatures of the ASSIM simulation were closer to observations; this is expected of a simulation with better cloud agreement.

Simulations for domains 2 and 3 also show similar improvements. Figure 2 shows a snapshot from simulations for domain 2.

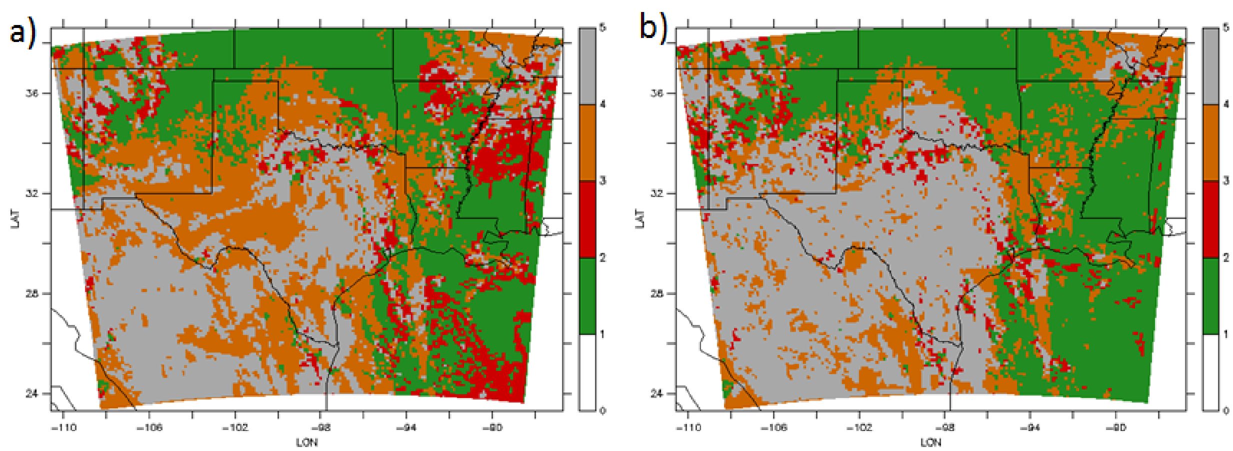

Figure 3: Agreement Index for August 27, 2013 at 22 UTC from a) CNTRL (AI=59.0%) b) ASSIM (AI=73.6%). Green indicates the model and GOES was clear, Red indicates locations where the model overpredicts clouds, Orange indicates locations where the model underpredicts clouds, and Grey indicates locations where the model and GOES are cloudy.

Overall, the results of the 12 km grid indicate that the assimilation technique still led to better cloud agreement. In doing so, the ASSIM simulation improved the model performance for surface temperature. As the grid size was reduced we also saw improvement in the wind speed statistics of the ASSIM simulation but there are still times where the error in the wind statistics is less for the CNTRL simulation. The mixing ratio results also started to become more variable between the two simulations but the CNTRL simulation tended to have less error on more days. With the reduction in the spatial coverage of the domain, it is likely that analyzing more spatial patterns would reveal the exact cause of the varying nature of which simulation performed better on a given day.

The results for domain 3 (4 km grid) indicate that the assimilation technique still led to better cloud agreement. In doing so, the ASSIM simulation once again improved the model performance for surface temperature. As the grid size was reduced, we also saw some further improvement in the wind speed statistics of the ASSIM simulation. However, there are still times where the error in the wind statistics is less for the CNTRL simulation. With the further reduction in the spatial coverage of the domain, it is likely that analyzing more spatial patterns would allow us to distinguish the physical processes responsible for the differences in the surface statistics. It is also apparent that there are distinct periods of time where one simulation out performs the other. This indicates that more analysis spatially still needs to be completed to determine the cause.

Project 14-020	**STATUS: Active – February 2, 2015**

Analysis of Ozone Formation Sensitivity in Houston Using the Data Collected during DISCOVER-AQ and SEAC4RS

University of Maryland – Xinrong Ren

AQRP Project Manager – Vincent Torres
TCEQ Project Liaison – Doug Boyer

Funding Amount: $70,000

Executive Summary

Despite great efforts undertaken in the past decades to address the problem of high ozone concentrations, our understanding of the key precursors that control tropospheric ozone production remains incomplete and uncertain. Sensitivity of ozone production to nitrogen oxides (NO_x) and volatile organic compounds (VOCs) represents a major uncertainty for oxidant photochemistry in urban areas and is expected to vary from location to location and from time of a day. Understanding of the non-linear relationship between ozone production and its precursors is critical for the development of an effective ozone control strategy.

The DISCOVER-AQ campaign in Houston in August/September 2013 provided rich data sets to examine and improve our understanding of atmospheric photochemical oxidation processes related to the formation of secondary air pollutants like ozone and particulate matter (PM). In this project, an analysis of ozone production and its sensitivity to NO_x and VOCs will be performed. An observation-constrained box model based on Carbon Bond mechanism, Version 5 (CB05) will be used to study the photochemical processes along the NASA P-3B flight track, as well as at eight surface sites where the P-3B conducted spiral profiles. Ozone (O_3) production rates will be calculated at different locations and at different times of day and its sensitivity to NO_x and VOCs will be investigated. Spatially and temporally resolved ozone production and its sensitivity will also be investigated.

This project specifically addresses one of the AQRP priority research areas: Improving the understanding of ozone and particulate matter (PM) formation, and quantifying the characteristics of emissions in Texas through analysis of data collected during the DISCOVER-AQ campaign. The following tasks will be performed in this project:

An investigation of spatial variations of ozone production and its sensitivity to NO_x and VOCs in Houston during DISCOVER-AQ.

(1) An investigation of temporal variations of ozone production and its sensitivity to NO_x and VOCs in Houston during DISCOVER-AQ.

Investigate non-uniform emission reduction of O_3 pollution in Houston using spatial and temporal variations of ozone production and its sensitivity to NO_x and VOCs.

(2) Calculation of ozone production efficiency (OPE) at different locations using the ratio of ozone production rate to the NO_x oxidation rate calculated in the box model.

These activities will strengthen our understanding of O_3 production, which is essential to meet the primary and secondary National Ambient Air Quality Standards (NAAQS) for ozone.

Project Update

During the period from March 1 to May 31, 2015, the team at University of Maryland College Park has accomplished the following tasks:

(1) We set up the box model with the Carbon Bond Version 5 (CB-05) mechanism.

(2) CMAQ model output created for 14-004 was extracted along the P-3B flight tracks for the month of September for input to the box model.

(3) We prepared input files for the CMAQ model run with process analysis.

(4) CMAQ model output was extracted along the P-3B flight tracks for the month of September and was used as input to constrain the CB05 box model for long-lived species that were not measured on the P-3B.

(5) We continued working on the programming of Matlab program that will be used to analyze the box model results for ozone production and its sensitivity to NOx and VOCs.

(6) Initial box model run has been conducted based on Carbon Bond Version 5 (CB05) mechanism. We compared the box model results with the CMAQ results. Figure 1 shows some comparison results between CB05 and CMAQ for the intermediate species: OH, HO_2, methylperoxy radical (MEO_2), and other higher alkylperoxy radicals (XO_2 that concerts NO to NO_2). These intermediate are very important for the calculation of ozone production. Any differences in these species will contribute to the difference in ozone production in the CB05 box model and CMAQ model.

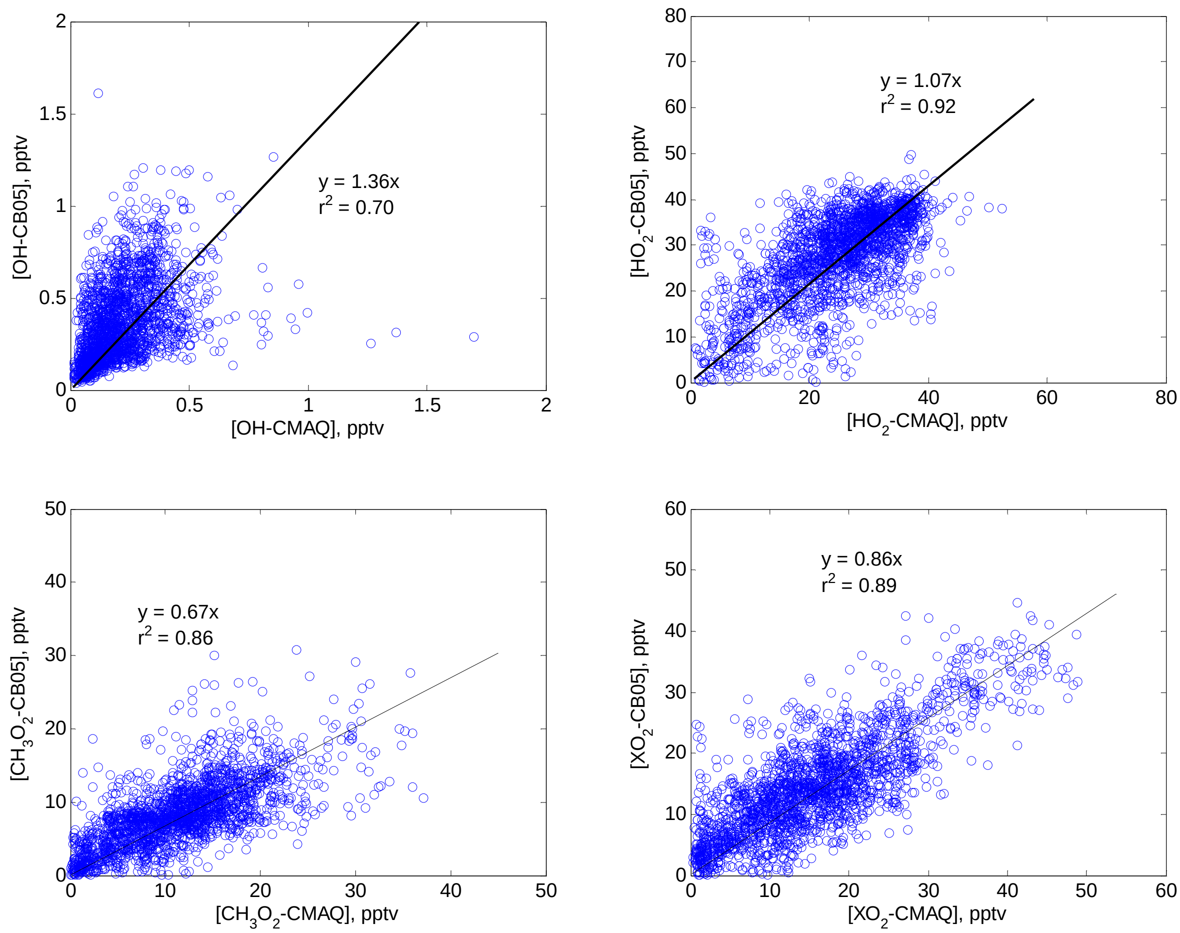

Figure 1. Comparison between CB05 and CMAQ for some intermediate species: OH, HO_2, methylperoxy radical (MEO_2), and other higher alkylperoxy radicals (XO_2 that concerts NO to NO_2).

As we can see in Figure 1, there are some differences in these intermediates and this will result in differences in ozone production rates calculated using the CB05 box model and the CMAQ model results. We found the reasons for these differences are the differences in some precursors in the box model (measured on the P-3B) and the CMAQ model (calculated from emissions) as shown in Figure 2. We noticed the correlation between the P-3B measured NOx (NO and NO_2) and the CMAQ modeled NOx is particularly poor. As we know the intermediates shown in Figure 1 are very sensitive to NO and NO_2. We will compare these species again after the new CMAQ simulations with updated emissions files.

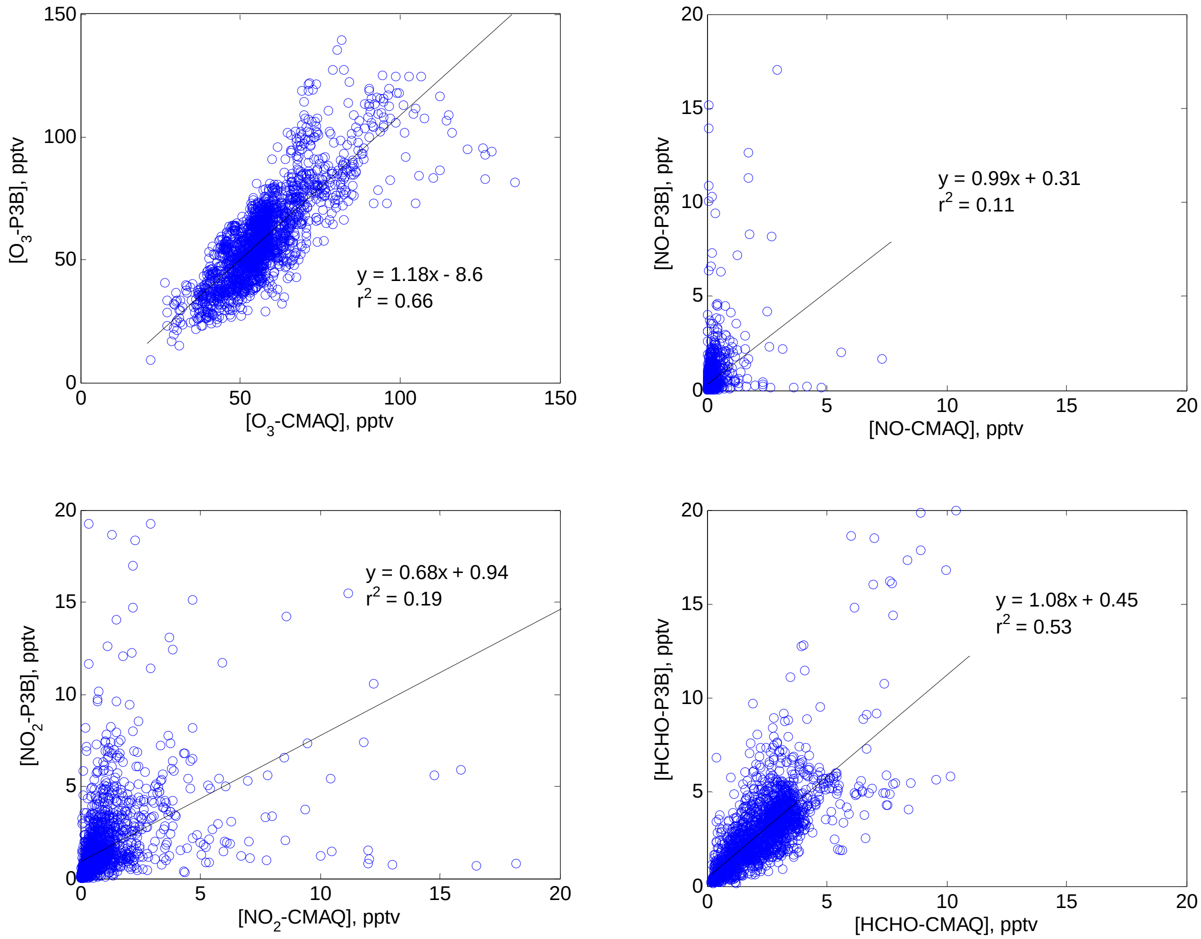

Figure 2. Comparison between P-3B observations and CMAQ model for some precursors: O_3, NO, NO_2, and formaldehyde (FORM).

During the next quarter, the following tasks are anticipated to be accomplished:

(1) The WRF-CMAQ model will be re-run using the updated emission files and new CMAQ model output will be extracted along the P-3B flight tracks for the month of September 2013 and will be used as input to constrain the box model.

(2) We will re-run the CB05 box model using the new input file.

(3) We will use the box model results to calculate ozone production and its sensitivity to NOx and volatile organic compounds (VOCs) along the NASA P-3 flight track during the DISCOVER-AQ study in Houston in 2013.

(4) We will also run CMAQ with process analysis in order to map the ozone production efficiency (OPE) and nitrogen oxides (NOx) and VOC limited areas throughout the Houston metropolitan area.

Project 14-022	STATUS: Active – February 19, 2015

Use of satellite data to improve specifications of land surface parameters

University of Alabama-Huntsville – Richard McNider
George Mason University – Daniel Tong

AQRP Project Manager – Vincent Torres
TCEQ Project Liaison – Bright Dornblaser

Funding Amount: $116,000
($71,004 UAH, $44,996 GMU)

Executive Summary

Land surface processes play a critical role in air quality model performance. Land surface temperatures impact boundary layer heights and turbulent mixing. Temperature gradients can also produce local wind patterns. For example in Houston the land-sea temperature gradient drives both the daytime sea breeze and nighttime land breeze. This growing temperature contrast in the morning is responsible for physical features such as a dead zone ahead of the sea breeze front, which develops as the land sea pressure gradient force opposes the large scale weather pattern. This dead zone allows the accumulation of precursors that are part of the peak ozone levels later in the day as this dead zone moves northward with the sea breeze front. Surface temperatures also impact air quality levels through temperature dependence of evaporative emissions and biogenic emissions. Temperatures also control the thermal decomposition of nitrogen species, which in turn impacts the efficiency of ozone production per NO molecule emitted. Thus, not only can temperatures affect ozone production, they can impact the efficacy and efficiency of control strategies.

It is the purpose of this project to evaluate and improve the performance of the land surface models used in the meteorological model (WRF) by the use of satellite skin temperatures to better specify physical parameters associated with land use classes. While considerable work has been done by the national community and especially in Texas to develop improved land use classifications, land use classes themselves are not directly used in models. Rather, physical parameters such as heat capacity, thermal resistance, roughness, surface moisture availability, albedo etc. associated with a land use class are actually used in the land surface model. Many of the land use class associated parameters such as surface moisture availability are dynamic and ill-observed depending on antecedent precipitation and evaporation, soil transport, the phenological state of the vegetation, irrigation applications etc. Other parameters such as heat capacity, thermal resistance or deep soil temperature are not only difficult to observe they are often unknowable *a priori.* This project will use satellite data to retrieve or adjust these critical land surface parameters.

The project will first develop skin temperature data sets from geostationary satellites and polar orbiting platforms and make direct comparisons to the skin temperatures from the WRF land surface model. This will be done for intensive field programs such as the recent DISCOVER-AQ and SEAC4RS campaigns. Second, techniques to use satellite observed skin temperatures to adjust land surface parameters such as surface moisture and surface thermal resistance will be tested to improve WRF skin and air temperatures. Extensive evaluation of model performance will be made against standard National Weather Service observations, special observations made

during the DISCOVERY-AQ field campaign in September 2013 and other independent satellite observations.

Project Update

This is the 2nd quarterly report of the project that covers the efforts in March, April, and May. During this period we provided two deliverable reports under Task 2 and 3 of the proposed work. The focus of Task 2 is to provide a diagnosis of a true skin temperature from the WRF Pleim-Xiu scheme. The Pleim-Xiu scheme uses a prognostic equation for the ground surface temperature given by equation (1) below.

$$\frac{1}{c_t}\frac{\partial T_g}{\partial t} = R_s + L_{dn} - \varepsilon\sigma T_g^4 - H - E - G$$

(1)

Here, R_s is the short wave radiation, L_{dn} is the longwave down radiation., H is the sensible heat flux, E is the latent heat flux, and G is the ground heat flux. However, this ground temperature,T_g, is associated with a finite heat capacity/resistance (the inverse of c_t in the prognostic equation) so that T_g does not have the dynamic range of a true skin temperature Here we recover a true skin temperature by taking the limit when the heat capacity/resistance goes to zero (see Mackaro et al. 2011).

$$0 = R_s + L_{dn} - \varepsilon\sigma T_s^4 - H - E - S$$

(2)

The skin temperature is found by rootfinding techniques in this algebraic equation.

Here S is the flux to the skin from both the canopy and bare soil

$$S = [(1-V)C_s + VC_v](T_s - T_g)$$

With V being the vegetative fraction and C_s and C_v the soil and vegetative heat capacities.

And the focus of Task 3 is the evaluation of satellite skin temperature products that we select to use in adjusting the skin temperature in the WRF simulations. This quarterly report includes highlights of the two deliverable reports.

<u>Background:</u> As part of this project we had proposed that satellite skin temperatures might be a better metric for model performance evaluation than standard National Weather Service (NWS) data in large part because of their ability to capture land use variations at fine resolution. Also, the project proposed that these satellite skin temperatures might also provide a better data set to nudge soil moisture than the use of NWS data in the Pleim-Xiu land surface assimilation scheme. However, the original Pleim-Xiu scheme did not have a true skin temperature but a ground temperature reflecting a 1 cm layer with a specific heat capacity. We describe a technique to

diagnose a skin temperature within the Pleim-Xiu land surface model. This is applied in the WRF model and examples of skin temperature provided during the Discovery AQ period. Horizontal spatial plots and selected time series plots demonstrate expected behavior.

Satellite skin temperatures are planned to be used to adjust soil moisture in a new version of the Pleim-Xiu (PX) scheme in a similar way that observed surface air temperatures are used to adjust moisture in the current PX scheme. However, skin temperatures as derived from satellite information have potential issues in terms of assumptions about surface emissivity and corrections for intervening atmosphere and cloud contamination. Under this activity we are to use a new product, the GSIP skin temperature data set developed by NOAA, rather than a previous MSFC skin temperature product. Thus, it is the purpose of this report to evaluate the utility of the GSIP product and also describe QA/QC plans for the skin temperature products. It also provides a first comparison to the skin temperatures from the Discovery AQ NASA aircraft.

The GSIP product is evaluated against skin temperature derived from MODIS data and measured at a surface station. The evaluation shows the GSIP skin temperature tends to give extremely high values in some vast areas and have cloud contamination issues. We are exploring three alternative paths to the GSIP skin temperature product. The evaluation of a third skin temperature dataset used in the ALEXI system (Anderson et al. 2007a, Anderson et al. 2007b) shows some promising results.

Highlights Task 2 Deliverable Report

This is the second deliverable report under this activity and its focus is the description and examples of diagnosing skin temperatures within the context of the Pleim–Xiu Land Surface Model (LSM) (Pleim and Xiu 1995, Xiu and Pleim 2001, and Pleim and Xiu 2003) as used in WRF and hereafter referred to as the PX model. The following describes the original task and deliverable to which this report is addressed.

Initial One-Dimensional Tests

The First International Satellite Land Surface Climatology Field Experiment (FIFE) provides observations for most of the relevant surface energy budget variables. The diagnosis technique discussed above in the Background section was first tested in a one-dimensional version of the PX model for a FIFE location for the approximate period 6-22 August 1987 with the results shown in Fig. 1. A three-dimensional WRF run provided the nudging field that we used above the boundary layer. The diagnosed skin temperatures agreed well with the observed FIFE values on several days, but with considerably higher values than observed during the period 9-11 August. This was likely due to a combination of two factors. The first is that we may not have nudged strongly enough above the boundary layer so that the impact of frontal passages is not being “felt” in the one-dimensional model, especially near the surface. The second is that the one-dimensional model used GOES-derived insolation which had a fixed water vapor value that in general overestimates the insolation which would lead to higher temperatures. This is related to the insolation issues we discussed in the first report.

Horizontal Plots from WRF Simulation

Figure 2 is an example of the diagnosed skin temperature for 1800 UTC 13 September 2013 for the simulation where the WRF internal downward shortwave radiation was replaced by the GOES-derived values from the GSIP archive (described in the previous report) which is the so-called “insolation” run

From the evidence thus far it appears that the implementation of a scheme to diagnose a skin temperature within the structure of the PX model is giving reasonable values. Large differences can occur in the skin temperature field between the control and insolation runs indicating the surface is responding to the GOES-derived estimated insolation. Relative to a discussion mentioned in the previous report, we have completed our own insolation retrieval for September 2013 and are in the process of comparing it to observed pyranometer data.

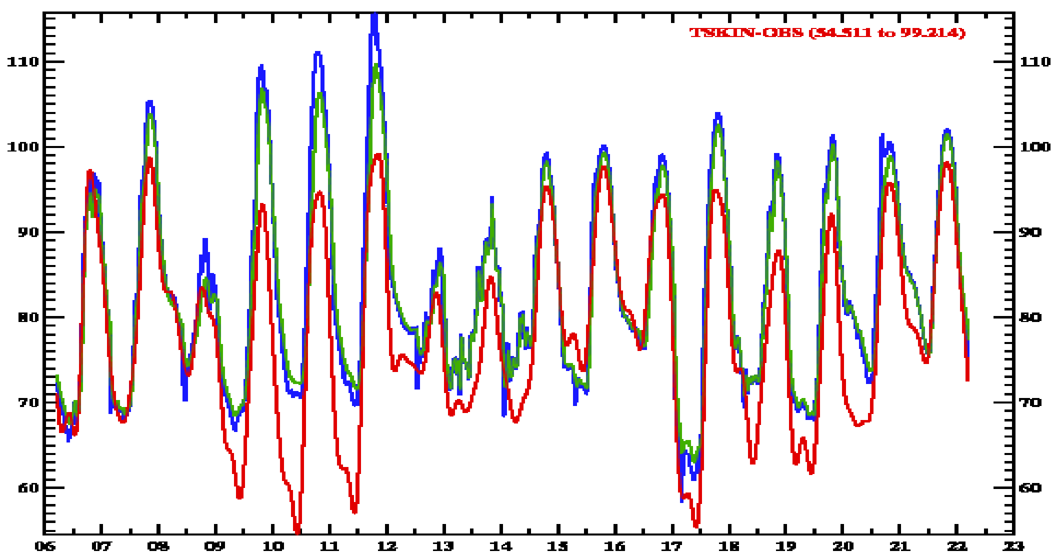

Fig. 1. Time series of diagnosed skin temperature (blue), top layer PX model temperature (green), and observed skin temperature (red) for the period 0515 UTC 6 August through 0445 UTC 22 August 1987 for FIFE location 1916. Results are from a 1-D model using the same PX model physics as the 3D WRF version. Units are in degrees F.

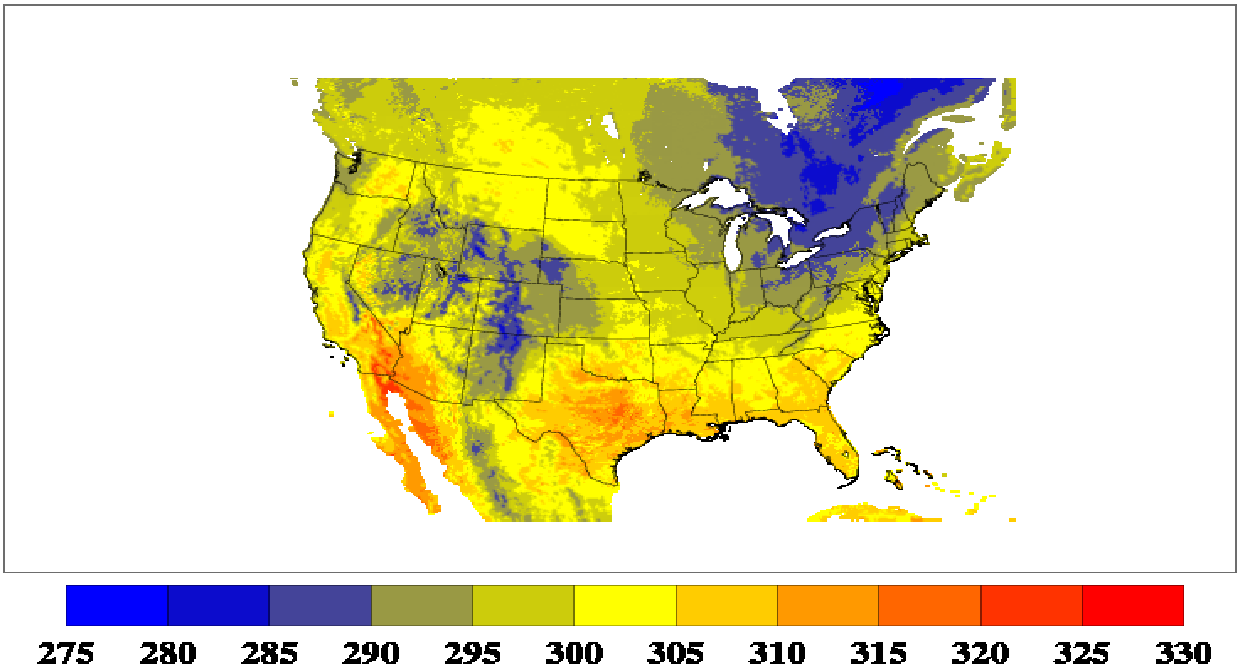

Fig. 2. WRF diagnosed skin temperature for the insolation simulation for 1800 UTC 13 September 2013 in units of K. Only land points shown.

<u>Highlights Task 3 Deliverable Report</u>
<u>Satellite Skin Temperature Comparisons</u>
Under this activity we provide initial inter-comparisons of three satellite Land Surface Temperature (LST) products – these are the GOES- GSIP standard LST product (Heidinger et al 2013 see also data links [NOAA GSIP Data]), a physical split window technique (Haines et al. 2001, Guillory et al. 1993) produced locally at MSFC and referred to as the SPoRT Skin Temperature and the MODIS operational LST product (see Wan and Dozier 1996 and updates). Though the GOES-GSIP product was new to our team we had chosen it as the primary data set to be used because it had complete CONUS (through both GOES EAST and GOES WEST) coverage and was an operational product supported by NOAA. The locally produced MSFC product only used GOES- EAST so that western areas beyond the Rockies were not included in the product.

However, when we first began an evaluation of the GSIP product we found some troubling aspects in the western U.S. in that afternoon skin temperatures appeared too large to be physically correct.

Figure 3 provide a spatial comparison between the WRF and GSIP Skin temperatures for the two day time passes of the MODIS LST for when skies were relatively clear over Texas. These two days give concern that over the western part (perhaps high altitude) part of the domain that GSIP skin temperatures are problematic.

Model Comparisons to With Discovery AQ Aircraft Data
During September 2013, in-situ air and surface temperature measurements were taken on the NASA P-3B aircraft on multiple days in the Greater Houston area in Texas in support of NASA's 3rd DISCOVER-AQ field campaign.

Hereafter we compared the WRF model simulations and the GSIP surface temperature product against the P-3B aircraft measurements on September 25, 2013. It was a clear day and thus the aircraft and GSIP surface temperature observations had less cloud contamination.

They were compared against in-situ temperature measurements onboard the flight. Figure 4 shows the spatial distributions of observed, WRF modeled (Base case) and GSIP surface temperature along the P-3B flight path on this day

Conclusions and Next Steps
While the problems with the GSIP skin temperature products in the west will require careful quality control, the variations in the East look physical and appear to suggest that they can be used for assimilation in the PX scheme. However, we will explore other alternatives to the GSIP data. There are three paths that we can explore further:

1. Blending of the GSIP and SPoRT products to replace GSIP with SPoRT if GSIP tendencies significantly exceed SPoRTt tendencies.
2. Use of MODIS data rather than GCIP data for the tendencies needed.
3. We are also exploring the use of a third skin temperature data set used in the ALEXI system (Anderson et al. 2007a, Anderson et al. 2007b) provided by Chris Hain of NOAA.

So far, the initial examination of the dataset provided by Dr. Hain has shown some promising results (see Fig. 5). The extreme high daytime temperature over some mountainous areas shown in the GSIP product is greatly reduced and cloud contamination pixels are removed. While we will continue to evaluate all these paths with more tests we may abandon some of these paths if a particular path looks like it will best provide a solution.

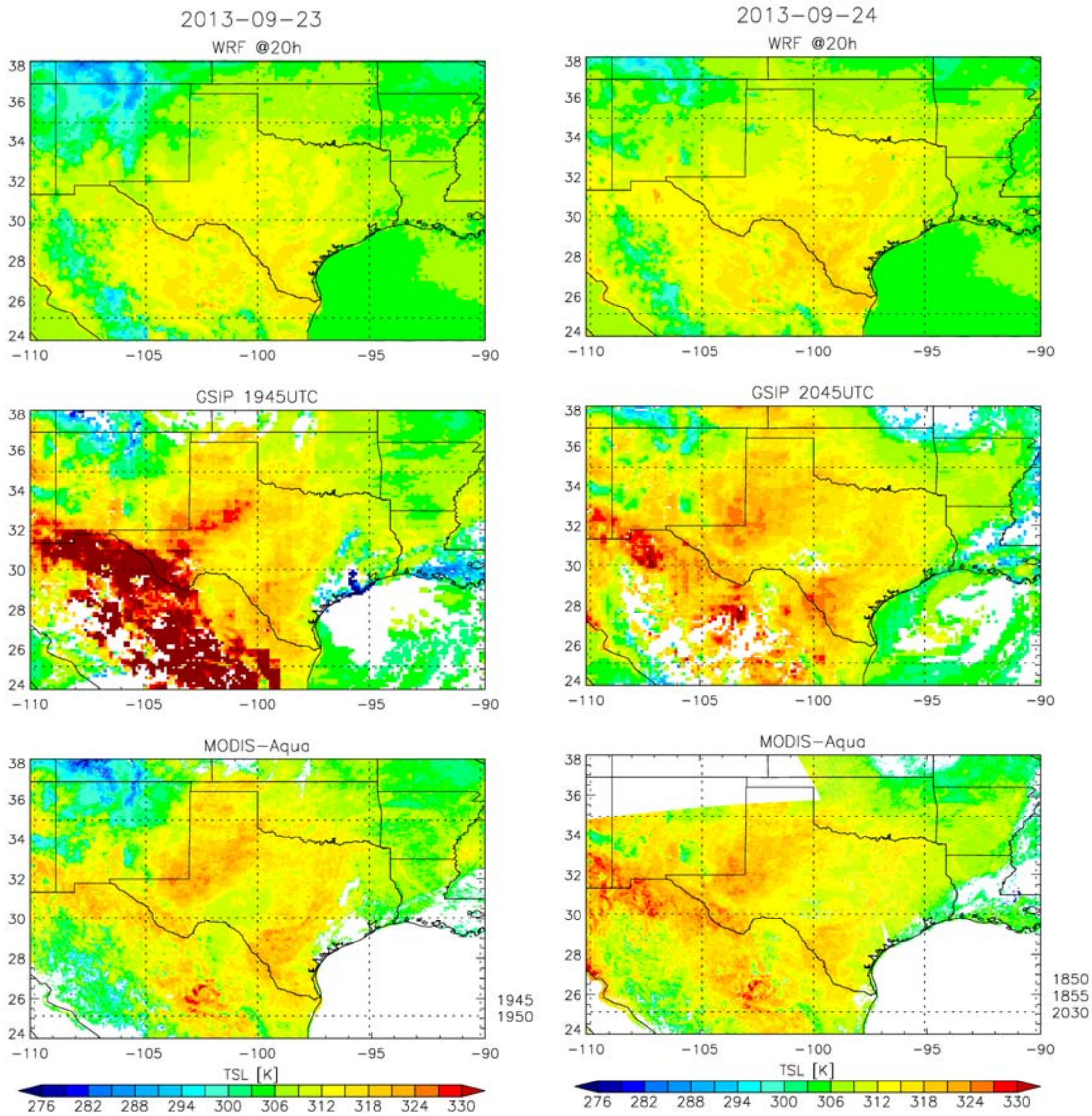

Fig. 3 Skin Temperature, from top to bottom—WRF, GSIP, and MODIS(Aqua). Left panels are for Sep 23, 2013 (Aqua overpass time was 19:45&19:50 GMT), right panels for Sep 24, 2013 (main Aqua overpass time was 20:30 GMT).

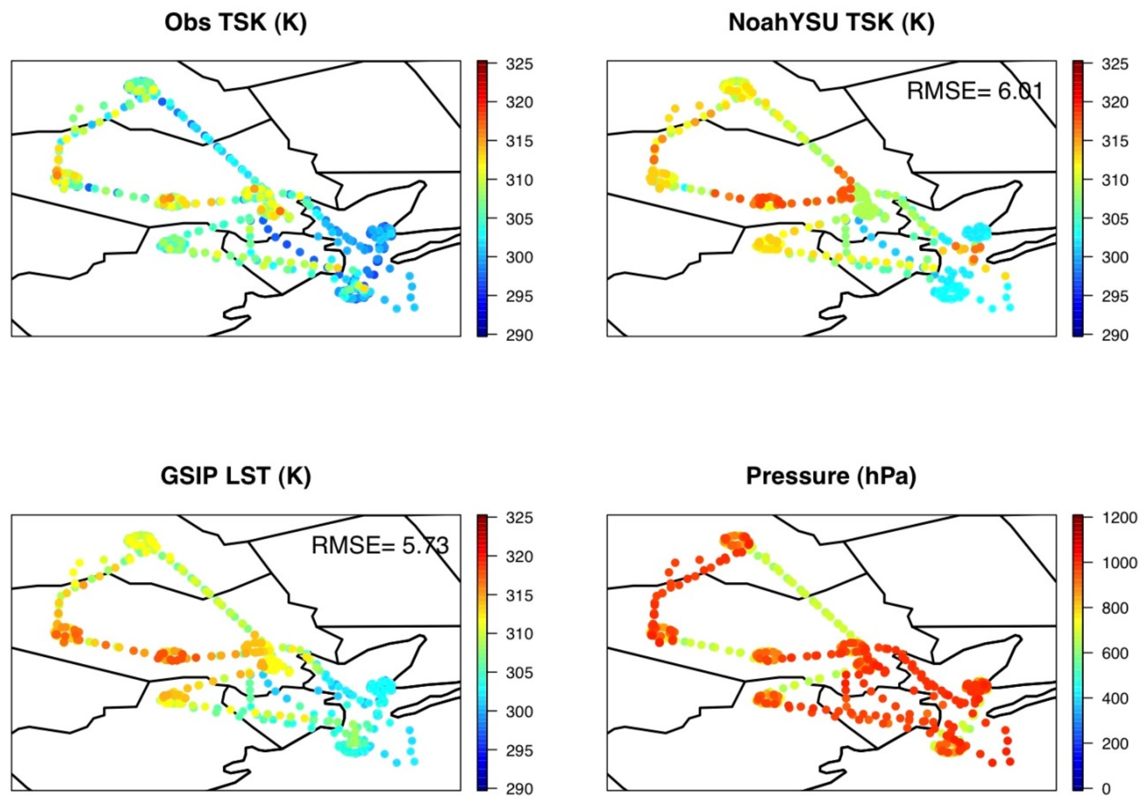

Fig. 4 Spatial distributions of observed, modeled (Base case) and GSIP surface temperature along the P-3B flight path on September 25, 2013. Aircraft altitude is indicated as pressure plot on lower right panel.

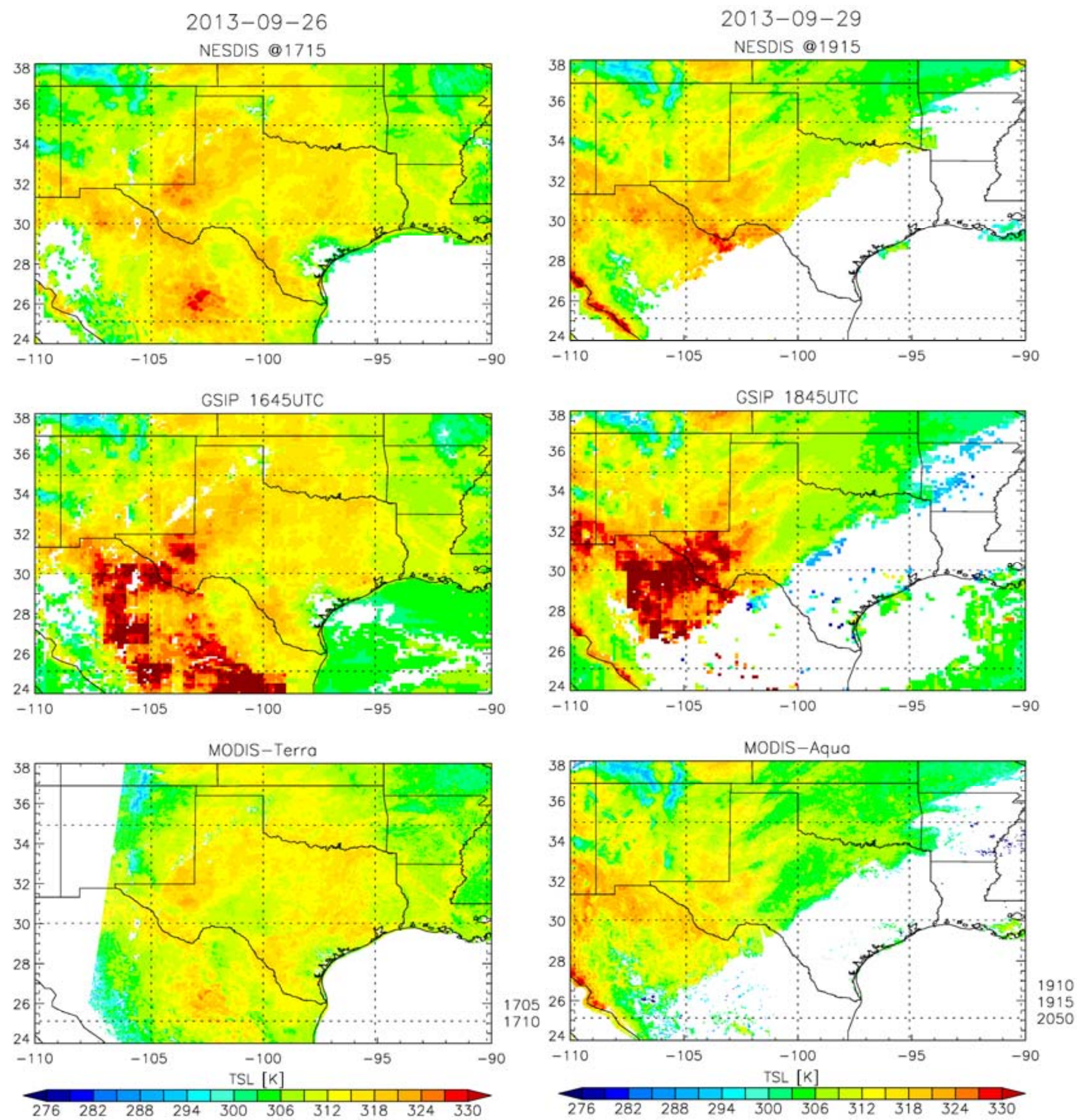

Fig. 5. Satellite skin temperature products at Terra overpass (left panels) on Sep 26, 2015 and Aqua over pass (right panels) on Sep 29, 2015. The panels in the top row are for the skin temperature product from Chris Hain at NESDIS (ALEXI); panels in the middle are for the GSIP Tskin product; and in the bottom are for the MODIS LST product.

References

Anderson, M.C., Norman, J.M., Mecikalski, J.R., Otkin, J.A. and Kustas, W.P., 2007a. A climatological study of evapotranspiration and moisture stress across the continental United States based on thermal remote sensing: 1. Model formulation. J. Geophys. Res., 112(D10): D10117.

Anderson, M.C., Norman, J.M., Mecikalski, J.R., Otkin, J.A. and Kustas, W.P., 2007b. A climatological study of evapotranspiration and moisture stress across the continental United States based on thermal remote sensing: 2. Surface moisture climatology. J. Geophys. Res., 112(D11): D11112.

Haines, S. L., R. J. Suggs, and G. J. Jedlovec, 2001: Inter-comparison of GOES-8 Imager and Sounder skin temperature retrievals. Preprints, 11th Conf. on Satellite Meteorology and Oceanography, Madison, WI, Amer. Meteor. Soc., 516-519.

Heidinger, A. K., I. Laszlo, C. C. Molling, and D. Tarpley (2013), Using SURFRAD to Verify the NOAA Single-Channel Land Surface Temperature Algorithm, J. Atmos. Oceanic Technol., 30(12), 2868-2884, doi:Doi 10.1175/Jtech-D-13-00051.1.

Jin, Minglen and Robert E. Dickinson (1999) Interpolation of surface radiative temperature measured from polar orbiting satellites to a diurnal cycle 1. Without clouds. J.Geophy, Res, 104, 2105–2116

Oleson,K. W., D. M. Lawrence, G. B. Bonan, M. G. Flanner, E. Kluzek, P. J. Lawrence, S. Levis, S. C. Swenson, P. E. Thornton, A. Dai, M. Decker, R. Dickinson, J. Feddema, C. L. Heald, F. Hoffman, J.-F. Lamarque, N. Mahowald, G.-Y. Niu, T. Qian, J. Randerson, S. Running, K. Sakaguchi, A. Slater, R. Stöckli, A. Wang, Z.-L. Yang, X. Zeng, X. Zeng, 2010: Technical Description of version 4.0 of the Community Land Model (CLM), NCAR Technical Note NCAR/TN-478+STR.

Pleim, E. F., A. Xiu, 1995: Development and testing of a surface flux and planetary boundary layer model for application in mesoscale models. *J. Appl. Meteor.*, **34**, 16-32.

Pleim, E. F., A. Xiu, 2003: Development of a land surface model. Part I: Application in a mesoscale meteorological model. *J. Appl. Meteor.*, **40**, 192-209.

Wan, Z., and J. Dozier, 1996: A generalized split-window algo-rithm for retrieving land-surface temperature from space.IEEE Trans. Geosci. Remote Sens.,34,892–905.

Xiu,A. and E. F. Pleim, 2001: Development of a land surface model. Part II: Data assimilation. *J. Appl. Meteor.*, **42**, 1811-1822.

Project 14-023	STATUS: Active – May 23, 2014 Ended – August 31, 2014

Assessment of Two Remote Sensing Technologies to Control Flare Performance

The University of Texas at Austin – Vincent Torres
Aerodyne Research, Inc. – Scott Herndon
Leak Surveys, Inc. – Joshua Furry
Providence Photonics, LLC – Yongshen Zeng

AQRP Project Manager – David Sullivan
TCEQ Project Liaison – Russell Nettles

Original Funding Amount: $480,741
($239,773 UT-Austin, $157,066 Aerodyne, $26,716 Leak Survey, $57,186 Providence Photonics)

Final Funding Amount: $36,587.11 ($25,874.37 UT-Austin, $10,712.74 Aerodyne)

Executive Summary

Industrial flares are devices used at industrial facilities to safely dispose of relief gases in an environmentally compliant manner through the use of combustion. Recent studies of industrial air- and steam-assisted flares have shown that merely complying with federal regulations like the Environmental Protection Agency's 40CFR § 60.18 and 40CFR § 63.11, do not ensure the flare will operate with at high combustion efficiency when combusting hydrocarbons over the entire range of operating scenarios for dual service flares. For vent gas streams containing hydrocarbons, the combustion efficiency (CE) is the percentage of the total hydrocarbon stream entering the flare that burns completely to form only carbon dioxide and water. It is desirable to have high combustion efficiency at all times to maximize flare performance.

The purpose of the proposed project was to conduct a series of field tests using an operational, full-scale industrial flare at a Petrologistics, LLC plant in Houston, Texas, to determine the technical, economic and operational feasibility of two approaches designed to maximize flare performance. These approaches continuously measure or determine the flare's combustion efficiency and would use this information to adjust the steam assist to the flare to adjust the flare's performance. To assess the technical performance of the approaches, the combustion efficiency measurements of each approach will be compared to an independent direct sampling measurement (the reference measurement) of the flare's combustion efficiency to determine the accuracy and completeness of the measurements obtained from the two approaches. For the field tests, the performance of the flare will not be controlled by either of the two approaches so that the prescribed test plan can be conducted with the flare. After the test series, the economic and operational feasibility will be evaluated based on the operational and safety characteristics observed during the tests and the estimated cost to implement each approach.

Project Update

On August 15, 2014, notice was sent to the AQRP Project Manager that the project would need to be ended and all unspent funds returned to the AQRP due to the plant where the testing was to be done no longer being able to participate.

No further work will be performed or costs incurred on this project.

Sources of Organic Particulate Matter in Houston: Evidence from DISCOVER-AQ Data, Modeling and Experiments

The University of Texas at Austin – Lea Hildebrandt Ruiz
Environ – Greg Yarwood
University of California – Riverside – Gookyoung Heo

AQRP Project Manager – Elena McDonald-Buller
TCEQ Project Liaison – Shantha Daniel

Funding Amount: $300,000
($163,282 UT-Austin, $101,404 Environ, $35,314 UC – Riverside)

Executive Summary
The United States Environmental Protection Agency recently lowered the annual National Ambient Air Quality Standard (NAAQS) for particulate matter smaller than 2.5 μm in diameter ($PM_{2.5}$) from 15 to 12 μg m^{-3}. This new annual standard brings the Houston region near to non-attainment for $PM_{2.5}$, underlining the importance of understanding the composition and sources of $PM_{2.5}$ in Houston. Recent measurements made during the month of September indicate that a majority of $PM_{2.5}$ in the Houston region is composed of organic material. An improved understanding of Houston organic aerosol is therefore essential and will directly benefit the Texas Commission on Environmental Quality (TCEQ) in understanding how to manage Houston's air quality.

Project 14-024 will focus on improving our understanding of the contributions of intermediate volatility organic compounds (IVOC) to formation of secondary organic aerosol (SOA). IVOCs, specifically large alkanes and polycyclic aromatic hydrocarbons, are largely excluded from current emission inventories because these compounds fall between the definitions of volatile organic compounds (VOC) and primary organic $PM_{2.5}$. Emissions of IVOC are expected to be high in Houston, due to the combination of petrochemical industry and mobile source emissions, and the contributions of IVOC to SOA appear to be important but underestimated. Work will include analysis of recently collected ambient data during DISCOVER-AQ on PM concentration and composition, new environmental chamber experiments on the SOA formation potential of IVOC, and photochemical modeling of the Houston region. Modeling of the formation of SOA from VOC and IVOC precursors will use a new state of the art approach based on the Volatility Basis Set (VBS) that has recently been implemented in the Comprehensive Air-quality Model with extensions (CAMx).

Project Update
In this quarter the UT Austin team continued analysis of DISCOVER-AQ data. This included finalizing analysis of data on bulk concentrations of organic and inorganic species collected by an aerosol chemical speciation monitor (ACSM) located at the Conroe measurement site. On average, 72 percent of non-refractory PM_1 (particulate matter smaller than 1 μm in diameter) was organic material, including a high fraction of organic nitrates. There was little diurnal variation in the concentrations of ammonium sulfate; however, concentrations of organic and organic

nitrate aerosol were consistently higher at night than during the day. Concentrations of inorganic ions in $PM_{2.5}$ filters collected at Conroe were quantified by the Dessert Research Institute (DRI). In general, results from the filter analysis agreed well with concentrations measured by the ACSM. Filter analysis results also confirmed that concentrations of inorganic nitrate were very low during the measurement campaign and that nitrate observed by the ACSM was due to organic nitrate species. Final quality-assured data on PM_1 mass concentrations (from the ACSM) as well as results from the inorganic filter analysis were shared with investigators of AQRP projects 14-009 and 14-029.

In addition to the bulk concentration analysis the UT Austin team also conducted positive matrix factorization (PMF) analysis on the aerosol mass spectrometer data collected by the ACSM and on the gas-phase data collected by the chemical ionization mass spectrometer (CIMS) operated with iodide-water cluster ionization. PMF analysis on the ACSM data suggests that the organic aerosol consisted mostly of oxygenated organic aerosol, as expected considering the distance of the measurement site from major primary sources as well as the high level of photochemical activity throughout the measurement campaign. PMF analysis on CIMS data is ongoing.

The UT Austin team also conducted environmental chamber experiments to measure the mass yield of secondary organic aerosol formed from the oxidation of the intermediate volatility organic compounds (IVOCs) of interest. Formation of secondary organic aerosol is observed from the oxidation of the IVOCs; quantification of the SOA mass yields is awaiting additional experiments and further quality assurance of the data. The team also characterized the temperature profile in the thermodenuder (TD) which will be used in environmental chamber experiments to measure the volatility of secondary organic aerosol. The location of heat tapes and insulation material was changed to flatten the temperature profile, and the TD is now ready to be used in the environmental chamber experiments.

Ramboll Environ prepared emissions inputs for the 3-D photochemical grid model simulations of the DISCOVER-AQ period using recently updated TCEQ 2013 emission inventory data for anthropogenic sources (on-road, off-road, non-road, area, oil & gas production, and point source sectors) and IVOC emissions estimated based on unspeciated fractions of total non-methane organic gas emissions. The base case simulation was conducted using the Comprehensive Air quality Model with extensions (CAMx) with the Volatility Basis Set (VBS) organic aerosol scheme.

Due to several instrument repairs environmental chamber experiments were delayed and an extension of the project through August 31, 2015 was requested and granted. We do intend to use all funds allocated to the project by August 31, 2015.

Project 14-025	STATUS: Active – May 21, 2014

Development and Evaluation of an Interactive Sub-Grid Cloud Framework for the CAMx Photochemical Model

Environ – Christopher Emery
Texas A&M University – John Nielson-Gammon
AQRP Project Manager – Gary McGaughey
TCEQ Project Liaison – Khalid Al-Wali

Funding Amount: $256,261
($135,735 Environ, $120,526 TAMU)

Executive Summary

The US Environmental Protection Agency (EPA) requires the use of photochemical models to demonstrate that emission control plans will achieve the federal standard for ground-level ozone (EPA, 2007). The TCEQ uses the Comprehensive Air quality Model with extensions (CAMx) for research and regulatory photochemical modeling. Previous research conducted for the TCEQ has concluded that improvements to the CAMx modeling system, including a sub-grid cloud convection treatment, are necessary to reduce model under prediction biases in oxidized nitrogen compounds in the upper troposphere. Cloud convection at sub-grid scales is an important mechanism for exchanging boundary layer air with the free troposphere and for chemical processing. The current sub-grid cloud approach within CAMx influences photolysis rates, scavenging by rainfall, and aqueous chemistry at grid scale, but does not explicitly treat these processes at cloud scale and does not include sub-grid convective transport.

Small-scale clouds are often widespread but they are not explicitly resolved by the grid scales employed in regional meteorological and photochemical modeling applications. The physical effects from these sub-grid clouds are difficult to characterize accurately, but they can substantially influence many different atmospheric processes, including: boundary layer mixing, ventilation, and deep vertical transport of heat, moisture, and chemical tracers; radiative transfer and surface heat budgets; spatio-temporal precipitation patterns, intensity and wet scavenging rates; chemistry via photolysis and aqueous reactions; and certain environmentally-sensitive emission sectors (e.g., biogenic). Cloud convection is also an important component for long-range transport of ozone, PM, and precursors. The effects of sub-grid clouds on vertical transport, chemistry, and wet scavenging are addressed to varying degrees in off-line photochemical models (i.e., models like CAMx that operate separately from meteorological models that supply environmental inputs). However, the spatio-temporal distributions of such clouds, and all the processes that occur within them, must be re-diagnosed because meteorological models do not export necessary information from their sub-grid cloud parameterizations. This leads to potentially large inconsistencies between the models.

Under this AQRP Project, ENVIRON and collaborators at the Texas A&M University (TAMU) will incorporate and extensively evaluate an explicit sub-grid cloud model within CAMx. The primary goal of this work is to introduce shallow and deep convective cloud mixing at sub-grid scales. Further, the investigators will develop an approach to improve interactions with chemistry and wet deposition to operate explicitly at sub-grid scales in tandem with the cloud mixing scheme. The approach will tie into recent updates implemented in the Weather Research and

Forecasting (WRF) model by researchers at EPA, whereby specific sub-grid cloud fields will be passed to CAMx to define their spatio-temporal distributions and mixing rates for the new sub-grid cloud algorithm. This will yield a more consistent cloud-mixing-chemistry system across the WRF and CAMx models. The new CAMx treatment will be tested for three convective episodes that occurred during the September 2013 Houston DISCOVER-AQ field study and the Spring 2008 START08 field study, particularly addressing tropospheric profiles of NOx, ozone, and other chemical tracers by comparing to in situ profiles from aircraft measurements. The new model will be provided to TCEQ to support future regulatory and research-oriented ozone and PM modeling.

Project Update

In March, TAMU completed installation of the Environ-modified versions of WRF and CAMx, and completed test runs of both models to confirm that all codes were working properly. TAMU ran WRF for all three test cases using a model configuration very similar to TCEQ's configuration, except the 4-km Texas nested grid was omitted since WRF's sub-grid convection option is not applicable at such fine scales. Initial CAMx runs were completed using inputs from two of the WRF runs. In general, the WRF simulations from all three cases exhibited much less convection than observed, and what convection was simulated by WRF was generally in the wrong place.

Environ received a pre-release "beta" version of WRF v3.7 from NCAR in early April. This version contains a new "multi-scale" Kain-Fritsch (MSKF) treatment for sub-grid convection that can be applied at finer resolution down to 1 km scales. We successfully tested the beta version to ensure that we could compile and run the model without errors and crashes. In late April, we obtained NCAR's public release of WRF v3.7 with MSKF. We implemented additional code modifications to output convective fluxes and time scale variables as needed to drive the CAMx sub-grid convection routine. We tested WRF v3.7 by applying the model to the September 1-8, 2013 DISCOVER-AQ period in southeast Texas to ensure that the model runs without errors and crashes. We also ran WRF v3.6.1 with the original Alapaty Kain-Fritsch (KF) updates (the model used to date) for the same period to inter-compare model versions. The first 5-6 days of this episode were characterized by local convective activity in eastern Texas, particularly along the Gulf Coast, which was transported from east to west each day. WRF v3.7 more correctly generated convection over southeast Texas on September 4, while WRF v3.6.1 shifted the convective band much too far south. Although actual convective activity continued through September 5-6, both versions of WRF did not exhibit sufficient convection on these later days. Environ began CAMx simulations of the September 1-8, 2013 period using both sets of WRF results; results will be forthcoming.

In April and May, work at TAMU continued along two fronts: optimization of WRF (v3.6.1) simulations of convective activity for cases of interest, and testing of CAMx with and without convective mixing. In an attempt to create a WRF simulation that was more consistent with observations, TAMU experimented with different model initialization times, different observational/analysis nudging configurations, different nesting interaction levels, different combinations of microphysics and boundary layer schemes, and different convective triggers within the KF scheme. Use of a longer spinup time, removal of analysis nudging, and selection of a different KF convective trigger produced the best results for the May START08 case. However, the June START08 WRF runs continued to be seriously deficient in convection. TAMU's best May START08 run produced convective initiation in eastern New Mexico, and the thunderstorms that formed there eventually developed into a squall line on May 6. However, the location of the squall line in the simulation occurred in Oklahoma rather than in North Texas. Using a combination of simulation results from the squall lines to the north and to the south, it should be possible to intelligently compare the convective mixing model performance with the in situ observations.

Further meteorological model testing by TAMU is focusing on the September 2013 DISCOVER-AQ case. WRF v3.6.1 simulates the development of unorganized convection in eastern Texas, but the location of convective activity is farther north than what was observed (opposite of Environ's WRF simulations, which placed convection too far south). While this TAMU run is usable, we hope to make further improvements to the fidelity of the simulation. This WRF simulation was used to drive an initial 2-day CAMx simulation (September 5-6) with and without its new convective mixing algorithm. The average simulated vertical profiles of ozone, NOx, and CO along all vertical flight spirals on September 6 were analyzed. The NOx profile was generally well simulated and the application of convective mixing suggests some improvements in boundary layer agreement. Ozone and CO tended not to agree well with measured profiles, and this may be related to a lack of spin-up days in the modelling conducted to date. Convection tends to slightly increase boundary layer ozone while slightly decreasing ozone in the free troposphere. This may be the result of net downward mixing of larger ozone concentrations aloft. Future CAMx simulations for this episode have been started on September 1 to allow for adequate spin-up.

Environ and TAMU developed a draft project final report for delivery to the University of Texas on May 18.

Delays or Technical Issues During the Reporting Period

Assessment of the performance of the WRF/CAMx convective treatment will be challenging if the convection simulated by WRF does not correspond to the convection that produced the redistribution of pollutants detected by aircraft. This is concerning, especially since TAMU has previously created successful WRF simulations for the May START08 case for other purposes using higher resolution grids and a different convective parameterization from KF. Based on WRF testing with alternative configurations, marginally satisfactory results have been achieved, as described above, for two of three episodes that produce a spatial and temporal pattern of convection that's reasonably consistent with the observations. Additional WRF tests are underway for the May START08 and September 2018 DISCOVER-AQ period. Interim CAMx simulations of these episodes are also underway.

The University of Texas granted a one-month no-cost extension for this contract. Project completion and delivery of the final AQRP-reviewed report is scheduled for July 31, 2015.

The project team intends to use all funds allocated to the project by July 31, 2015.

Project 14-026	STATUS: Active – May 21, 2014

Quantifying ozone production from light alkenes using novel measurements of hydroxynitrate reaction products in Houston during the NASA SEAC4RS project

Environ – Greg Yarwood
(NOAA – Thomas Ryerson)

AQRP Project Manager – Gary McGaughey
TCEQ Project Liaison – Chris Kite

Funding Amount: \$165,562 (Reduced from 231,182)
(\$165,562 increased from \$135,782 Environ, \$0 reduced from \$95,400 CalTech)

Executive Summary

The objective of this project is to improve and quantify our understanding of ozone (O_3) and formaldehyde (HCHO) production from industrial emissions of Highly Reactive Volatile Organic Compounds (HRVOCs) in the Houston area. Aircraft flights during the National Aeronautics and Space Administration (NASA) Studies of Emissions and Atmospheric Composition, Clouds and Climate Coupling by Regional Surveys (SEAC^{4}RS) project encountered plumes with enhanced O_3 downwind of petrochemical facilities in Houston. For example, on 25 September 2013, ground monitoring downwind of the Ship Channel showed 5-minute average O_3 values peaking at 165 ppb and are associated with elevated concentrations of the oxidation products of HRVOCs. HRVOCs, specifically ethene, propene, butenes and 1,3-butadiene, have been implicated in these types of high ozone events but quantifying the relative contributions of individual HRVOCs to O_3 formation has been difficult.

The project objective will be accomplished by a combination of data analysis and reactive plume modeling. Data taken aboard the NASA DC-8 research aircraft during the 2013 SEAC^{4}RS project in Houston will be analyzed. Chemical compounds called β-hydroxynitrates are formed when HRVOCs react in the atmosphere in the presence of nitrogen oxides (NOx). Measurements of the C_2-C_4 hydroxynitrates aboard the DC-8 provide a novel means to link observed enhancements of O_3 and HCHO to reactions of specific HRVOCs. Analyzing the data will provide a robust first-order attribution of observed O_3 and HCHO enhancements to the oxidation of individual HRVOCs emitted from the Houston Ship Channel. The plumes of HRVOCs and O_3 that the DC-8 intercepted will be analyzed further to estimate what emissions of HRVOCs and NOx gave rise to each plume. A reactive plume model (SCICHEM) will be used to model these plumes and test chemical reaction mechanisms for individual HRVOCs. The model sensitivity to plume expansion rates will be evaluated to test how plume dilution influences chemical processing and therefore how grid model resolution can influence assessments for HRVOC sources. The benefits of this project to the TCEQ will be a data-driven assessment of the contributions of individual HRVOCs to O_3 and HCHO enhancements downwind of the Houston ship channel and improved modeling tools for assessing the air quality impacts of HRVOC emissions in the Texas State Implementation Plan (SIP).

Project Update

Project activities are described below.

Data Analysis

Dr. Parrish downloaded and reviewed the QA/QC'd Caltech β-hydroxynitrate data for all SEAC[4]RS flights over Texas to identify flights of interest for the data analysis and reactive plume modelling. The review identified four flights (18 September 2013, 19 August 2013, 4 September 2013, and 23 September 2013) that potentially tracked plumes originating in the Houston Ship Channel. Trajectory analysis was conducted for these plumes to confirm their origin and to provide a semi-quantitative indication of the plume transport history. Back trajectories were calculated from the DC-8 flight track for specific plume transects, with the origin generally taken as the location where the highest β-hydroxynitrates concentrations were observed.

The data analysis examined β-hydroxynitrate data in conjunction with observations of NOx (NO + NO_2), hydrocarbon, peroxyacetyl nitrate (PAN), nitric acid (HNO_3), total reactive nitrogen oxides (NOy), O_3, formaldehyde (HCHO), acetaldehyde (CH_3CHO), and other chemical and meteorological parameters measured aboard the NASA DC-8. The goals were to determine the relationships between the ambient concentrations of photochemical products (particularly the β-hydroxynitrates, O_3 and aldehydes) and precursor species and to elucidate net O_3 and aldehyde production rates and yields.

Dr. Parrish used the simplified kinetics scheme for the HRVOC chemistry developed in the previous reporting period to calculate the quantitative relationships between aldehydes and β-hydroxynitrates and compared the calculated HCHO and CH_3CHO values with the aircraft observations. Excellent correlations were found between calculated aldehyde values and the measured values for all 4 flights selected for analysis.

The above analysis was extended to understand the quantitative relationships of ozone to β-hydroxynitrates. Calculated ozone values from the simplified HRVOC chemistry were compared with aircraft measurements. While the correlations were still high, the slopes of the best fit lines were significantly less than unity at large downwind distances, and the calculation of ozone from the β-hydroxynitrates greatly underestimated the observed O_3 concentrations. The results suggest that rapid removal of the β-hydroxynitrates is a likely explanation for the O_3 underestimation in the downwind transects. Aldehydes are also rapidly removed from the atmosphere, explaining the better performance for the aldehyde estimates from the β-hydroxynitrate values.

Photochemical plume modeling

The simplified kinetics scheme for the HRVOC chemistry has been implemented in the development version of the reactive plume model, SCICHEM 3.0. The updates will be ported to the final version, which completed development on May 28, 2015 and is planned for public release in June 2015. Ramboll Environ is the co-developer of SCICHEM 3.0 and has access to the final version of the model. Background surface NOx and VOC emissions for areas to the west (urban), south (suburban) and northeast (high biogenics) of the ship channel have been developed using CAMx modeling inputs for the HGB 4-km domain. These areas characterize the background for possible trajectories of ship channel plumes. Other model inputs for simulating the 18 September 2013 Ship Channel plume have been prepared for the modeling with SCICHEM 3.0.

Final Report

A preliminary draft report describing the data analysis has been submitted to AQRP; this draft will serve as the initial starting point of the peer-reviewed publication. The SCICHEM modeling results and additional data analysis results will be included in the final draft report.

Delays or Technical Issues during the Reporting Period

A 3-month no-cost extension for this study has been requested by the study team due to the delays in getting the project started and in receiving QA/QC'd hydroxynitrate data for review and analysis. We intend to use all funds allocated to the project by 06/30/2015.

Project 14-029	STATUS: Active – July 10, 2014

Spatial and temporal resolution of primary and secondary particulate matter in Houston during DISCOVER-AQ

Baylor University – Rebecca Sheesley

AQRP Project Manager – Elena McDonald-Buller
TCEQ Project Liaison – Shantha Daniel

Funding Amount: $178,679

Executive Summary

This project builds on a previously-funded AQRP project tasked at the initial elemental carbon (EC), organic carbon (OC), and optical black carbon (BC) characterization of particulate matter (PM) at Moody Tower and Manvel Croix during DISCOVER-AQ Houston Texas 2013 (AQRP 12-032). Under the original framework of PIs Sheesley and Usenko's AQRP ECOC Project, samples were to be collected over the entire DISCOVER-AQ sampling period at two primary sites in Houston: Moody Tower (urban) and Manvel Croix (southern suburb). Collaborations developed during the early stages of this project increased the sampling intensity at the two primary sites and expanded PM sampling efforts to Conroe (far north suburb) and La Porte (urban industrial).

The overall goals of this project are to analyze the filter samples collected in the previous project and to quantify the strength of PM formation and PM emission sources, including shipping emissions, motor vehicle exhaust, biomass burning and biogenic emissions, across the Houston metropolitan area. This work builds on the strengths of DISCOVER-AQ, specifically the spatial and temporal sampling strategies (i.e. multiple ground-based sites sampled for approximately 28 days). These strategies allow for the examination of both regional and long-range transport as well as anthropogenic and biogenic influences on air quality. The project will characterize PM through the quantification of water-soluble OC, organic tracers, EC, OC, ^{14}C, select inorganic ions, and elemental tracers from PM filters collected from four DISCOVER-AQ anchor sites including Moody Tower, Manvel Croix, Conroe, and La Porte. The PIs will apply a combination of radiocarbon source apportionment of organic and elemental carbon with source-specific organic and inorganic molecular tracers to tightly constrain urban and regional, fossil and biomass burning/biogenic sources.

Progress Report

The major focus of this quarter was data retrieval, collection, and handling. Raw data received from Desert Research Institute (DRI) and the National Ocean Sciences Accelerator Mass Spectrometry Facility (NOSAMS) was examined for errors and quality control. Specific datasets (e.g. inorganic ions) were converted to ambient concentrations. In addition, select datasets were distributed to other AQRP DISCOVER-AQ project leaders as specified in the project's collaboration and data sharing sections. The focus of this period was inorganic ions, elemental tracers (i.e. metals), radiocarbon, and organic tracers. Inorganic ions and elemental tracers were measured by an independent laboratory, DRI. DRI is an accredited laboratory for the analysis of inorganic ions and elemental tracers and has been approved by TCEQ. Inorganic ions and elemental tracer data was received by Baylor in March. Inorganic ions data was later distributed to PI Hildebrandt Ruiz (14-024). Invoices associated with the analysis of inorganic ions and elemental tracers have been submitted. Radiocarbon measurements were performed by NOSAMS. The first batch of radiocarbon data was received by Baylor in late May. Invoices associated with the analysis of the first batch of radiocarbon are currently being submitted. The second batch of radiocarbon is forthcoming. Organic tracers are measured at Baylor University under the supervision on PIs Sheesley and Usenko and are currently ongoing.

Project PIs participated in a number of data sharing conference calls and the Texas Air Quality Symposium. Specifically, the project PIs participate in conference calls with other AQRP DISCOVER-AQ project PIs as well as conference calls with the project's AQRP program manager and TCEQ liaison.

On May 18th, a final report draft was submitted to AQRP and TCEQ. The report provides a detailed list of project organization and success as they pertain to the ten project deliverables. The final report also provides tables of the raw datasets (e.g. elemental tracers) as well as copies of publications associated with the project. Finally, the report provides a future work section that highlights the need for an improved understanding of aerosol chemistry as it relates to different emission sources (biogenic and anthropogenic) and under a wide range of meteorological conditions including rain scavenging efficiency.

Data Retrieval (from independent laboratories)
Inorganic Ion. Inorganic ion datasets including Moody Tower (14-029; filter-based measurements), Conroe (14-024; filter-based), and Manvel Croix (14-009; Particle-into-liquid sampler; PILS). Inorganic ions data was distributed to PI Hildebrandt Ruiz (14-024) and PIs Sheesley and Usenko received ambient sulfate concentrations measured at Manvel Croix from PI Griffin (PILS; 14-009).

Filter-based measurements were conducted to obtain inorganic ion (SO4, Cl, NO3, NH4 and K) mass concentrations. Inorganic ions were measured using ion chromatography. The four filter blanks had non-detects for all ions. Of the 27 samples (9/4/2013 – 9/28/2013; note that these are 4-14 h samples and the sampler was down for 9/6-9/7), there was the following detects for each reported anion and cation: 16 detects for chloride, 23 detects for particulate nitrate, 27 detects for sulfate, 26 detects for ammonium, 26 detects for soluble sodium and 24 detects for soluble potassium.

Elemental Tracers. Teflon filters (MV PM2.5) were analyzed for 51 elemental tracers. Filter-based elemental tracer measurements were conducted by the certified contract laboratory DRI.Elemental tracers were measured using X-Ray Fluorescence. Detection frequency for the 51 elemental tracers detected above filter blanks are in parentheses: Sodium (15), Magnesium (5), Aluminum (8), Silicon (22), Phosphorous (0), Sulfur (25), Chlorine (25), Potassium (25), Calcium (25), Scandium (0), Titanium (17), Vanadium (18), Chromium (17), Manganese (14), Iron (25), Cobalt (0), Nickel (24), Copper (25), Zinc (25), Gallium (1), Arsenic (0), Selenium (9), Bromine (22), Rubidium (14), Strontium (17), Yttrium (3), Zirconium (21), Niobium (11), Molybdenum (14), Palladium (6), Silver (4), Cadmium (2), Indium (7), Tin (12), Antimony (8), Cesium (2), Barium (Ba), Lanthanum (9), Cerium (12), Samarium (5), Europium (15), Terbium

(7), Hafnium (0), Tantalum (0), Wolfram (8), Iridium (0), Gold (2), Mercury (6), Thallium (2), Lead (21) and Uranium (4). The ambient concentrations of the detected metals were distributed to AQRP project (14-029) PI. In addition, select metals, when detected, will be used as molecular tracers in the chemical mass balance (CMB) model in partial fulfillment of that deliverable.

Radiocarbon. Filter preparation and carbon isolation was accomplished by the PIs prior to radiocarbon analysis by accelerator mass spectrometry at NOSAMS. Aliquots of selected filters were cut to obtain at least 60 µg of total carbon, placed in an ashed glass petri dish (glass was cleaned via heat in a muffle oven to 500 ºC), acidified in a dessicator over HCl and sealed in the glass petri dish by wrapping completely in ashed aluminum foil. These prepared samples were then shipped to NOSAMS, frozen, overnight. Radiocarbon analysis was accomplished at NOSAMS by measuring the ratio of ^{14}C to ^{12}C for the sample, a blank and a modern reference standard. The reference is 0.95 times the specific activity of National Bureau of Standards Oxalic Acid I (Standard Reference Material 4990B), which is a $^{14}C/^{12}C$ ratio of $1.176 \pm 0.010 \times 10^{-12}$ (Karlen et al. 1964; Olsson 1970). These three ratios are combined in the following expression to calculate the raw F_{modern} which is reported by NOSAMS: $F_{modern} = (^{14}C_{sample}/^{12}C_{sample} - {}^{14}C_{blank}/^{12}C_{blank})/(^{14}C_{modern\ reference\ standard}/^{12}C_{modern\ reference\ standard} - {}^{14}C_{blank}/^{12}C_{blank})$.

Organic Tracers

Aliquots of quartz fiber filters collected from Moody Tower, Manvel Croix, Conroe, and La Porte are analyzed for organic tracers (e.g. polycyclic aromatic hydrocarbons; PAHs, hopanes, steranes, alkanes, levoglucosan, and tracers for non-combustion sources). Typically, 10 to 60% of filter is dedicated for organic tracer analysis as highlighted in previous months' technical reports and site-specific filter plans. Aliquot size is dependent on specific bulk carbon measurements and the relationship between organic carbon mass and tracer concentrations.

Preliminary data demonstrate the presence of at least ten different classes of contaminants in particulate matter samples collected during DISCOVER-AQ Houston 2013. For example, a large number of alkanes were measured in samples collected from Moody Tower and La Porte. The alkane profile measured at these two sites showed an enhancement of alkanes with odd numbered of carbon atoms (e.g. nonacosane – $C_{29}H_{60}$). Sources of alkanes in the atmosphere include biogenic (waxy plants) and anthropogenic sources (incomplete combustion of fossil fuels). This preliminary data suggest that alkanes measured at these two sites had high contributions from biogenic sources.

As organic tracer data continues to be produced through the analysis of quartz fiber filters and project PIs have begun the process of combining tracer datasets. These datasets serve as the foundation for the examination of the spatial and temporal strength of PM formation and contributions of PM emission sources in the Houston metropolitan area. These datasets will also house the specific ambient concentrations for the molecular and elemental tracers for use in the CMB Model (see below).

Chemical Mass Balance Model
Organic and elemental tracer ambient concentrations are combined to model contribution of primary emission sources to organic carbon at Moody Tower, Manvel Croix, Conroe, and La Porte during the week of 9/21-28/13. This is accomplished using the Chemical Mass Balance Model (EPA v8.2) and primary emission source profiles from the literature. The finalized list of profiles will be included in the project's final report. For the model runs, hopanes, PAHs, alkanes, levoglucosan, elemental carbon, aluminum and silicon are used as tracers. As with the organic tracer analysis, the initial runs of the CMB model were completed with 9/11-9/14 samples. Initial runs using only organic tracers and EC indicate 20% contribution of motor vehicles (diesel and gasoline) and minimal biomass burning.

Results
Preliminary results for the project were presented at the April 2015 Texas Air Quality Symposium. PIs and student presented oral and posters at the symposium. Over the course of the symposium many great ideas/concepts were presented. Baylor's addition to this focused on aerosol chemistry including source apportionment using radiocarbon, bulk carbon measurements, and specific molecular markers.

Poster Presentations for Regional SETAC conference

- Poster titled "Spatial trends in inorganic atmospheric particulate matter composition during DISCOVER-AQ in Houston, TX"
- Poster titled "Spatial trends in surface-based carbonaceous aerosol measurements during DISCOVER-AQ in Houston, TX"

Manuscript submission/publication

- A.E. Clark, S. Yoon, R.J. Sheesley, S. Usenko, Pressurized liquid extraction technique for the analysis of pesticides, PCBs, PBDEs, OPEs, PAHs, alkanes, hopanes, and steranes in atmospheric particulate matter, Chemosphere 137 (2015) 33-44.

Delays or Issues Report
In March, an issue was identified in routine laboratory blanks and filter extracts from Manvel Croix, Conroe and La Porte (frequency of blanks are described in the project's QAPP). This issue had the potential to alter the recovery of organic tracers. Quartz fiber filter extraction and analysis stopped as soon as the potential problem was identified. QAPPs are specifically designed to help identify this type of laboratory issues. The routine analysis of laboratory blanks and immediate analysis of sample extracts, as described in the project's approved QAPP, identified the issue and allowed the project's PIs and student to identify and correct it. Steps were taken to eliminate the issue. The elimination of the issue was verified using filter laboratory blanks.

Research Funds Report
Supplies and salary expenses were reported by the Office of Sponsored Programs at Baylor University. DRI invoices have been submitted and the first batch invoice from NOSAMS is currently being processed. Salary buyout (with the approval of the project's AQRP program manager) for PIs Sheesley and Usenko were requested and approved. This buyout help correct for differences in fund distribution last summer due to the July 2014 start date. Details of specific invoices are included in monthly financial reports.

Project 14-030	STATUS: Active – June 25, 2014

Improving Modeled Biogenic Isoprene Emissions under Drought Conditions and Evaluating Their Impact on Ozone Formation

Texas A&M University – Qi Ying

AQRP Project Manager – Elena McDonald-Buller
TCEQ Project Liaison – Mark Estes

Funding Amount: $176,109

Executive Summary

Isoprene emitted from biogenic sources plays an important role in atmospheric chemistry that leads to the formation of ozone and secondary particulate matter (PM). Although drought has been thought to affect biogenic emissions, the capability of the current drought parameterization to adjust the impact of soil moisture on isoprene emissions has not been critically evaluated, especially under severe drought conditions in Texas. The impact of this change in isoprene emissions on regional ozone concentrations is also unclear. In this study, biogenic isoprene emissions during two seven-month episodes, one representing a relatively wet year (2007) and one representing a severe drought year (2011) will be estimated using the most recent version of the MEGAN biogenic emission model (MEGAN v2.1). Emissions during the severe drought year 2011 will be estimated using several different soil moisture parameterization schemes, including one that will be developed in this study based on additional field and climate-controlled laboratory measurements of isoprene emissions at leaf-level for selected Texas tree species. The Community Multiscale Air Quality Model (CMAQ) will be used to simulate isoprene, isoprene oxidation products and ozone concentrations during the dry and wet episodes. The predicted concentrations will be evaluated against all available measurements to evaluate the ability of different drought parameterization schemes and quantify the impact of drought on biogenic isoprene emission and ozone concentrations in Texas. Optimal configuration of the WRF model that is most appropriate for meteorology and soil moisture simulations during the drought seasons will also be investigated.

Project Update

Project activities are described by task below.

Task 1: Meteorology simulation with WRF.

We performed an additional set of WRF simulations for both 2007 and 2011, using the same input data as we used in the previous set of simulations. Instead of running the simulations in segments of 8-days (including 1-day spin-up), we run the simulations this time in 1-day segments with 3 hour spin-up. This appears to improve the performance for both the meteorological parameters (temperature, relative humidity, wind speed and wind direction) and the CMAQ predicted ozone concentrations.

Task 2: Perform field and laboratory measurements on common Texas tree species.

Isoprene emissions from new growths in early 2015 have been monitored. While emissions are present, they are low. Photosynthesis rates are lower than from mature leaves of these species, so leaf physiology is still developing. A high variability is observed, meaning the leaves' physiology has not yet reached a stage where a high reproducibility is achieved. Since variability is high, we cannot guarantee that useful results can be obtain before the end of the funding period.

Task 3: Evaluate drought parameterization for isoprene emissions.
Isoprene emissions measured during the 2011 drought season in east Texas as well as soil moisture measurements at the top soil were used evaluate the default parameterization scheme in the MEGAN model. Two sets of soil moisture data were used in the evaluation. The first set of soil moisture data were based on observed top soil moisture and derived root zone soil moisture from a simple model. Two possible root zone depths (1 m and 2 m) were used in the analysis. The second set of soil moisture data were predicted using WRF, using the Noah land use scheme. The results indicate ambiguity of the drought response of isoprene emitting oaks that results from 1) the root-zone soil depth of the species, and 2) the drought response parametrization. They demonstrate that a uniform root-zone depth selection and a uniform drought response parametrization may lead to regionally paradoxical results. In regions dominated by drought resistant oak species such as Quercus stellata a deeper root zone may have to be considered alongside a narrower range of soil moistures that affect isoprene emissions, while the opposite should be considered in regions dominated by less drought resistant species such as Quercus nigra.

Task 4: Perform regional BVOC modeling using MEGAN.
In the past quarter, we regenerated MEGAN simulated BVOC emissions for 2007 and 2011. These two sets of BVOC emissions (referred to as ‘new’ simulations hereafter) were based on the new met fields generated from the new WRF simulations mentioned in Task 1 above. One set of emissions (base case - new) was based on the original MEGAN model obtained from Dr. Alex Guenther without considering the soil moisture effect (drought effect) on BVOC emissions. The second set of emissions (soil moisture case 1 - new) were based on our modified MEGAN with drought effect parameterization based on Dr. Guenther’s original parameterization as documented in his MEGAN papers.

Task 5: Perform regional air quality simulations.
In the past quarter, we have accomplished the following items: 1) Update all anthropogenic emissions for 2007 and 2011 using the new WRF simulation mentioned in Task 1; 2) Finished air quality simulation using the CMAQ model for both 2007 and 2011 with inputs from the new WRF, BVOC and anthropogenic missions. We found that 1) predicted isoprene concentrations are still significantly higher than observations, even when the drought effect was considered in most cases; 2) predicted ozone concentrations generally agree with the observed concentrations, although peak ozone concentrations are constantly over-predicted, possibly due to over-predictions of isoprene emissions, and 3) predicted peak ozone concentrations were reduced with reduced isoprene concentrations, and in some cases, led to better agreement in the predicted and observed peak ozone concentrations. This suggests the necessity in improving the MEGAN-predicted isoprene emissions.

FINANCIAL STATUS REPORT

Initial funding for fiscal year 2010 was established at $2,732,071.00. In late May 2010 an amendment was issued increasing the budget by $40,000. Funding for fiscal year 2011 was established at $2,106,071, for a total award of $4,878,142 for the FY 2010/2011 biennium. FY 2010 funds were fully expended in early 2012 and the FY 2011 funds expired on June 30, 2013 with a remaining balance of $0.11.

In February 2012, funding of $1,000,000 was awarded for FY 2012. In June 2012, an additional $160,000 was awarded in FY 2012 funds and $1,000,000 was awarded in FY 2013 funds, for a total of $2,160,000 in funding for the FY 2012/2013 biennium.

In April 2013, the grant was amended to reduce the FY 2012 funds by $133,693.60 and increase the FY 2011 funds by the same amount.

In June 2013, the grant was amended to increase the FY 2013 funds by $2,500,000.

In October 2013, the grant was amended to award FY 2014 funds of $1,000,000 and FY 2015 funds of $1,000,000. The budget for each fiscal year can be found in Appendix C.

FY 2012 funds were fully expended at the end of April 2014. FY 2013 funds will be fully expended by June 2015.

For each biennium (and fiscal year) the funds were distributed across several different reporting categories as required under the contract with TCEQ. The reporting categories are:

<u>Program Administration</u> – limited to 10% of the overall funding (per Fiscal Year)
This category includes all staffing, materials and supplies, and equipment needed to administer the overall AQRP. It also includes the costs for the Council meetings.

<u>ITAC</u>
These funds are to cover the costs, largely travel expenses, for the ITAC meetings.

<u>Project Management</u> – limited to 8.5% of the funds allocated for Research Projects
Each research project will be assigned a Project Manager to ensure that project objectives are achieved in a timely manner and that effective communication is maintained among investigators in multi-institution projects. These funds are to support the staffing and performance of project management.

<u>Research Projects</u> / Contractual
These are the funds available to support the research projects that are selected for funding.

Program Administration

Program Administration includes salaries and fringe benefits for those overseeing the program as a whole, as well as, materials and supplies, travel, equipment, and other expenses. This category allows indirect costs in the amount of 10% of salaries and wages.

During the reporting period several staff members were involved, part time, in the administration of the AQRP. Dr. David Allen, Principal Investigator and AQRP Director, is responsible for the overall administration of the AQRP. James Thomas, AQRP Manager, is responsible for assisting Dr. Allen in the program administration. Maria Stanzione, AQRP Grant Manager, with Rachael Bushn, Melanie Allbritton, and Susan McCoy each provided assistance with program organization and financial management. This included assisting with the contracting process. Denzil Smith is responsible for the AQRP Web Page development and for data management.

Fringe benefits for the administration of the AQRP were initially budgeted to be 22% of salaries and wages across the term of the project. It should be noted that this was an estimate, and actual fringe benefit expenses have been reported for each month. The fringe benefit amount and percentage fluctuate each month depending on the individuals being paid from the account, their salary, their FTE percentage, the selected benefit package, and other variables. For example, the amount of fringe benefits is greater for a person with family medical insurance versus a person with individual medical insurance. At the end of the project, the overall total of fringe benefit expensed is expected to be at or below 22% of the total salaries and wages. Actual fringe benefit expenses to date are included in the spreadsheets above.

As discussed in previous Quarterly Reports, the AQRP Administration requested and received permission to utilize funds in future fiscal years. This is for all classes of funds including Administration, ITAC, Project Management, and Contractual. As of the writing of this report, the FY 2010, FY 2011, and FY 2012 funds have been fully expended. This same procedure will be followed for the FY 2013, FY 2014, and FY 2015 funds.

In May 2014, UT-Austin received a Contract Extension for the AQRP. This extension will continue the program through April 27, 2016.

Table 1: AQRP Administration Budget

Administration Budget (includes Council Expenses)
FY 2010/2011

Budget Category		FY10 Budget	FY11 Budget	Total	Expenses	Pending Expenses	Remaining Balance
Personnel/Salary		$202,816.67	$172,702.06	$375,518.73	$375,518.73	$0.00	$0.00
Fringe Benefits		$38,665.65	$33,902.95	$72,568.60	$72,568.60	$0.00	$0.00
Travel		$346.85	$0	$346.85	$346.85	$0.00	$0.00
Supplies		$15,096.14	$101.25	$15,197.39	$15,197.39	$0.00	$0.00
Equipment		$0	$0	$0			$0.00
Total Direct Costs		$256,925.31	$206,706.26	$463,631.57	$463,631.57	$0.00	$0.00
Authorized Indirect Costs		$20,281.69	$17,270.20	$37,551.89	$37,551.89	$0.00	$0.00
10% of Salaries and Wages							
Total Costs		**$277,207.00**	**$223,976.46**	**$501,183.46**	**$501,183.46**	**$0.00**	**$0.00**
Fringe Rate		22%	22%		19%		

Administration Budget (includes Council Expenses)
FY 2012/2013

Budget Category		FY12 Budget	FY13 Budget	Total	Expenses	Pending Expenses	Remaining Balance
Personnel/Salary		$74,238.65	$256,479.00	$330,717.65	$330,393.11	$0.00	$324.54
Fringe Benefits		$17,068.38	$59,428.95	$76,497.33	$76,474.25		$23.08
Travel		$339.13	$0.00	$339.13	$339.13		$0.00
Supplies		$3,560.62	$8,352.05	$11,912.67	$11,912.65	$0.00	$0.02
Equipment		$0.00	$0.00	$0.00			$0.00
Total Direct Costs		$95,206.78	$324,260.00	$419,466.78	$419,119.14	$0.00	$347.64
Authorized Indirect Costs		$7,423.86	$25,740.00	$33,163.86	$33,039.30	$0.00	$124.56
10% of Salaries and Wages							
Total Costs		**$102,630.64**	**$350,000.00**	**$452,630.64**	**$452,158.44**	**$0.00**	**$472.20**
Fringe Rate		23%	23%		23%		

Administration Budget (includes Council Expenses)
FY 2014/2015

Budget Category		FY14 Budget	FY15 Budget	Total	Expenses	Pending Expenses	Remaining Balance
Personnel/Salary		$70,000.00	$70,000.00	$140,000.00	$8,675.45	$0.00	$131,324.55
Fringe Benefits		$15,150.00	$15,150.00	$30,300.00	$2,530.94	$0.00	$27,769.06
Travel		$350.00	$350.00	$700.00	$0.00	$0.00	$700.00
Supplies		$7,500.00	$7,500.00	$15,000.00	$400.24	$0.00	$14,599.76
Equipment							
Total Direct Costs		$93,000.00	$93,000.00	$186,000.00	$11,606.63	$0.00	$174,393.37
Authorized Indirect Costs		$7,000.00	$7,000.00	$14,000.00	$867.55	$0.00	$13,132.45
10% of Salaries and Wages							
Total Costs		**$100,000.00**	**$100,000.00**	**$200,000.00**	**$12,474.18**	**$0.00**	**$187,525.82**
Fringe Rate		22%	22%		29%		

ITAC

No ITAC activities occurred during this period and none are planned through the end of the AQRP Grant period. In June, the program administration will request permission to transfer the FY 14 and FY 15 ITAC funds to the Research Projects.

Table 2: ITAC Budget

ITAC Budget
FY 2010/2011

Budget Category		FY10 Budget	FY11 Budget	Total Budget	Expenses	Pending Expenses	Remaining Balance
Personnel/Salary							
Fringe Benefits							
Travel		$16,378.86	$6,292.97	$22,671.83	$22,671.83		$0
Supplies		$1,039.95	$284.67	$1,324.62	$1,324.62		$0
Total Direct Costs		$17,418.81	$6,577.64	$23,996.45	$23,996.45		$0
Authorized Indirect Costs							
10% of Salaries and Wages							
Total Costs		**$17,418.81**	**$6,577.64**	**$23,996.45**	**$23,996.45**	**$0.00**	**$0**

ITAC Budget
FY 2012/2013

Budget Category		FY12 Budget	FY13 Budget	Total Budget	Expenses	Pending Expenses	Remaining Balance
Personnel/Salary							
Fringe Benefits							
Travel		$5,323.31	$0.00	$5,323.31	$5,323.31		$0.00
Supplies		$231.86	$0.00	$231.86	$231.86		$0.00
Total Direct Costs		$5,555.17	$0.00	$5,555.17	$5,555.17		$0.00
Authorized Indirect Costs							
10% of Salaries and Wages							
Total Costs		**$5,555.17**	**$0.00**	**$5,555.17**	**$5,555.17**	**$0**	**$0.00**

ITAC Budget
FY 2014/2015

Budget Category		FY14 Budget	FY15 Budget	Total Budget	Expenses	Pending Expenses	Remaining Balance
Personnel/Salary							
Fringe Benefits							
Travel		$7,000.00	$7,000.00	$14,000.00	$0.00		$14,000.00
Supplies		$500.00	$500.00	$1,000.00	$0.00		$1,000.00
Total Direct Costs		$7,500.00	$7,500.00	$15,000.00	$0.00		$15,000.00
Authorized Indirect Costs							
10% of Salaries and Wages							
Total Costs		**$7,500.00**	**$7,500.00**	**$15,000.00**	**$0.00**	**$0.00**	**$15,000.00**

Project Management

During this quarter, Project Managers continued to work with the project teams to ensure all reporting requirements were met and projects were moving forward as described in the Work Plans. Project managers began reviewing draft final reports which were due on May 18, 2015, for all projects ending on June 30, 2015.

Table 3: Project Management Budget

Project Management Budget
FY 2010/2011

Budget Category		FY10 Budget	FY11 Budget	Total Budget	Expenses	Pending Expenses	Remaining Balance
Personnel/Salary		$145,337.70	$121,326.64	$266,664.34	$266,664.34	$0	$0
Fringe Benefits		$28,967.49	$23,102.60	$52,070.09	$52,070.26	$0	($0.17)
Travel		$0	$0	$0	$0		$0
Supplies		$778.30	$207.98	$986.28	$986.22	$0	$0.06
Total Direct Costs		$175,083.49	$144,637.22	$319,720.71	$319,720.82	$0	($0.11)
Authorized Indirect Costs		$14,533.77	$12,132.66	$26,666.43	$26,666.32	$0	$0.11
10% of Salaries and Wages							
Total Costs		**$189,617.26**	**$156,769.88**	**$346,387.14**	**$346,387.14**	**$0**	**$0.00**

Project Management Budget
FY 2012/2013

Budget Category		FY12 Budget	FY13 Budget	Total Budget	Expenses	Pending Expenses	Remaining Balance
Personnel/Salary		$53,384.46	$123,279.85	$176,664.31	$176,664.31		$0.00
Fringe Benefits		$10,991.04	$23,666.75	$34,657.79	$34,657.79		$0.00
Travel		$0.00	$0.00	$0.00	$0.00		$0.00
Supplies		$967.98	$698.82	$1,667.38	$1,452.52		$214.86
Total Direct Costs		$65,343.48	$147,645.42	$212,989.48	$212,774.62	$0.00	$214.86
Authorized Indirect Costs		$5,338.44	$12,328.58	$17,666.44	$17,666.44		$0.00
10% of Salaries and Wages							
Total Costs		**$70,681.92**	**$159,974.00**	**$230,655.92**	**$230,441.06**	**$0.00**	**$214.86**

Project Management Budget
FY 2014/2015

Budget Category		FY14 Budget	FY15 Budget	Total Budget	Expenses	Pending Expenses	Remaining Balance
Personnel/Salary		$52,000.00	$52,000.00	$104,000.00	$36,180.76	$0.00	$67,819.24
Fringe Benefits		$9,300.00	$9,300.00	$18,600.00	$7,738.98	$0.00	$10,861.02
Travel							
Supplies		$1,000.00	$1,000.00	$2,000.00	$587.25	$0.00	$1,412.75
Total Direct Costs		$62,300.00	$62,300.00	$124,600.00	$44,506.99	$0.00	$80,093.01
Authorized Indirect Costs		$5,200.00	$5,200.00	$10,400.00	$3,618.08	$0.00	$6,781.92
10% of Salaries and Wages							
Total Costs		**$67,500.00**	**$67,500.00**	**$135,000.00**	**$48,125.07**	**$0.00**	**$86,874.93**

Research Projects

FY 2010-2011

The FY 2010 Research/Contractual budget was originally funded at $2,286,000. After all transfers, it was increased by $1,827.93. The FY 2011 Research/Contractual budget was originally funded at $1,736,063. After all transfers, it was increased by $377.62, plus an additional $116,000 from FY 2012 funds that were changed to FY 2011 funds. This is an overall net increase of $13,205.55 to the Research/Contractual funds (and net reduction in Project Management/ITAC funds). ($105,000 in FY 2012 research funds were transferred to FY 2011, the remaining $11,000 were transfers from Project Management funds.)

All FY 2010 Research Project funding was fully expensed before the expiration of FY 2010 funds in June 2012. The FY 2011 Research Project funding that remained after all FY 2011 research projects were completed was allocated to FY 2012-2013 projects. This included the funds that were reallocated from FY 2012 to FY 2011. The funds were allocated to project 13-016 Valparaiso and project 13-004 Discover AQ Infrastructure. Both projects utilized their FY 2011 funds (project 13-004 $116,000 and project 13-016 $20,168.90) by June 30, 2013. A remaining balance of $0.11 was returned to TCEQ.

Table 4 on the following 2 pages illustrates the 2010-2011 Research Projects, including the funding awarded to each project and the total expenses reported on each project through the expiration of the FY 2011 funds on June 30, 2013.

FY 2012-2013

The FY 2012 Research/Contractual budget was originally funded at $815,000. Transfers to date have increased the budget by $32,438.67. These funds were fully expended as of April 2014. The FY 2013 Research Contractual budget was originally funded at $835,000. In June 2013, Amendment 9 increased this budget by $2,100,000. (The remaining $400,000 was allocated to Admin and Project Management.) Transfers to date have increased that by an additional $55,026 for a total FY 2013 Research Contractual budget of $2,990,026. This includes funds transferred from the FY 13 Project Management budget to the Research Projects budget, in order to fund as many research projects as possible, and the return of $53,974 to FY 13 Project Management to cover the additional Project Manager needed for the additional 5 projects.

Funds that were not expended by the FY 2012 – 2013 research projects totaling $1,716,863.39 (including an April 2015 refund of $18.40 to a project that ended in March 2014) were allocated to projects from the FY 2014-2015 RFP, with $53,974 of the funds allocated to Project Management. Table 5 illustrates the 2012-2013 Research Projects, including the funding awarded to each project and the total expenses reported on each project as of May 31, 2015.

As noted in Table 7, many of the projects from the FY 2014-2015 RFP were funded from a combination of FY 2013 funds and either FY 2014 or FY 2015 funds. In order to expend all FY 2013 funding by June 30, 2015, adjustments were made to the amount of FY 2013 funding allocated to specific projects, and project expenses that were originally charged to the FY 2014 or FY 2015 portion of the project funds were transferred to the FY 2013 portion.

FY 2014-2015

The FY 2014 and 2015 Research/Contractual budgets were originally funded at $825,000 each. As noted above, research projects were awarded to FY 2013, 2014, and 2015 funds. In May 2015 adjustments were made to the specific allocation amount across the fiscal year accounts for several projects.

As the projects neared the June 30, 2015 end date, several investigators requested extensions to their projects. For those that requested them, extensions were granted for either one, two, or three months. No project has an end date beyond September 30, 2015. Draft final reports were due from all projects with a June 30, 2015 end date.

Table 4: 2010/2011 Contractual Expenses

Contractual Expenses

FY 10 Contractual Funding		$2,286,000		
FY 10 Contractual Funding Transfers		$1,827.93		
FY 10 Total Contractual Funding		**$2,287,827.93**		
Project Number		Amount Awarded (Budget)	Cumulative Expenditures	Remaining Balance
10-008	Rice University	$128,851	$126,622.32	$2,228.68
10-008	Environ International	$49,945	$49,944.78	$0.22
10-009	UT-Austin	$591,332	$591,306.66	$25.34
10-021	UT-Austin	$248,786	$248,786.41	-$0.41
10-022	Lamar University	$150,000	$132,790.80	$17,209.20
10-032	University of Houston	$176,314	$176,314	$0
10-032	University of New Hampshire	$23,054	$18,850.65	$4,203.35
10-032	UCLA	$49,284	$47,171.32	$2,112.68
10-034	University of Houston	$195,054	$186,657.54	$8,396.46
10-042	Environ International	$237,481	$237,479.31	$1.69
10-045	UCLA	$149,773	$142,930.28	$6,842.72
10-045	UNC - Chapel Hill	$33,281	$33,281	$0
10-045	Aerodyne Research Inc.	$164,988	$164,988.10	-$0.10
10-045	Washington State University	$50,000	$50,000	$0
10-DFW	UT-Austin	$37,857	$37,689.42	$167.58
FY 10 Total Contractual Funding Awarded		$2,286,000		
FY 10 Contractual Funding Expended (Init. Projects)			$2,244,812.59	
FY 10 Contractual Funds Remaining Unspent after Project Completion				$41,187.41
FY 10 Additional Projects				
	Data Storage	$7,015.34	$7,015.34	$0
10-SOS	State of the Science	$36,000.00	$36,000.00	$0
FY 10 Contractual Funds Expended to Date*			$2,287,827.93	
FY 10 Contractual Funds Remaining to be Spent				$0

FY 11 Contractual Funding		$1,736,063.00		
FY 11 Contractual Funding Transfers		$116,377.62		
FY 11 Total Contractual Funding		**$1,852,440.62**		
Project Number		Amount Awarded (Budget)	Cumulative Expenditures	Remaining Balance
10-006	Chalmers University of Tech	$262,179	$262,179	$0
10-006	University of Houston	$222,483	$217,949.11	$4,533.89
10-015	Environ International	$201,280	$201,278.63	$1.37
10-020	Environ International	$202,498	$202,493.48	$4.52
10-024	Rice University	$225,662	$223,769.99	$1,892.01
10-024	University of New Hampshire	$70,747	$70,719.78	$27.22
10-024	University of Michigan	$64,414	$60,597.51	$3,816.49
10-024	University of Houston	$98,134	$88,914.46	$9,219.54
10-029	Texas A&M University	$80,108	$78,276.97	$1,831.03
10-044	University of Houston	$279,642	$277,846.38	$1,795.62
11-DFW	UT-Austin	$50,952	$29,261.75	$21,690.25
FY 11 Total Contractual Funding Awarded		$1,758,099		
FY 11 Contractual Funds Expended (Init. Projects)			$1,713,287.06	
FY 11 Contractual Funds Remaining Unspent after Project Completion				$44,811.94
FY 11 Additional Projects				
	Data Storage	$2,984.66	$2,984.66	$0.00
	12-016 Valparaiso	$20,168.90	$0.00	$21,168.90
	12-004 Discover AQ Infrastructure	$116,000.00	$115,999.89	$0.11
FY 11 Contractual Funds Expended to Date*			$1,852,440.51	
FY 11 Contractual Funds Remaining to be Spent				$0.11
Total Contractual Funding		$4,022,063.00		
Total Contractual Funding Transfers		$118,205.55		
Total Contractual Funding Available		$4,140,268.55		
Total Contractual Funds Expended to Date			$4,140,268.44	
Total Contractual Funds Remaining				$0.11

Table 5. 2012/2013 Contractual Expenses

Contractual Expenses

FY 12 Contractual Funding	$815,000.00
FY 12 Contractual Funding Transfers	$32,438.67
FY 12 Total Contractual Funding	**$847,438.67**

Project Number		Amount Awarded (Budget)	Cumulative Expenditures	Remaining Balance
12-004	UT-Austin (Torres)	$20,174.10	$20,174.10	$0.00
12-006	UC-Riverside	$101,765.00	$101,765.00	$0.00
12-006	TAMU/TEES	$44,494.00	$42,134.22	$2,359.78
12-011	Environ International	$77,420.00	$77,410.16	$9.84
12-012	UT-Austin (Hildebrandt)	$79,463.00	$79,173.94	$289.06
12-012	Environ International	$69,374.00	$69,372.64	$1.36
12-013	Environ International	$59,974.00	$59,960.93	$13.07
12-018	UT-Austin (McDonald-Buller)	$85,282.00	$85,197.80	$84.20
12-018	Environ International	$21,688.00	$21,686.26	$1.74
12-028	University of Houston	$19,599.00	$16,586.51	$3,012.49
12-028	UCLA	$17,944.00	$17,709.51	$234.49
12-028	Environ International	$44,496.00	$44,496.00	$0.00
12-028	UNC - Chapel Hill	$35,230.00	$35,230.00	$0.00
12-032	Baylor	$45,972.00	$43,642.21	$2,329.79
12-TN1	Maryland	$64,994.00	$64,537.12	$456.88
12-TN2	Maryland	$69,985.00	$68,362.27	$1,622.73
FY 12 Total Contractual Funding Awarded		$847,438.67		
FY 12 Contractual Funds Expended to Date			$847,438.67	
FY 12 Contractual Funds Remaining to be Spent				$0.00

Note:
Project 12-004 on this page and Project 13-004 on the following page were the same project, with funding split across fiscal years. After all FY12 projects were completed and fully invoiced, the remaining FY12 funds were transferred to 12-004 and 13-004 was reduced by the same amount, so that the total project budget remained the same, but all FY12 funds could be expended.

FY 13 Contractual Funding		$835,000		
FY 13 Contractual Funding Transfers		$2,209,000		
FY 13 Total Contractual Funding		**$3,044,000**		
Project Number		Amount Awarded (Budget)	Cumulative Expenditures	Remaining Balance
13-004	UT-Austin (Torres)	$1,555,770	$805,209.66	$750,560.24
13-005	Chalmers University of Tech	$129,047	$129,047.00	$0.00
13-005	University of Houston	$48,506	$44,928.24	$3,577.76
13-016	Valparaiso	$46,652	$46,652.10	$0.00
13-016	University of Houston	$19,846	$14,101.40	$5,744.60
13-022	Rice University	$89,912	$75,881.86	$14,030.14
13-022	University of Houston	$116,903	$116,122.47	$780.53
13-024	Maryland	$90,444	$89,658.88	$785.12
FY 13 Total Contractual Funding Awarded		$2,097,080		
FY 13 Contractual Funds Expended (Init. Projects)			$1,321,601.61	
FY 13 Contractual Funds Remaining Unspent				$1,722,398.39
FY 13 Additional Expenditures				
	DATA Storage	$5,535	$5,535	$0.00
FY 13 Contractual Funds Expended			$1,327,136.61	
FY 13 Contractual Funds Remaining Unspent				$1,716,863.39

Note:
After all FY13 projects were completed contractual funds in the amount of $1,716,844.99 remained. In April 2015, a refund of an expense totaling $18.40 was reimbursed to project 13-004, increasing the remaining funds to $1,716,863.39. The funds will be utilized for FY14 projects and will be accounted for on the following page.

FY 13 Remaining Contractual Funding		**$1,716,863.39**		
FY 13 Remaining Contractual Funding Transfers		**($53,974.00)**		
FY 13 Total Remaining Contractual Funding		**$1,662,889.39**		
Project Number		Amount Awarded (Budget)	Cumulative Expenditures	Remaining Balance
14-002	Univ. of CO - Boulder	$136,818.02	$126,321.61	$10,496.41
14-003	UNC Chapel Hill	$80,632.41	$68,238.28	$12,394.13
14-006	Sonoma Technology	$48,985.00	$37,467.30	$11,517.70
14-006	Valparaiso	$3,578.11	$3,578.11	$0.00
14-007	Chalmers Univ.	$65,233.00	$55,880.00	$9,353.00
14-007	Univ. of Houston	$23,081.00	$10,000.00	$13,081.00
14-008	UT-Austin (McDonald-Buller)	$156,500.00	$155,378.82	$1,121.18
14-009	Rice University	$60,000.00	$49,378.60	$10,621.40
14-011	UT-Austin (McDonald-Buller)	$131,166.00	$111,426.21	$19,739.79
14-011	Environ	$6,000.00	$3,065.94	$2,934.06
14-016	Environ	$240,000.00	$223,179.91	$16,820.09
14-017	Univ. of Alabama-Huntsville	$25,000.00	$22,997.48	$2,002.52
14-017	Rice University	$25,000.00	$18,152.98	$6,847.02
14-023	UT-Austin (Torres)	$25,874.37	$25,874.37	$0.00
14-023	Aerodyne	$10,712.74	$10,712.74	$0.00
14-024	UT-Austin (Hildebrandt Ruiz)	$143,282.00	$138,585.78	$4,696.22
14-024	Environ	$25,000.00	$25,000.00	$0.00
14-024	UC Riverside	$33,270.50	$30,875.39	$2,395.11
14-025	Environ	$89,000.00	$71,272.52	$17,727.48
14-025	TAMU	$20,000.00	$20,000.00	$0.00
14-026	Environ	$80,000.00	$68,819.12	$11,180.88
14-029	Baylor University	$109,650.32	$96,946.21	$12,704.11
14-030	TEES	$112,056.23	$99,237.61	$12,818.62

FY 13 Total Remaining Contractual Funding Awarded		$1,650,839.70		
FY 13 Remaining Contractual Funds Expended			$1,472,388.98	
FY 13 Remaining Contractual Funds Remaining to be Spent				$190,500.41
Total Contractual Funding		$3,837,465		
Total Contractual Funding Awarded		$3,825,415		
Total Contractual Funding Remaining to be Awarded		$12,050		
Total Contractual Funds Expended to Date			$3,646,964.26	
Total Contractual Funds Remaining to be Spent				$190,500.41

Table 6. 2014/2015 Contractual Expenses

Contractual Expenses

FY 14 Contractual Funding		**$825,000**		
FY 14 Contractual Funding Transfers		**$0**		
FY 14 Total Contractual Funding		**$825,000**		
Project Number		Amount Awarded (Budget)	Cumulative Expenditures	Remaining Balance
14-002	CU - Boulder	$13,689.98	$0.00	$13,689.98
14-002	Univ. of Maryland	$49,387.00	$13,287.63	$36,099.37
14-003	UNC Chapel Hill	$119,367.59	$0.00	$119,367.59
14-004	Univ. of Maryland	$55,056.00	$48,578.50	$6,477.50
14-004	Morgan State Univ.	$54,055.00	$27,522.50	$26,532.50
14-006	St. Edwards Univ.	$11,025.00	$0.00	$11,025.00
14-009	Rice Univ.	$49,867.00	$19,397.28	$30,469.72
14-009	Univ. of Houston	$109,635.00	$26,193.23	$83,441.77
14-014	Univ. of Houston	$84,927.00	$8,351.25	$76,575.75
14-022	Univ. of Alabama–Huntsville	$71,004.00	$0.00	$71,004.00
14-022	George Mason Univ.	$44,996.00	$0.00	$44,996.00
14-026	Environ	$85,562.00	$25,261.86	$60,300.14
14-030	TAMU/TEES	$64,052.77	$0.00	$64,052.77
FY 14 Total Contractual Funding Awarded		$812,624.34		
FY 14 Contractual Funding Remaining to be Awarded		$12,375.66		
FY 14 Contractual Funds Expended to Date			$168,592.25	
FY 14 Contractual Funds Remaining to be Spent				$656,407.75

FY 15 Contractual Funding		**$825,000**		
FY 15 Contractual Funding Transfers		**$0**		
FY 15 Total Contractual Funding		**$825,000**		
Project Number		Amount Awarded (Budget)	Cumulative Expenditures	Remaining Balance
14-005	TAMU	$103,890.00	$2,367.68	$101,522.32
14-006	Sonoma Technology	$2,000.00	$0.00	$2,000.00
14-007	Chalmers University	$8,946.00	$0.00	$8,946.00
14-007	Univ. of Houston	$0.00	$13,081.00	-$13,081.00
14-008	Univ. of Texas - Austin	$18,500.00	$0.00	$18,500.00
14-010	TAMU	$79,325.00	$4,568.74	$74,756.26
14-011	Univ. of Texas - Austin	$20,001.00	$287.53	$19,713.47
14-011	Environ	$22,419.00	$0.00	$22,419.00
14-016	Environ	$31,911.00	$0.00	$31,911.00
14-017	Univ. of Alabama - Huntsville	$112,003.00	$9,433.75	$102,569.25
14-017	Rice University	$37,979.00	$0.00	$37,979.00
14-020	Univ. of Maryland	$70,000.00	$0.00	$70,000.00
14-023	Aerodyne Research	$0.00	$0.00	$0.00
14-024	Univ. of Texas - Austin	$20,000.00	$387.44	$19,612.56
14-024	Environ	$76,404.00	$14,738.69	$61,665.31
14-025	Environ	$46,735.00	$9,840.60	$36,894.40
14-025	TAMU	$100,526.00	$44,214.30	$56,311.70
14-029	Baylor University	$69,028.68	$0.00	$69,028.68
FY 15 Total Contractual Funding Awarded		$819,667.68		
FY 15 Contractual Funding Remaining to be Awarded		$5,332.32		
FY 15 Contractual Funds Expended to Date			$98,919.73	
FY 15 Contractual Funds Remaining to be Spent				$726,080.27

Total Contractual Funding	$1,650,000		
Total Contractual Funding Awarded	$1,632,292		
Total Contractual Funding Remaining to be Awarded	$17,708		
Total Contractual Funds Expended to Date		$267,511.98	
Total Contractual Funds Remaining to be Spent			$1,382,488

Table 7. Breakdown of Project Funding Across Fiscal Years

Project	Final Approved Budget by Entity	FY 13	FY 14	FY 15	
14-002 - UC Boulder	150,508.00	136,818.02	13,689.98		$150,508.00
14-002 - Maryland	49,387.00		49,387.00		$49,387.00
14-003 - UNC - CH	200,000.00	80,632.41	119,367.59		$200,000.00
14-004 - Maryland	55,056.00		55,056.00		$55,056.00
14-004 - Morgan State	54,055.00		54,055.00		$54,055.00
14-005 - TAMU	103,890.00			103,890.00	$103,890.00
14-006 - Sonoma Tech	50,985.00	48,985.00		2,000.00	$50,985.00
14-006 - Valpo	3,578.11	3,578.11			$3,578.11
14-006 - St. Edwards	11,025.00	0.00	11,025.00		$11,025.00
14-007 - Chalmers	74,179.00	65,233.00		8,946.00	$74,179.00
14-007 - UH	23,081.00	23,081.00		0.00	$23,081.00
14-008 - UT Austin	175,000.00	156,500.00		18,500.00	$175,000.00
14-009 - Rice	109,867.00	60,000.00	49,867.00		$109,867.00
14-009 - UH	109,635.00		109,635.00		$109,635.00
14-010 - TAMU	79,325.00			79,325.00	$79,325.00
14-011 - UT	151,167.00	131,166.00		20,001.00	$151,167.00
14-011 - Environ	28,419.00	6,000.00		22,419.00	$28,419.00
14-014 - UH	84,927.00		84,927.00		$84,927.00
14-016 - Environ	271,911.00	240,000.00		31,911.00	$271,911.00
14-017 - UA - Huntsville	137,003.00	25,000.00		112,003.00	$137,003.00
14-017 - Rice	62,979.00	25,000.00		37,979.00	$62,979.00
14-020 - Maryland	70,000.00			70,000.00	$70,000.00
14-022 - UA - Huntsville	71,004.00		71,004.00		$71,004.00
14-022 - GMU	44,996.00		44,996.00		$44,996.00
14-023 - UT	25,874.37	25,874.37		0.00	$25,874.37
14-023 - ARI	10,712.74	10,712.74		0.00	$10,712.74
14-023 - Leak Sys	0.00				$0.00
14-023 - Provid	0.00				$0.00
14-024 - UT	163,282.00	143,282.00		20,000.00	$163,282.00
14-024 - Environ	101,404.00	25,000.00		76,404.00	$101,404.00
14-024 - UC-Riverside	30,875.39	30,875.39			$30,875.39
14-025 - Environ	135,735.00	89,000.00		46,735.00	$135,735.00
14-025 - TAMU	120,526.00	20,000.00		100,526.00	$120,526.00
14-026 - Environ	165,562.00	80,000.00	85,562.00		$165,562.00
14-026 - CalTech	0.00		0.00		$0.00
14-029 - Baylor	178,679.00	109,650.32		69,028.68	$178,679.00
14-030 - TAMU	176,109.00	112,056.23	64,052.77		$176,109.00
Amt in Projects	3,280,736.61	1,648,444.59	812,624.34	819,667.68	
Available Funding		1,662,889.39	825,000.00	825,000.00	
Funding Remaining		14,444.80	12,375.66	5,332.32	

Appendix A

Financial Reports by Fiscal Year

FY 10 and 11

(Expenditures reported as of November 30, 2014.)

Administration Budget (includes Council Expenses)

FY 2010

Budget Category		FY10 Budget	Cumulative Expenditures	Pending Expenditures	Remaining Balance
Personnel/Salary		$202,816.67	$202,816.67		$0
Fringe Benefits		$38,665.65	$38,665.65		$0
Travel		$346.85	$346.85		$0
Supplies		$15,096.14	$15,096.14		$0
Equipment		$0.00			$0
Other					
Contractual					
Total Direct Costs		$256,925.31	$256,925.31		$0
Authorized Indirect Costs		$20,281.69	$20,281.69		$0
10% of Salaries and Wages					
Total Costs		**$277,207.00**	**$277,207.00**	**$0**	**$0**

Administration Budget (includes Council Expenses)

FY 2011

Budget Category		FY11 Budget	Cumulative Expenditures	Pending Expenditures	Remaining Balance
Personnel/Salary		$172,702.06	$172,702.06	$0.00	$0.00
Fringe Benefits		$33,902.95	$33,902.95	$0.00	$0.00
Travel		$0.00		$0.00	$0.00
Supplies		$101.25	$101.25	$0.00	$0.00
Equipment					
Other		$0.00			$0.00
Contractual					
Total Direct Costs		$206,706.26	$206,706.26	$0.00	$0.00
Authorized Indirect Costs		$17,270.20	$17,270.20	$0.00	$0.00
10% of Salaries and Wages					
Total Costs		**$223,976.46**	**$223,976.46**	**0.00**	**$0.00**

ITAC Budget

FY 2010

Budget Category		**FY10 Budget**	**Cumulative Expenditures**	**Pending Expenditures**	**Remaining Balance**
Personnel/Salary					
Fringe Benefits					
Travel		$16,378.86	$16,378.86	$0	$0
Supplies		$1039.95	$1,039.95		$0
Equipment					
Other					
Total Direct Costs		$17,418.81	$17,418.81	$0	$0
Authorized Indirect Costs					
10% of Salaries and Wages					
Total Costs		**$17,418.81**	**$17,418.81**	**$0**	**$0**

ITAC Budget

FY 2011

Budget Category		**FY11 Budget**	**Cumulative Expenditures**	**Pending Expenditures**	**Remaining Balance**
Personnel/Salary					
Fringe Benefits					
Travel		$6,292.97	$6,292.97	$0.00	$0
Supplies		$284.67	$284.67	$0.00	$0
Equipment					
Other					
Total Direct Costs		$6,577.64	$6,577.64	$0.00	$0
Authorized Indirect Costs					
10% of Salaries and Wages					
Total Costs		**$6,577.64**	**$6,577.64**	**$0.00**	**$0**

Project Management Budget
FY 2010

Budget Category		FY10 Budget	Cumulative Expenditures	Pending Expenditures	Remaining Balance
Personnel/Salary		$145,337.70	$145,337.70		$0
Fringe Benefits		$28,967.49	$28,967.49		$0
Travel		$0	$0		$0
Supplies		$778.30	$778.30		$0
Equipment					
Other					
Total Direct Costs		$175,083.49	$175,083.49	$0	$0
Authorized Indirect Costs		$14,533.77	$14,533.77		$0
10% of Salaries and Wages					
Total Costs		**$189,617.26**	**$189,617.26**	**$0**	**$0**

Project Management Budget
FY 2011

Budget Category		FY11 Budget	Cumulative Expenditures	Pending Expenditures	Remaining Balance
Personnel/Salary		$121,326.64	$121,326.64	$0	$0
Fringe Benefits		$23,102.60	$23,102.77	$0	($0.17)
Travel		$0			$0
Supplies		$207.98	$207.92	$0	$0.06
Equipment					
Other					
Total Direct Costs		$144,637.22	$144,637.33	$0	($0.11)
Authorized Indirect Costs		$12,132.66	$12,132.55	$0	$0.11
10% of Salaries and Wages					
Total Costs		**$156,769.88**	**$156,769.88**	**$0**	**$0.00**

AQRP Budget

FY 2010

Budget Category		FY10 Budget	Cumulative Expenditures	Pending Expenditures	Remaining Balance
Personnel/Salary		$202,816.67	$202,816.67	$0.00	$0.00
Fringe Benefits		$38,665.65	$38,665.65	$0.00	$0.00
Travel		$346.85	$346.85	$0.00	$0.00
Supplies		$15,096.14	$15,096.14	$0.00	$0.00
Equipment		$0	$0.00	$0.00	$0.00
Other		$0	$0.00	$0.00	$0.00
Contractual		$2,287,827.93	$2,287,827.93	$0.00	$0.00
ITAC		$17,418.81	$17,418.81	$0.00	$0.00
Project Management		$189,617.26	$189,617.26	$0.00	$0.00
Total Direct Costs		$2,751,789.31	$2,751,789.31	$0.00	$0.00
Authorized Indirect Costs		$20,281.69	$20,281.69	$0.00	$0.00
10% of Salaries and Wages					
Total Costs		**$2,772,071.00**	**$2,772,071.00**	**$0.00**	**$0.00**

AQRP Budget

FY 2011

Budget Category		FY11 Budget	Cumulative Expenditures	Pending Expenditures	Remaining Balance
Personnel/Salary		$172,702.06	$172,702.06	$0.00	$0.00
Fringe Benefits		$33,902.95	$33,902.95	$0.00	$0.00
Travel		$0.00	$0.00	$0.00	$0.00
Supplies		$101.25	$101.25	$0.00	$0.00
Equipment		$0.00	$0.00	$0.00	$0.00
Other		$0.00	$0.00	$0.00	$0.00
Contractual		$1,852,440.62	$1,852,440.51	$0.00	$0.11
ITAC		$6,577.64	$6,577.64	$0.00	($0.00)
Project Management		$156,769.88	$156,769.88	$0.00	$0.00
Total Direct Costs		$2,222,494.40	$2,222,494.29	$0.00	$0.11
Authorized Indirect Costs		$17,270.20	$17,270.20	$0.00	$0.00
10% of Salaries and Wages					
Total Costs		**$2,239,764.60**	**$2,239,764.49**	**$0.00**	**$0.11**

Appendix B

Financial Reports by Fiscal Year

FY 12 and 13

(Expenditures reported as of November 30, 2014.)

Administration Budget (includes Council Expenses)

FY 2012

Budget Category		**FY12 Budget**	**Cumulative Expenditures**	**Pending Expenditures**	**Remaining Balance**
Personnel/Salary		$74,238.65	$74,238.65	$0.00	$0.00
Fringe Benefits		$17,068.38	$17,068.38	$0.00	$0.00
Travel		$339.13	$339.13		$0.00
Supplies		$3,560.62	$3,560.62	$0.00	$0.00
Equipment		$0.00			$0.00
Other					
Total Direct Costs		$95,206.78	$95,206.78	$0.00	$0.00
Authorized Indirect Costs		$7,423.86	$7,423.86	$0.00	$0.00
10% of Salaries and Wages					
Total Costs		**$102,630.64**	**$102,630.64**	**$0.00**	**$0.00**

Administration Budget (includes Council Expenses)

FY 2013

Budget Category		**FY13 Budget**	**Cumulative Expenditures**	**Pending Expenditures**	**Remaining Balance**
Personnel/Salary		$256,479.00	$256,154.46		$324.54
Fringe Benefits		$59,428.95	$59,405.87		$23.08
Travel		$0.00	$0.00		$0.00
Supplies		$8,352.05	$8,352.03		$0.02
Equipment					
Other		$0.00			
Total Direct Costs		$324,260.00	$323,912.36	$0.00	$347.64
Authorized Indirect Costs		$25,740.00	$25,615.44		$124.56
10% of Salaries and Wages					
Total Costs		**$350,000.00**	**$349,527.80**	**$0.00**	**$472.20**

ITAC Budget
FY 2012

Budget Category		FY12 Budget	Cumulative Expenditures	Pending Expenditures	Remaining Balance
Personnel/Salary					
Fringe Benefits					
Travel		$5,323.31	$5,323.31		$0.00
Supplies		$231.86	$231.86		$0.00
Equipment					
Other					
Contractual					
Total Direct Costs		$5,555.17	$5,555.17	$0.00	$0.00
Authorized Indirect Costs					
10% of Salaries and Wages					
Total Costs		**$5,555.17**	**$5,555.17**	**$0.00**	**$0.00**

ITAC Budget
FY 2013

Budget Category		FY13 Budget	Cumulative Expenditures	Pending Expenditures	Remaining Balance
Personnel/Salary					
Fringe Benefits					
Travel		$0.00	$0.00		$0.00
Supplies		$0.00	$0.00		$0.00
Equipment					
Other					
Contractual					
Total Direct Costs		$0.00	$0.00	$0.00	$0.00
Authorized Indirect Costs					
10% of Salaries and Wages					
Total Costs		**$0.00**	**$0.00**	**$0.00**	**$0.00**

Project Management Budget

FY 2012

Budget Category		FY12 Budget	Cumulative Expenditures	Pending Expenditures	Remaining Balance
Personnel/Salary		$53,384.46	$53,384.46	$0.00	$0.00
Fringe Benefits		$10,991.04	$10,991.04	$0.00	$0.00
Travel		$0.00	$0.00		$0.00
Supplies		$967.98	$967.98		$0.00
Equipment					
Other					
Contractual					
Total Direct Costs		$65,343.48	$65,343.48	$0.00	$0.00
Authorized Indirect Costs		$5,338.44	$5,338.44	$0.00	$0.00
10% of Salaries and Wages					
Total Costs		**$70,681.92**	**$70,681.92**	**$0.00**	**$0.00**

Project Management Budget

FY 2013

Budget Category		FY13 Budget	Cumulative Expenditures	Pending Expenditures	Remaining Balance
Personnel/Salary		$123,279.85	$123,279.85		$0.00
Fringe Benefits		$23,666.75	$23,666.75		$0.00
Travel					
Supplies		$699.40	$484.54		$214.86
Equipment					
Other					
Contractual					
Total Direct Costs		$147,646	$147,431.14	$0	$214.86
Authorized Indirect Costs		$12,328.00	$12,328.00		$0.00
10% of Salaries and Wages					
Total Costs		**$159,974.00**	**$159,759.14**	**$0.00**	**$214.86**

AQRP Budget

FY 2012

Budget Category		FY12 Budget	Cumulative Expenditures	Pending Expenditures	Remaining Balance
Personnel/Salary		$74,238.65	$74,238.65	$0.00	$0.00
Fringe Benefits		$17,068.38	$17,068.38	$0.00	$0.00
Travel		$339.13	$339.13	$0.00	$0.00
Supplies		$3,560.62	$3,560.62	$0.00	$0.00
Equipment		$0.00	$0.00	$0.00	$0.00
Other		$0.00	$0.00	$0.00	$0.00
Contractual		$847,438.67	$847,438.67	$0.00	$0.00
ITAC		$5,555.17	$5,555.17	$0.00	$0.00
Project Management		$70,681.92	$70,681.92	$0.00	$0.00
Total Direct Costs		$1,018,882.54	$1,018,882.54	$0.00	$0.00
Authorized Indirect Costs		$7,423.86	$7,423.86	$0.00	$0.00
10% of Salaries and Wages					
Total Costs		**$1,026,306.40**	**$1,026,306.40**	**$0.00**	**$0.00**

AQRP Budget

FY 2013

Budget Category		FY13 Budget	Cumulative Expenditures	Pending Expenditures	Remaining Balance
Personnel/Salary		$256,479.00	$256,154.46	$0.00	$324.54
Fringe Benefits		$59,428.95	$59,405.87	$0.00	$23.08
Travel		$0.00	$0.00	$0.00	$0.00
Supplies		$8,352.05	$8,352.03	$0.00	$0.02
Equipment		$0.00	$0.00	$0.00	$0.00
Other		$0.00	$0.00	$0.00	$0.00
Contractual		$2,990,026.00	$2,799,525.59	$0.00	$190,500.41
ITAC		$0.00	$0.00	$0.00	$0.00
Project Management		$159,974.00	$159,759.14	$0.00	$214.86
Total Direct Costs		$3,474,260.00	$3,283,197.09	$0.00	$191,062.91
Authorized Indirect Costs		$25,740.00	$25,615.44	$0.00	$124.56
10% of Salaries and Wages					
Total Costs		**$3,500,000.00**	**$3,308,812.53**	**$0.00**	**$191,187.47**

Appendix C

Financial Reports by Fiscal Year

FY 14 and 15

(Expenditures reported as of November 30, 2014.)

Administration Budget (includes Council Expenses)

FY 2014

Budget Category		FY14 Budget	Cumulative Expenditures	Pending Expenditures	Remaining Balance
Personnel/Salary		$70,000.00	$8,675.45	$0.00	$61,324.55
Fringe Benefits		$15,150.00	$2,530.94	$0.00	$12,619.06
Travel		$350.00	$0.00	$0.00	$350.00
Supplies		$7,500.00	$400.24	$0.00	$7,099.76
Equipment					
Other					
Total Direct Costs		$93,000.00	$11,606.63	$0.00	$91,393.37
Authorized Indirect Costs		$7,000.00	$867.55	$0.00	$6,132.45
10% of Salaries and Wages					
Total Costs		**$100,000.00**	**$12,474.18**	**$0.00**	**$87,525.82**

Administration Budget (includes Council Expenses)

FY 2015

Budget Category		FY15 Budget	Cumulative Expenditures	Pending Expenditures	Remaining Balance
Personnel/Salary		$70,000.00	$0.00	$0.00	$70,000.00
Fringe Benefits		$15,150.00	$0.00	$0.00	$15,150.00
Travel		$350.00	$0.00	$0.00	$350.00
Supplies		$7,500.00	$0.00	$0.00	$7,500.00
Equipment					
Other					
Total Direct Costs		$93,000.00	$0.00	$0.00	$93,000.00
Authorized Indirect Costs		$7,000.00	$0.00	$0.00	$7,000.00
10% of Salaries and Wages					
Total Costs		**$100,000.00**	**$0.00**	**$0.00**	**$100,000.00**

ITAC Budget

FY 2014

Budget Category		FY14 Budget	Cumulative Expenditures	Pending Expenditures	Remaining Balance
Personnel/Salary					
Fringe Benefits					
Travel		$7,000.00	$0.00	$0.00	$7,000.00
Supplies		$500.00	$0.00	$0.00	$500.00
Equipment					
Other					
Total Direct Costs		$7,500.00	$0.00	$0.00	$7,500.00
Authorized Indirect Costs					
10% of Salaries and Wages					
Total Costs		**$7,500.00**	**$0.00**	**$0.00**	**$7,500.00**

ITAC Budget

FY 2015

Budget Category		FY15 Budget	Cumulative Expenditures	Pending Expenditures	Remaining Balance
Personnel/Salary					
Fringe Benefits					
Travel		$7,000.00	$0.00	$0.00	$7,000.00
Supplies		$500.00	$0.00	$0.00	$500.00
Equipment					
Other					
Total Direct Costs		$7,500.00	$0.00	$0.00	$7,500.00
Authorized Indirect Costs					
10% of Salaries and Wages					
Total Costs		**$7,500.00**	**$0.00**	**$0.00**	**$7,500.00**

Project Management Budget
FY 2014

Budget Category		FY14 Budget	Cumulative Expenditures	Pending Expenditures	Remaining Balance
Personnel/Salary		$52,000.00	$36,180.76	$0.00	$15,819.24
Fringe Benefits		$9,300.00	$7,738.98	$0.00	$1,516.02
Travel		$0.00	$0.00	$0.00	$0.00
Supplies		$1,000.00	$0.00	$0.00	$1,000.00
Equipment					
Other					
Total Direct Costs		$62,300.00	$43,919.74	$0.00	$18,380.26
Authorized Indirect Costs		$5,200.00	$3,618.08	$0.00	$1,581.92
10% of Salaries and Wages					
Total Costs		**$67,500.00**	**$47,537.82**	**$0.00**	**$19,962.18**

Project Management Budget
FY 2015

Budget Category		FY15 Budget	Cumulative Expenditures	Pending Expenditures	Remaining Balance
Personnel/Salary		$52,000.00	$0.00	$0.00	$52,000.00
Fringe Benefits		$9,300.00	$0.00	$0.00	$9,300.00
Travel		$0.00	$0.00	$0.00	$0.00
Supplies		$1,000.00	$587.25	$0.00	$412.75
Equipment					
Other					
Total Direct Costs		$62,300.00	$0.00	$0.00	$61,712.75
Authorized Indirect Costs		$5,200.00	$0.00	$0.00	$5,200.00
10% of Salaries and Wages					
Total Costs		**$67,500.00**	**$0.00**	**$0.00**	**$66,912.75**

AQRP Budget

FY 2014

Budget Category		**FY14 Budget**	**Cumulative Expenditure s**	**Pending Expenditures**	**Remaining Balance**
Personnel/Salary		$70,000.00	$7,360.66	$0.00	$61,324.55
Fringe Benefits		$15,150.00	$2,088.54	$0.00	$12,619.06
Travel		$350.00	$0.00	$0.00	$350.00
Supplies		$7,500.00	$400.24	$0.00	$7,099.76
Equipment		$0.00	$0.00	$0.00	$0.00
Other		$0.00	$0.00	$0.00	$0.00
Contractual		$825,000.00	$168,592.25	$0.00	$656,407.75
ITAC		$7,500.00	$0.00	$0.00	$7,500.00
Project Management		$67,500.00	$47,537.82	$0.00	$19,962.18
Total Direct Costs		$993,000.00	$227,736.70	$0.00	$765,263.30
Authorized Indirect Costs		$7,000.00	$867.55	$0.00	$6,132.45
10% of Salaries and Wages					
Total Costs		**$1,000,000.00**	**$228,604.25**	**$0.00**	**$771,395.75**

AQRP Budget

FY 2015

Budget Category		**FY15 Budget**	**Cumulative Expenditures**	**Pending Expenditures**	**Remaining Balance**
Personnel/Salary		$70,000.00	$0.00	$0.00	$70,000.00
Fringe Benefits		$15,150.00	$0.00	$0.00	$15,150.00
Travel		$350.00	$0.00	$0.00	$350.00
Supplies		$7,500.00	$0.00	$0.00	$7,500.00
Equipment		$0.00	$0.00	$0.00	$0.00
Other		$0.00	$0.00	$0.00	$0.00
Contractual		$825,000.00	$98,919.73	$0.00	$726,080.27
ITAC		$7,500.00	$0.00	$0.00	$7,500.00
Project Management		$67,500.00	$587.25	$0.00	$66,912.75
Total Direct Costs		$993,000.00	$99,506.98	$0.00	$893,493.02
Authorized Indirect Costs		$7,000.00	$0.00	$0.00	$7,000.00
10% of Salaries and Wages					
Total Costs		**$1,000,000.00**	**$99,506.98**	**$0.00**	**$900,493.02**